Stony Brook University

OFFICIAL COPY

The official electronic file of this thesis or dissertation is maintained by the University Libraries on behalf of The Graduate School at Stony Brook University.

© All Rights Reserved by Author.

Structural and Functional Significance of the Additional Transmembrane Segment in Mammalian Glutamate Receptors

A Dissertation Presented

by

Alexandra Victoria Corrales Higuera

to

The Graduate School

In Partial Fulfillment of the

Requirements

for the Degree of

Doctor of Philosophy

in

Molecular and Cellular Pharmacology

Stony Brook University

May 2009

Copyright by

Alexandra Victoria Corrales Higuera

2009

Stony Brook University

The Graduate School

Alexandra Victoria Corrales Higuera

We, the dissertation committee for the above candidate for the

Doctor of Philosophy degree,

hereby recommend acceptance of this dissertation.

Lonnie P. Wollmuth, Ph.D. Advisor
Associate Professor, Neurobiology and Behavioral Sciences

Joav Prives, Ph.D. Chairperson of Defense
Professor, Pharmacological Sciences

Ira S. Cohen, M.D. Ph.D.
Professor, Physiology and Biophysics

Styliani-Anna E. Tsirka Ph.D.
Professor, Pharmacological Sciences

James R. Howe, Ph.D.
Professor, Pharmacology, Yale University School of Medicine

This dissertation is accepted by the Graduate School.

Lawrence Martin
Dean of The Graduate School

Abstract of the Dissertation

Structural and Functional Significance of the Additional Transmembrane Segment in Mammalian Glutamate Receptors

by

Alexandra Victoria Corrales Higuera

Doctor of Philosophy
in
Molecular and Cellular Pharmacology

Stony Brook University
2009

Glutamate receptors (GluRs) are ligand gated ion channels. They bind glutamate, the major excitatory neurotransmitter in the brain, and are essential to normal brain function and, when dysfunctional, contribute to numerous brain diseases. GluRs are integral membrane proteins with four subunits per functional receptor. Each subunit has four domains each with independent evolutionary origin: the amino terminal and ligand binding domain are extracellular, the transmembrane domain is located in the lipid bilayer, and C-terminal domain is intracellular. The transmembrane domain includes 4 hydrophobic segments, M1-M4, with M1 to M3 forming the ion channel core and having a structural homology to two transmembrane K^+ channels but with an inverted orientation in the membrane. Supporting this relationship are two transmembrane prokaryotic GluRs (e.g., GluR0) that are functional though they display gating kinetics quite different from mammalian GluRs. The M4 segment (as well as the C-terminal domain) has an unknown

evolutionary origin. During my thesis I studied the structural and functional significance of the additional transmembrane segment, M4, in mammalian GluRs.

Mammalian GluRs need the additional transmembrane segment (M4) to function, in contrast to prokaryotic GluRs. Specifically, I found that deletion of M4 in AMPA (GluR-A) receptors abolishes glutamate-activated current although the receptor expresses at the membrane. This lack of functionality is not due to any apparent interaction of M4 with the ligand-binding domain since decoupling M4 from the ligand-binding domain by introducing multiple glycines into the linker (joining M4 to the ligand-binding domain) has no notable effect on function. In contrast, mutagenesis scans of M4 as well as recovery of function from polyleucine M4 transmembrane helped us to define a unique face of the M4 helix that is required for glutamate receptor function. These interactions are in part involved in gating transitions in transmembrane segments. Hence, my work indicates that the interaction of M4 with other transmembrane segments is required for channel gating in mammalian GluRs, presumably to allow key gating elements (M3 and/or M1) to undergo their conformational change.

For Eduardo, Markus and Myriam Sophia

TABLE OF CONTENTS

LIST OF FIGURES

LIST OF TABLES

Abbreviations

AMPA	alpha-amino-3-Hydroxy-methyl-4-isoxazolepropionate
APV	(2R)-amino-5-phosphonovaleric acid
ATD	Amino terminal domain
CNQX	6-cyano-7-nitroquinoxaline-2,3,-dione 7-nitro-2,3-dioxo-1,4-dihydroquinoxaline-6-carbonitrile
CTD	C-terminal domain
CTZ	Cyclothiazide
D1	Domain 1 of ligand binding domain
D2	Domain 2 of ligand binding domain
EPSC	Excitatory post-synaptic current
EPSP	Excitatory post-synaptic potential
ER	Endoplasmic reticulum
GluR-A, -B, -C, -D	Ionotropic Glutamate receptor subunit A, or B, or C, or D Same as GluR-1 or 2, or 3 or 4
GluRs	Ionic Glutamate Receptors
KA	Kainate
LBD	Ligand binding domain
MAGUKs	Membrane associated guanylate kinases
MTSET	2-(trymethylamonium)ethyl methanethiosulfonate
NMDA	N-methyl-D-aspartate receptors
NR1 2A 2B 2C 2D 3A 3B	NMDA receptor subunit 1, or 2A, or 2B, or 2C, or 2D, or 3A, or 3B
PDZ	Acronym combining the first letters of three proteins — post synaptic density protein (PSD95), Drosophila disc large tumor suppressor (DlgA), and zonula occludens-1 protein (zo-1) — which were first discovered to share the domain
PKA	Protein kinase A
PKC	Protein kinase C
PSD	Post-synaptic density
SCAM	Substituted Cysteine accessibility method
TARPs	Transmembrane AMPA receptor auxiliary subunits

Acknowledgments

I would like to thank the many people that have made it possible for me to reach this point.

First, many thanks to Dr. Lonnie P. Wollmuth for his guidance, support and accommodations during the course of my studies. He laid the path that facilitated my work and scientific achievements.

Second, my gratitude to Dr. Markus Eilers for his patience, persistence and scientific recommendations in the structural sections of my project.

Thank you to several people that taught me different skills necessary for the development of my work:

Dr. Paul Bremm for handling and experimentation with *Xenopus laevis* oocytes.

Dr. Steven O. Smith from the Center for structural Biology, for the access to biochemistry and computational equipment. Additional thanks to Ian Brett, Miki Itaya and Tzu-Chun (Tony) Tang for their instruction.

Dr. Gerald H. Thomsen, Dr. David Talmage and the Center for Nervous System Disorders for access to their microscopy equipment. Also, thanks to Dr. Arif Kirmizitas, Sarah Canetta and Julie Rosenbaum for their technical guidance

Dr. Mark L. Mayer from the National Institutes of Health (NIH) for the clone of bacterial glutamate receptor (GluR0).

Thank you to all the members of the Wollmuth lab, especially the efforts in data acquisition of Iehab Talukder, Janeth Allopena, Rashek Kazi and Martin Prieto. Their support was invaluable. My gratitude is extended to Gulcan Akgul, Catherine Salussolia,

my good friend Jessica Helm and other previous members of the lab who aided in this work.

I would like to acknowledge the support staff from the pharmacology department, Lynda Perdomo-Ayala, Beverly Campbell and June Moriarty. Also, thanks to Nina Maung from SUNY AGEP and the graduate school children accommodation policy (CAP) that provided financial support during my graduate studies.

I would like to recognize the support of my friends from room 8 at SBCCSI, the Cooking club especially Martine Ziliox, and Brookwolves and Loquitos de Aldrich soccer teams. Such activities allowed me to keep a fresh perspective on my work.

Thanks to the many friends who have supported and encourage me along the years, especially the playground group of Sebastian, Catalina, Luba and Walton.

Always thank you to my Family, in Colombia and Germany, who have believed in me and helped me achieve my goals.

Finally thank you to my daughter Myriam Sophia and my husband Markus. Your love, support and encouragement have helped me to be here today.

CHAPTER ONE

General Introduction

1 INTRODUCTION

Underneath the complex circuit of the neuronal network that gives rise to mental activity is synaptic transmission. Fast synaptic transmission underlies how we think and perceive our environment and most motor actions. Synaptic transmission can be excitatory increasing the activity of the postsynaptic cell or inhibitory decreasing the activity of the postsynaptic cell. This rapid signaling involves ligand gated ion-channels in the membrane. Glutamate is the major excitatory neurotransmitter in the brain and spinal cord. A family of glutamate receptors has been identified. During neuronal signaling, postsynaptic receptors produce effects in the cell that vary in their biochemical mechanism, duration of action and physiological function. Activation of glutamate receptors open ion channels that produce a fast and brief synaptic action.

The focus of my thesis is to define mechanisms regulating the coupling between the ligand binding domain and opening/closing of the glutamate receptor ion channel.

1.1 Glutamatergic Synaptic Transmission

Ionotropic glutamate receptors (GluRs) are ligand-gated ion channels that are essential to fast cell-to-cell communication in the brain and spinal cord. They are activated by glutamate, the major excitatory neurotransmitter in the mammalian central

nervous system. GluRs are implicated in the development of synaptic connections, pain perception, and the synaptic plasticity underlying higher order processes such as learning and memory, as well as a variety of neurological disorders. This family of receptors has been divided into three major subtypes based on their pharmacology as well as molecular cloning: α-amino-3-hydroxy-methyl-4-isoxazolepropionate receptors (AMPA receptors), N-methyl-D-aspartate receptors (NMDA receptors) and kainate receptors (KA receptors) (Dingledine et al., 1999). AMPA and NMDA receptors are found at all synapses, whereas KA receptors have a less widespread distribution and are modulatory in function. All functional glutamate receptors are multimeric proteins, composed of four subunits assembled as a dimer of dimers (Lerma, 2006; Mayer, 2006; Paoletti and Neyton, 2007).

Each subtype has distinct biophysical and molecular properties which are important for their flexibility and diversity in synaptic function. For all subtypes, the associated ion channel is cation selective. Hence, activation of GluRs leads to a depolarizing or excitatory postsynaptic potential (EPSP), tending to increase the activity of the post synaptic cell. However, because of differences in pore properties, channel kinetics, affinity for agonist, interaction with other proteins, and cellular regulation, the specific contribution of the subtypes to EPSPs varies widely. Heterogeneity within each subtype also originates from the homo- or hetero-oligomeric assembly of distinct subunits into tetramers, mRNA editing, splice variants and post-translational modifications (Dingledine et al., 1999; Hall and Ghosh, 2008; Paoletti and Neyton, 2007; Rodriguez-Moreno and Sihra, 2007).

1.1.1 α-amino-3-hydroxy-methyl-4-isoxazolepropionate receptors (AMPA receptors)

AMPA receptors generate the large early component of the excitatory postsynaptic current (EPSC) (Figure 1-1). Pharmacologically dissected EPSC shows that the activation and deactivation kinetics of AMPA-receptor-mediated currents are fast (Figure 1-1), occurring on the time scale of several milliseconds. The heterologously expressed AMPA receptor subunits also show fast gating kinetics.

Structurally, AMPA receptors can assemble as homo- or hetero-tetramers from a pool of four subunits (GluRA-D, alternatively GluR1-4, Figure 1-2). The tetrameric composition determines the channel's functional properties, but the subunit selectivity of the assembly process is poorly understood (Dingledine et al., 1999; Greger and Esteban, 2007; Rosenmund et al., 1998).

AMPA receptor cation channels have relative low conductances (<<20 pS) and are permeable to Na^+ and K^+ but usually not to Ca^{2+} ions (Dingledine et al., 1999). Ca^{2+} permeability depends on the presence and RNA editing of the GluR-B (or GluR2) transcript. In a tightly regulated process, specific adenosines are deaminated to inosines by dsRNA adenosine desaminases. The editing of RNA causes single amino acid exchanges in GluR-B, which renders the entire channel Ca^{2+} impermeable. The change in amino-acid codon happens because inosines base-pair like guanosines. Although AMPA receptors are edited at multiple positions, the most highly edited and essential for survival is the Q/R site in the M2 loop. In this case, a glutamine (Q) codon (CAG) is

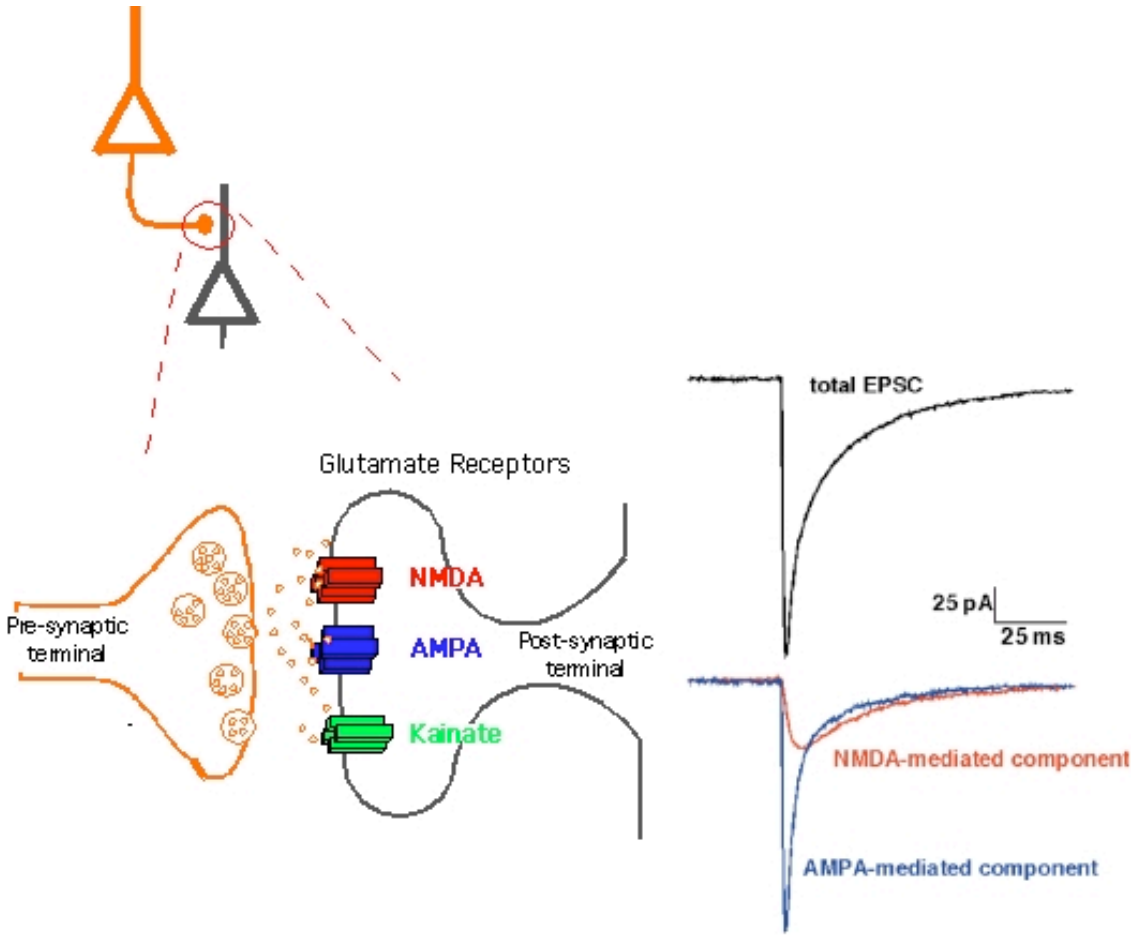

Figure 1-1 Glutamate-mediated post-synaptic currents

Excitatory post-synaptic currents (EPSC) elicited by release of presynaptic glutamate. The EPSC (top) was pharmacologically dissected into its component GluR subtypes. In the presence of the NMDA receptors antagonist APV ((2R)-amino-5-phosphonovaleric acid) AMPA-mediated components are revealed. The competitive antagonist CNQX (6-cyano-7-nitroquinoxaline-2,3-dione or 7-nitro-2,3-dioxo-1,4-dihydroquinoxaline-6-carbonitrile) of AMPA receptors reveals the NMDA-receptor-mediated component.

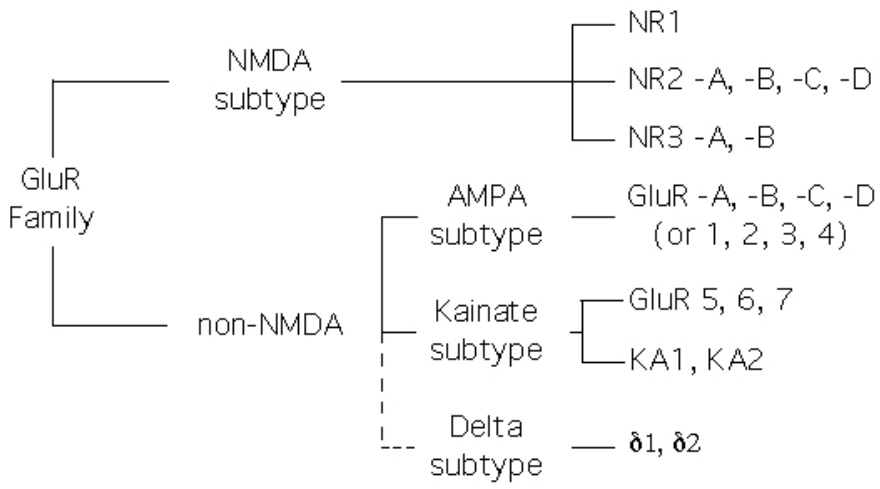

Figure 1-2 The ionotropic Glutamate Receptor family.

The diagram describes relations between the different subtypes but does not represent evolutionary distance. The molecular diversity of each family is promoted by RNA editing, post-translational modifications and the genetic regulation of receptor expression. The molecular, biophysical and pharmacological properties vary between GluR subtypes and specify their contributions to synaptic physiology (see Dingledine et al., 1999; Mayer, 2004). The range of the glutamatergic response is determined by the functional diversity of GluRs.

edited to an arginine (R) codon (CIG) (Dingledine et al., 1999; Seeburg and Hartner, 2003).

This Q/R site greatly influences the biophysical properties of the receptor including Ca^{2+} permeability, single channel conductance and polyamine block. Heteromeric receptors with GluR-B are Ca^{2+} impermeable and have a linear current-voltage relationship (IV). On the other hand, heteromeric receptors lacking GluR-B are Ca^{2+} permeable and show a strong block by intracellular polyamines (Bowie and Mayer, 1995; Kamboj et al., 1995; Koh et al., 1995).

Another characteristic of AMPA receptors is their fast and strong desensitization. In the continuous presence of glutamate, AMPA receptors rapidly enter into a non-conducting desensitized state (<5% of peak current) on the time scale of several milliseconds. Although the full physiological significance of desensitization at glutamatergic synapses is unknown, it contributes to shaping the EPSC decay at mature synapses (Wall et al., 2002; Zucker and Regehr, 2002).

1.1.2 N-methyl-D-aspartate receptors (NMDA receptors)

NMDA receptors contribute to the late component of the EPSC. A pharmacologically dissected NMDA-receptors-mediated EPSC shows slow gating kinetics (Figure 1-1), with slow activation and deactivation components (Wyllie et al.,

1998). Because of their slow gating kinetics and high Ca^{2+} permeability, NMDA receptors mediate an electrical and biochemical signal at the glutamatergic synapse. Normally, without the activation of AMPA receptors, this channel does not contribute greatly to an EPSP due to a strong voltage-dependent block by Mg^{2+} (see below). This enables the receptor to act as coincidence detector at the synapse (Cull-Candy and Leszkiewicz, 2004), requiring ligand binding and membrane depolarization to activate. NMDA receptors have also been implicated in a number of diseases including stroke, schizophrenia, Huntington's disease and ischemia (Cull-Candy et al., 2001; Kalia et al., 2008).

NMDA receptors are obligate heterotetramers in contrast to AMPA receptors. The receptors assemble as heteromers from a pool of seven members in the subtype (Figure 1-2). All NMDA receptors contain NR1, the essential subunit, in combination with any NR2 (NR2A, B, C, D), or NR3 (NR3-A, -B). NR1:NR2A is the typical, and most studied, functional receptors. Alternative splicing can generate eight functional isoforms of NR1 with receptors of different pharmacological properties. Other splice variants for NR2 and NR3 also exist (Cull-Candy et al., 2001; Dingledine et al., 1999b; Paoletti and Neyton, 2007). The receptor composition follows "the dimer of dimers" arrangement of the GluR family with the dimer element NR1:NR2 (Furukawa et al., 2005). The expression pattern of NMDA receptors shows that the subunits are differentially distributed throughout the brain, and their distributions change during development (Cull-Candy and Leszkiewicz, 2004). NR2A appears late in development to replace NR2B and

NR2D, the first subunits present during development. Each subunit gives different properties to the receptor function.

The cation channel of NMDA receptors formed by NR1:NR2A subunits has a high conductance (50 pS) that is permeable to Ca^{2+}, Na^{+} and K^{+} (Dingledine et al., 1999). They exhibit high Ca^{2+} permeability and are blocked by Mg^{2+} at membrane resting potential (Kuner and Schoepfer, 1996). Other receptor subtypes have smaller conductances and in the case of NR1:NR3 the sensitivity to Mg^{+} and Ca^{2+} is greatly reduced (Cavara and Hollmann, 2008).

The activation of NMDA receptors require glutamate as well as the coagonist glycine. NR1 and NR2. bind glycine and glutamate respectively (Dingledine et al., 1999; Dingledine et al., 1990). The extracellular glycine concentration in the brain is thought to be sufficient for channel gating. NMDA receptors conductance is voltage as well as chemical transmitter dependent. Mg^{2+} is tightly bound to the channel at resting membrane potential (-65 mV) and is expelled from the channels by electrostratic repulsion when the membrane is depolarized, allowing Na^{+} and Ca^{2+} to enter. NMDA receptor channels therefore allow current flow only when glutamate is bound and the cell is depolarized.

The influx of Ca^{2+} after NMDA receptors activation can trigger LTP or LTD of synaptic currents. The activation of NMDA in the CA1 region is required for the induction of LTP. Mechanistically, strong post-synaptic depolarization activates

biochemical processes via the increase in Ca^{2+} to threshold levels. The system regulation is tight, but dramatic Ca^{2+} entry and cell death can occur, as observed during ischemia (Cull-Candy and Leszkiewicz, 2004). The basic properties of LTP (cooperativity, associativity and input specificity) arise from the NMDA receptors properties as a "coincidence detector". NMDA receptors require both the presynaptic release of glutamate and the postsynaptic depolarization, resulting from the simultaneous activation of a population of synapses, to achieve its contribution to the postsynaptic response.

1.1.3 Kainate Receptors (KA receptors)

KA receptors are not found at all glutamatergic synapses although they are present in various neuronal populations (for general reviews see Lerma, 2006). KA receptors are restricted cellularly and subcellularly, adding further diversity to the synaptic response where they mainly have a modulatory function. The efficiency of KA receptors to regulate network activity depends on their repetitive synaptic activation within physiological ranges of firing frequencies.

Five KA receptor subunits have been identified and are distinguished into low affinity receptors (GluR-5, -6 and -7) and high affinity receptors (KA1 and KA2) (Figure 1-2) (Huettner, 2003; Jaskolski et al., 2005; Pinheiro and Mulle, 2006). GluR-5 -6 and -7 can function as homomeric or heteromeric receptors. In contrast KA1 and KA2 do not form functional receptors by themselves but require GluR –5, -6 or –7 subunits to form

functional receptors (though in heterologous expression system KA1 and KA2 can form homomers) (Kew and Kemp, 2005).

Similar to AMPA receptors, GluR –5 and –6 have an edited Q/R site at the M2 reentry loop. This modification, like in AMPA receptors, determines the extent of permeation to Ca^{2+}. In the edited or R-form (arginine), the receptors have low Ca^{2+} permeability whereas in the unedited Q-form (glutamine) the permeability to Ca^{2+} is high (Pinheiro and Mulle, 2006). Unlike AMPA receptors, the editing is incomplete. Similar to AMPA receptors, the Ca^{2+} permeability is correlated with the intracellular polyamine block that produces inwardly rectifying current-voltage (I-V) relationship for unedited Ca^{2+} permeable receptors and linear I-V curves for edited Ca^{2+} impermeables receptors (Pinheiro and Mulle, 2006). GluR –5, -6 and –7 undergo alternative splicing, with eight splice variants identified so far, introducing additional heterogeneity to the subtype (Dingledine et al., 1999). KA1 and KA2 subunits are not subjected to known RNA editing or alternative splicing.

The KA receptor cation channel has a conductance around 20 pS, similar to AMPA receptors but shorter in opening duration (Huettner, 2003). The in vitro kainate affinity of GluR –5, -6 and 7 is in the range of 50-100 nM (low affinity subunits), while for KA1 and KA2 it is 5-15 nM (high affinity kainate binding) (Dingledine et al., 1999).

KA receptors regulate network activity and are found at the presynaptic and postsynaptic level (Huettner, 2003; Lerma, 2006; Pinheiro and Mulle, 2006; Rodriguez-Moreno and Sihra, 2007).

1.1.3.1 Presynaptic KA receptors

The role of presynaptic KA receptors is reported extensively with the use of exogenous kainate and few reports describe the activation by endogenous glutamate. It is assumed that the facilitatory action of presynaptic GluRs require a slight depolarization of the presynaptic membrane that may lead to large changes in synaptic release. When synapatic terminals express receptors to their own neurotransmitters, an autoregulatory loop is formed that may facilitate feedback (Kwon and Castillo, 2008). KA presynaptic autoreceptors strongly influence LTP by changing the induction threshold. In the presynapse of mossy fibers, KA autoreceptors are implicated in synaptic facilitation. GluR-6 and GluR-7 located close to the glutamate release site can generate depolarization or the influx of Ca^{2+} can induce intracellular Ca^{2+} release (Lerma, 2006).

Presynaptic KA autoreceptors also modulate synaptic depression. High frequency pulses inhibit synaptic transmission between synapses of parallel fibers and stellate cells in the cerebellum. The modulatory effect is influenced by KA receptor composition, receptor density and precise location at the synapse. Presynaptic KA receptors can also act as heteroreceptors. This mechanism is not clear and experimentally requires strong stimulation conditions (Huettner, 2003). The response is influenced by GluR6 or KA2 presence at the tetrameric receptor. KA receptors regulate the release of GABA but more

details are required to determine if KA receptors are on the membrane of somatodedritic or GABAergic terminals (Pinheiro and Mulle, 2006).

1.1.3.2 Postsynaptic KA receptors

Postsynaptic KA receptors carry an inward depolarizing current. KA receptors activation generates an EPSC when the synapse between mossy fibers and pyramidal cell of the hippocampus is stimulated. The EPSC generated by KA receptors is small in amplitude (<10% compared to AMPA), with slow rise and decay times . These are also much slower than those found just from heterologous expression of KA receptors subunits. The basis for this is unknown but may reflect protein-protein interactions (Zhang et al., 2009). KA-receptors-mediated EPSCs provide extended depolarization under repetitive firing using a broad spectrum of physiological frequencies.

1.1.3.3 Extrasynaptic KA receptors

Somatodendritic extrasynaptic KA receptors activated by non-synaptic glutamate, contribute to the KA receptors neural regulation, but the mechanism of this pathway is not clear (Pinheiro and Mulle, 2006).

1.2 Post-Synaptic Glutamate Receptors

GluRs organization at the synapse is carefully monitored. The localization and stabilization at the membrane result from a coordinated process of cell trafficking from and toward the secretory and endocytic pathway. The C-terminal domain (CTD) of

GluRs is the major participant in this activity. It has Cis-acting regulatory elements that control trafficking, surface expression and protein-protein interaction (Derkach et al., 2007). The CTD also modulates GluR downstream signaling (Collingridge and Isaac, 2003). The CTD are of variable length, according to subunit. Their sequences exhibit phosphorylation sites (Barria et al., 1997; Chen et al., 2006; Hirbec et al., 2003; Oh et al., 2006; Soderling and Derkach, 2000), PDZ domains (Kim and Sheng, 2004), glycosaminoglycan attachment sites, myristoylation sites, and lysine residues where ubiquitin can be covalently bound (Burbea et al., 2002; DiAntonio and Hicke, 2004; Ehlers, 2003; Wheeler et al., 2002). All these regulatory elements have proven functional in some GluR subunits (Moriyoshi et al., 2004). Differences arise between subunits regarding their cytosolic interaction partners (Greger and Esteban, 2007).

The strength of the synaptic response is regulated among other factors by the number and type of GluRs at the synapse.

One mechanism for this modulation is the removal of receptors from the plasma membrane. Indeed, the process of endocytosis at the synapse produces a dynamic regulation in the number of receptors at the membrane. This process has been demonstrated to be a clathrin-dependent event in the case of AMPA and NMDA receptors (Burbea et al., 2002; Lavezzari et al., 2003; Lee et al., 2002).

The removal of AMPA receptors from the membrane is ubiquitin-dependent (Burbea et al., 2002) like metabotropic GluRs (Moriyoshi et al., 2004). Stimulation of

NMDA receptors generates endocytosis of KA receptors to early endosomes by a Protein Kinase C (PKC), Protein Kinase A (PKA) and Calcium (Ca^{2+}) dependent process. Additionally direct stimulation of KA receptors targets receptors to lysosomes in a PKC dependent mechanism (Cho et al., 2003; Ehlers, 2000; Martin and Henley, 2004).

Second, the insertion of GluRs at the membrane is regulated by an early endoplasmic reticulum (ER) control mechanism. KA1, KA2 and NR1 subunits present intracellular signals that favor ER retention (Pinheiro and Mulle, 2006; Xia et al., 2001). The formation of heteromeric receptors can mask the presence of these ER retention signals.

A third mechanism is binding and stabilization of GluRs in the plasma membrane. GluRs interact with scaffolding proteins from the postsynaptic density (PSD) region. The interaction occurs through the CTD of GluRs and PDZ domains of PSD proteins. The PDZ domains are responsible for binding and stabilizing GluRs in the plasma membrane. One family of PSD proteins is the membrane associated guanylate kinases (MAGUKs). Some of their members that express at the postsynapse are PSD95, PSD-93, SAP97 and SAP102 (Sheng and Hoogenraad, 2007). The interaction of MAGUKs with GluRs is subunit specific. The PSD-95 binds NMDA receptors subunits through the PDZ domain (Kornau et al., 1995). PSD-93 binds indirectly to AMPA receptors through TARPs (transmembrane AMPA receptor auxiliary subunits). SAP97 interact with AMPA receptors (Leonard et al., 1998). The primary effect of these proteins is to modulate receptor localization but they also affect activation and deactivation kinetics of the GluRs

that they bind. Interestingly, genetic manipulations of individual MAGUKs (such as PSD-95) often have minimal effects on the NMDA receptor mediated-EPSCs. One possible explanation is the existence of multiple pathways to coordinate the trafficking of GluR subunits at immature and mature synapses.

TARPs are a family of proteins that associate with AMPA receptors. The best known and characterized is Stargazin. A PDZ binding site on its extreme C-terminus provides a linkage to PDZ domain proteins such as PDS95 and SAP97 (Chen et al., 2000). These interactions are likely to be critical in stargazin's role in the trafficking of AMPA receptors. In addition stargazin is also important as an acute modulator of AMPA receptor function. It has been shown to enhance AMPA receptor mediated currents (Yamazaki et al., 2004), affect desensitisation kinetics and agonist responsiveness (Bowie et al., 2003) and mediate AMPA receptor induced NMDA receptor clustering (Mi et al., 2004). To reconstitute native AMPA receptors properties in heterologous cells it is necessary to coexpress TARPs (Morimoto-Tomita et al., 2009; Tomita et al., 2005).

1.3 Disease

The release of glutamate at the synapse is a highly regulated process. If the homeostasis of glutamate release and reuptake is altered and high concentrations of neurotransmitter are present an excessive activation of GluRs can occur. Overactivation of GluRs generates excitotoxicity (Dirnagl et al., 1999; Heintz and Zoghbi, 2000; Olney et al., 1972) that promotes neuronal death through necrosis as well as apoptosis, characteristics present in several neurodegenerative diseases like epilepsy, ischemic stroke, Parkinson's or Alzheimer's disease, Huntington's chorea and amyotrophic lateral sclerosis.

The neurotoxic effects of GluRs excessive activation are mainly due to increase in intracellular Ca^{2+}, though imbalance in other pathways (e.g. K^{+}, Na^{+}) may also exist. The elevation in intracellular calcium can activate Ca^{2+}-dependent proteases, alter cellular metabolism, increase free radicals to toxic levels and enhance protein degradation. GluR overactivation is correlated with enhanced neuronal excitation that can produce seizures as a result of circuit overload. This cascade of events can produce even more glutamate release, increasing the autoexcitation and leading to neural network collapse (Citri and Malenka, 2008). Excitotoxicity can result from the ingestion of GluR agonists, ischaemia or neurodegenerative disorders (Dirnagl et al., 1999).

Drugs that block glutamate receptors attenuate some of the pathological symptoms but produce psychomimetic or cardiovascular side effects. The strategy in the

field of the neuroprotective drugs is to search for non-antagonist compounds that interact with GluRs. New targets for drug interaction that modulate channel activity would open new avenues for drug design.

The extensive family of GluRs and its central role in synaptic physiology open multiple pathways that can influence disease. The following references are centered on AMPA receptors, the focus of my research. However, it is difficult to determine if AMPA receptor dysfunction is the initial cause or consequence of a disorder. Here I present what AMPA receptors dysfunctions have been related to neurological disease.

1.3.1.1 RNA editing

Mutations in conserved regions or failure in the RNA editing process can generate alterations in the synaptic phenotype.

GluRs are subjected to RNA editing that define their physiological characteristics. Adenosine deaminases acting on RNA (ADAR1-3) convert adenosine to inosine, and edit residues in GluRs. The order of editing as well as the mechanisms controlling editing in native neurons is poorly understood. Deletion of the binding site (ECS intronic sequence) for proper operation of the editing enzyme eliminate the essential Q/R editing in AMPA receptors. AMPA receptors with the unedited GluR-2 (Q) have a higher Ca^{2+} permeability opposite the GluR-2 (R) edited form (Kwak and Kawahara, 2005). Mice with the ECS deletion are normal until the second week of life, when they develop spontaneous and recurrent seizures and die before they are 3 weeks old (Peng et al.,

2006). This editing defect is observed also in amyotrophic lateral sclerosis (ALS) patients (Kawahara et al., 2004), where failure of GluR-2 editing occurs in a disease specific and region selective manner. RNA editing of AMPA receptors is a crucial event for neuronal survival and its deficiency can be a direct cause of neuronal death.

1.3.1.2 Receptor activity

AMPA receptors are also implicated in neurodegenerative disorders. Modulation of AMP receptors activity or synaptic expression is altered during pathological conditions.

Alzheimer's disease (AD) results from a progressive and irreversible loss of neuronal function that leads to cell death. The hallmark pathology includes deposition of amyloid plaques, composed of β-amyloid peptide (Aβ) and neurofibrillary tangles. Aβ modulates synaptic function, and in pathological levels inhibits synaptic plasticity (Shepherd and Huganir, 2007). It reduces AMPA and NMDA receptor-mediated currents in slices by a mechanism similar to a signaling pathway involved in LTD. The number of synaptic AMPA receptors is reduced by Aβ overexpression, apparently by the phosphorylation of Ser880. The activity of this residue is linked to the endocytosis of AMPA receptors and long term depression (LTD) (Hsieh et al., 2006). How Aβ can modulate AMPA receptors function by an intracellular cascade is still an object of study.

1.3.1.3 Synaptic expression

Modification in the number of synaptic AMPA receptors is observed in other neuronal pathologies.

During amyotrophic lateral sclerosis (ALS), a reduction in GluR2 expression in spinal moto-neurons consistent with increased Ca^{2+} permeability and excitotoxicity (Samarasinghe et al., 1996; Virgo et al., 1996) is observed. Together with marked reduction of RNA editin (Kwak and Kawahara, 2005), this may be a direct cause of the selective motor neuron death seen in ALS.

During Huntington's disease AMPA receptors removal from the synapse is impaired. The NMDA-receptor-dependent removal of surface AMPA receptors is modified, producing defects in long term potentiation (LTP; (Benn et al., 2007; Metzler et al., 2007).

The glutamatergic hypothesis of schizophrenia postulates a link between glutamatergic transmission and the disease. The evidence is clear to connect the hypo-function of NMDA receptors to the pathologic mechanism (Coyle et al., 2002). However with AMPA receptors the evidence is scarce. Data show a reduced expression of GluR2 in the population of pyramidal neurons of the para-hippocampal gyrus. Nevertheless, it is unclear if GluR2 reduction is a cause or consequence of the disease (Eastwood et al., 1995). Recent studies have evaluated the association of AMPA receptor genes (GRIA1,GRIA2, GRIA3 and GRIA4) with the disease (Guo et al., 2004; Magri et al.,

2008). Only GRIA3 gene is associated with the susceptibility to schizophrenia in women (Magri et al., 2008).

The Olivopontocerebellar (OPCA) degeneration is a progressive neurodegenerative condition. It is not a definite single disease, but a condition that may be present in several distinct degenerative ataxic disorders like: autosomal dominant ataxia, complicated spastic paraplegia, multiple-system atrophy (MSA) and many cases of idiopathic late-onset cerebellar ataxia (ILOCA). Is also a hallmark in prion disorders, mitochondrial encephalomyopathies and hereditary metabolic disease (Berciano et al., 2006).

MSA involves abnormalities in alpha-synuclein. On the gross level, the brains common characteristics are diminute pons, cerebellum degeneration, loss of Purkinje cells (Gilman et al., 2000; Jellinger, 2003). Studies of the brain of patients with OPCA indicate a reduction in mRNA of GluR-2 and GluR-3 and suggest the role of an excitotoxic mechanism (Dirson et al., 2002). There is also an increase in autoantibodies against GluR2 in OPCA brains (Gahring et al., 1997).

1.3.1.4 Autoantibodies

Autoimmunity for GluRs has been proposed in several progressive nervous system degeneration pathophysiologies.

In Rasmussen's encephalitis (Andrews and McNamara, 1996) GluR3 autoantibodies are found in the plasma of patients affected. Patients have severe epilepsy, hemiplegia, dementia and inflammation of the brain. Only one cerebral hemisphere is affected by progressive atrophy (Granata et al., 2003; McNamara et al., 1999). This rare progressive disorder appears in childhood. The autoantibodies can activate AMPA and Kainate receptors in cortical neurons. The antibody epitope is located at the agonist binding site of GluRs. Antibody GluR activation may produce the epileptic seizures that characterize the disease and contribute to excitotoxic cell death (Rogers et al., 1994). As part of the immunological response elicited, complement activation kills cortical cells. Still, it is not clear how Rasmussen's encephalitis is initiated, how it is restricted to a single cerebral hemisphere, and how the antibodies have access to the brain.

1.4 General Receptor Structure

Functional GluRs are tetramers composed of individual subunits that are thought to share a similar topology (Figure 1-3; see Dingledine et al., 1999; Mayer, 2006; Oswald et al., 2007; Wollmuth and Sobolevsky, 2004).

Each GluR subunit has a modular design (Oswald et al., 2007; Wo and Oswald, 1995) being composed of four domains: an extracellular amino terminal domain (ATD), a ligand binding domain (LBD), a transmembrane (ion channel) domain and an intracellular C-terminal domain (CTD). Some of these domains have well-defined evolutionary relationships (Wo and Oswald, 1995). The extracellular region of a GluR subunit includes the amino terminal domain and the ligand binding domain for agonist. The amino terminal domain shows sequence homology to bacterial leucine, isoleucine, valine-binding proteins (LIVBP), and presumably shares an evolutionary history with them (O'Hara et al., 1993; Stern-Bach et al., 1994). It has several subtle roles in oligomerization, desensitization, and membrane expression (Ayalon and Stern-Bach, 2001; Kuusinen et al., 1999; Leuschner and Hoch, 1999). Interestingly, in AMPA receptors, partial deletion of the ATD eliminates membrane expression whereas total deletion of it does not affect membrane expression, ligand binding, channel activation or desensitization (Pasternack et al., 2002). The ATD in NMDA receptors is involved in desensitization and binding of small molecules and zinc ions (Huggins and Grant, 2005). Bacterial GluR subunits lack a prominent ATD. Still, the receptor is targeted to the

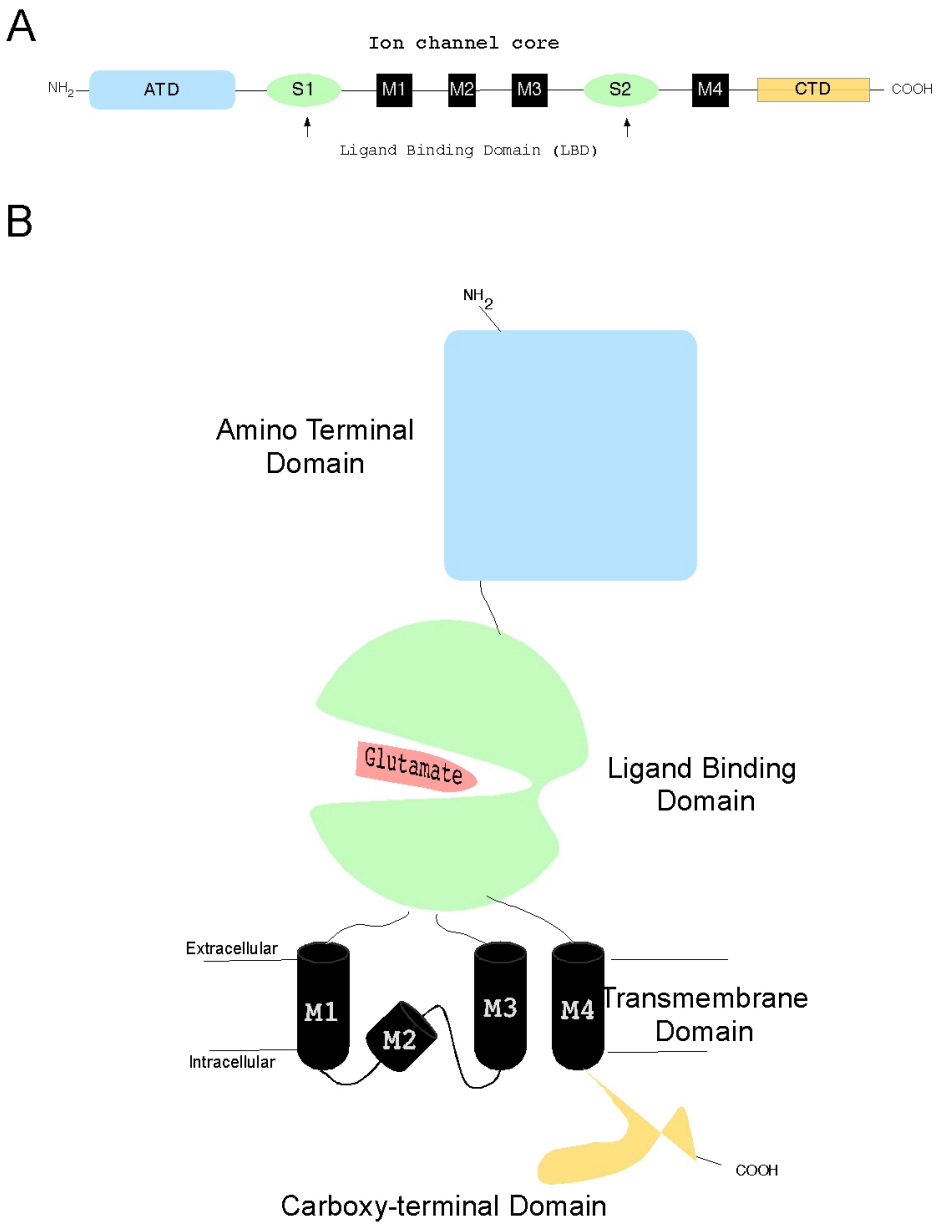

Figure 1-3 Schematic representation of an individual subunit of ionotropic GluR

A) GluR linear sequence: Amino Terminal Domain (ATD, light blue), Ligand Binding domain (LBD, green), ion channel (black) and C-terminal domain (CTD, gray)

B) Topology of an individual GluR subunit. Four such subunits come together to form a functional receptor. The amino terminal domain and the ligand binding domain are located in the extracellular space. The ion channel is at the plasma membrane. The carboxy-terminal domain is intracellular and has a regulatory activity. The various domains are not drawn to scale.

membrane. Electron microscopy reconstruction of AMPA receptors shows that the ATD orientation relative to each other and the membrane change according to the state (resting or desensitized) of the receptor (Midgett and Madden, 2008; Nakagawa et al., 2006; Oswald et al., 2007).

The ligand binding domain is formed by the region N-terminal to M1 (S1 lobe) and the M3-M4 extracellular loop (S2 lobe). It has an evolutionary relationship to lysine, arginine, ornithine-binding proteins (LAOBP, (O'Hara et al., 1993)) and will be considered in more detail below. The transmembrane domain has four hydrophobic regions M1, M2, M3 and M4 (Dingledine et al., 1999). However one of the hydrophobic segments, M2, does not span the membrane but rather is a reentrant pore loop (Figure 1-3). The other three segments (M1, M3 and M4) are considered to span the bilayer as α-helices (Wollmuth and Sobolevsky, 2004). M1 to M3 are thought to form the core of the ion channel and have structural homology and an evolutionary relationship to K^+ channels (Wo and Oswald, 1995). The C-terminal domain (CTD) of the protein is highly regulated and is thought to be responsible for intracellular interaction with proteins and trafficking of the protein to the plasma membrane (Kim and Sheng, 2004). It also contains numerous phosphorylation sites important for regulating channel activity (Chen et al., 2006). The M4 segment and the CTD are the only elements of a GluR that do not have identified evolutionary homologous domains yet (Wo and Oswald, 1995).

The modular organization of GluRs, especially for the ligand binding domain and the ion channel, has facilitated the study of their structure-function relationship.

Although all of the domains are essential for receptor function and diversity, I will focus mainly on the ligand binding domain and the ion channel.

1.4.1 Ligand Binding domain

As noted above, the ligand binding domain (LBD) is formed by two discontinuous peptide sequences, S1 and S2 which are separated from the core of the ion channel (M1, M2 and M3).

Isolated LBD, termed S1S2 construct, is the only domain of ionotropic GluRs for which there are presently high resolution structures. The structures were obtained by creating isolated, water soluble S1S2 constructs: The ATD and the M4 segment were removed and a GT linker between S1 and S2 replaced the M1 to M3 segment (Armstrong et al., 1998; Chen et al., 1998). This S1S2 construct retains ligand affinity, comparable to the intact receptors, when expressed separately of the ion channel (Kuusinen et al., 1995). Crystal structures of the LBD for non-NMDA and NMDA receptors have been solved. For the non-NMDA's crystal structures, the apo state (no ligand bound; Protein data bank (PDF) entry 1fto), antagonist (1lbc), partial agonist (1lbb, 1ftk) and full agonist bound (1ftj) conformations have been determined (Ahmed et al., 2008; Armstrong and Gouaux, 2000; Armstrong et al., 1998; Furukawa et al., 2005; Mayer, 2005). The bilobed structure of LBD (Domain 1 (D1) and Domain 2 (D2)) forms a conserved "clam shell-like domain" (Maier et al., 2007). Each lobe presents portions of S1 (domain 1) and S2

(domain 2) sequences (Armstrong et al., 1998). The domains are held together by two linker sequences analogous to the hinge region of periplasmic binding proteins (PBP (Kang et al., 1992)) (Figure 1-4).

The cleft between domains provides the binding site for agonist. Like the structural periplasmic binding proteins family members, the bilobular structure works like a Venus-flytrap-style cleft (Acher and Bertrand, 2005). Multiple primary polar residues from both lobes anchor agonist binding. Binding of full and partial agonists, like kainate, quisqualate, and willardiine derivatives, also takes place in the same coordination cleft (Armstrong and Gouaux, 2000; Jin et al., 2003). The cleft closes around 20º relative to the apo state with the agonist and 10-18º with partial agonist. Antagonist (like DNQX (Armstrong and Gouaux, 2000), cyclothiazide (CTZ; (Sun et al., 2002)) do not close the cleft but bind at different site in the structure. Comparison of the ligand binding pockets of the LBD suggests that the ligand binding mechanisms of GluR family may be conserved. The agonist selectivity is inherent to features of the AMPA, kainate and NMDA receptor binding pockets (Chen and Wyllie, 2006).

The structural mobility of the LBD facilitates binding and dissociation of agonist. Residues in the cleft that bind agonist display two types of motion (McFeeters and Oswald, 2002). The residues that interact with the gamma-constituents (C-5) of glutamate are mobile while the ones that bind the alpha substituents (C-1) have minimal

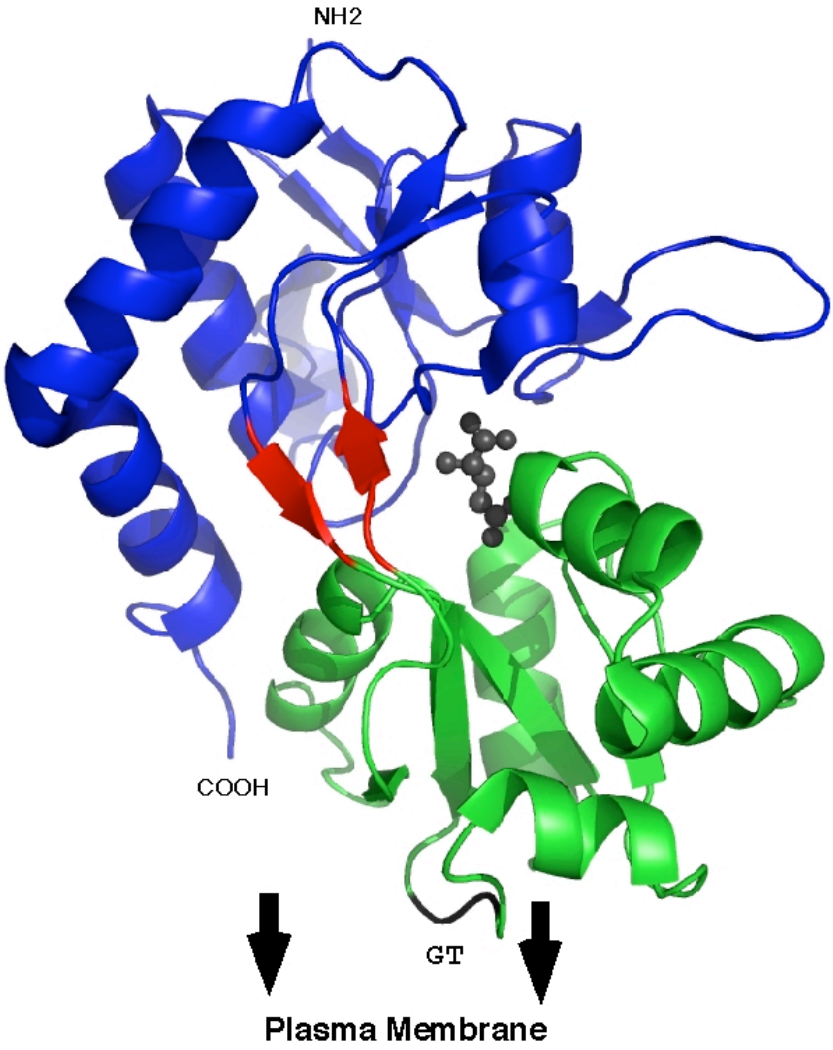

Figure 1-4 Ribbon presentation of the bilobular LBD of GluR2 (1FTJ)

The lobes are held together by a hinge (red) that in the apo state (1FTO) are expanded and contract upon ligand binding reducing the separation between domain 1 (blue) and domain 2 (green) of the LBD. In this structure the core of the ion channel (M1-M3) is replaced by a GT linker (black, glycine-threonine) (Armstrong and Gouaux, 2000).

internal motion. Two residues present at the hinge region show motions that indicate a degree of intervention during closing of the lobes concurrent with ligand binding. For dissociation, it is thought that the concerted motion of helix F (in domain 2) facilitates the reopening of the clamp.

Crystals of GluR-2 complex with AMPA are non-crystallographic symmetric dimers (Sun et al., 2002). The subunits present their N-termini distal to the plasma membrane and C-termini, proximal to the potential location of the ion channel (Figure 1-4). The dimer interface is mediated by domain 1 of the LBD. The interactions include specific amino-acids in the intersubunit contact area. Modification of these residues can alter the stability of the dimer. Mutations or chemicals that eliminate desensitization (Stern-Bach et al., 1998; Sun et al., 2002) modify the interface in a similar manner. An important finding is that the obtained crystals are symmetrical dimers involving residues in domain 1. This suggests that the tetrameric structure of GluRs are assembled from dimers of dimers. Contiguous S1S2 domains are linked by multiple electrostatic interactions present between domain 1 of subunits. Crystallographic studies suggest that the dimer-dimer interaction occurs by translation and rotation of one subunit over the second one. These interactions are located in a lateral interface that involves domain 1 and domain 2 structural features

1.4.1.1 Desensitization

GluRs desensitize in the continuous presence of Glutamate. During desensitization the receptor is in an inactive state although agonist is bound (Figure 1-5).

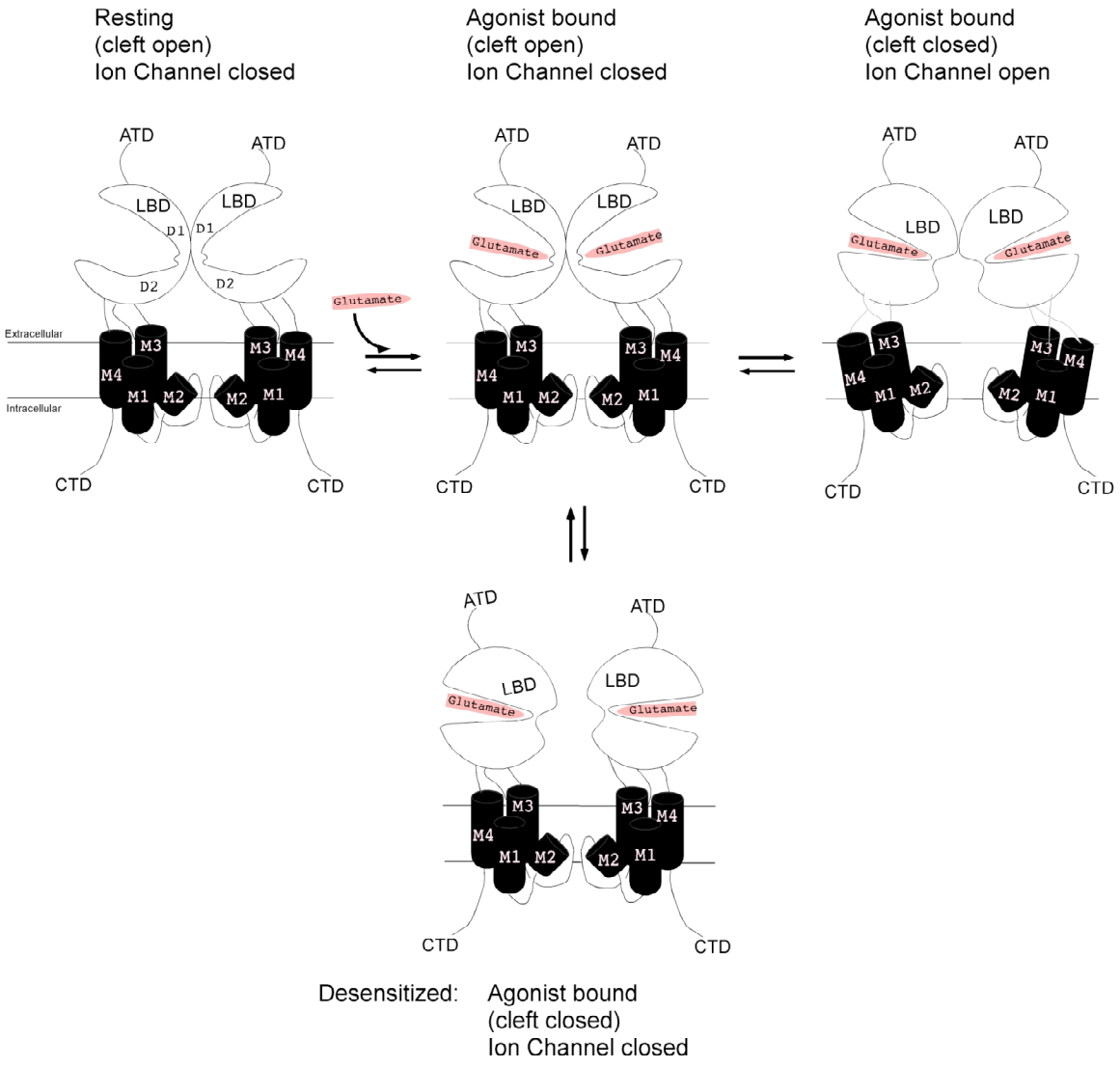

Figure 1-5 A model of GluR function

In the resting state, the dimer of LBD is held together by interactions between domain 1 interfaces. When glutamate binds to the cleft, movements of the domain 2 (D2) accompany the closing of the LBD. The structural changes experienced in the LBD are transduced into opening of the ion channel. The receptor enter the desensitize state when domain 1 interaction of the dimeric LBD are disrupted. ATD and CTD have been removed for clarity.

Desensitization is a complex phenomenon that is influenced by several domains of GluRs. ATD (Krupp et al., 1998), LBD, flip/flop alternative splicing and CTD have different effects on desensitization. Many regions affect desensitization in different degree, but all may contribute to the phenomenon.

One explanation of how the desensitization process occurs comes from the structural model of the LBD. The LBD of GluRs form dimers with a stable intradimer interface (Domain 1). Mutations that affect the interface, like L479Y (GluR-A or L483Y for GluR-B), reduce desensitization. This effect is also observed with the allosteric modulator CTZ that block desensitization by promoting dimerization of the subunits through domain 1 interactions (Sun et al., 2002; Weston et al., 2006; Zhang et al., 2006). Perturbations that destabilize the dimer interface of LBD affect desensitization. Rearrangements of the dimer interface disconnect the LBD from the ion channel producing desensitization.

1.4.2 Ion Channel

The general elements forming the ion channel of GluRs are known (Wollmuth and Sobolevsky, 2004), though high resolution structures of the intact receptor (LBD and ion channel) or of the ion channel itself have not been elucidated. However, there is strong evidence that the core of the ion channel (hydrophobic segments M1-M3) is structurally homologous to K^+ channels (Wo and Oswald, 1995), for which crystal

structures do exist (Doyle et al., 1998). The bacterial K^+ channel KscA, as the prototype for P-loop ion channels, is tetrameric, with the four subunits surrounding the central or water-filled pore. Each subunit consists of two transmembrane helices (TM1 and TM2) and a pore forming P loop (MacKinnon, 2003) (Fig. 1-6, left panel).

Prokaryotic GluRs are considered evidence of the missing link between K^+ and mammalian glutamate receptors (Chen et al., 1999). In prokaryotic GluRs, the ion channel has a similar architecture to K^+ channels, but inverted in the membrane 180°, placing the P-loop on the intracellular rather than the extracellular side of the membrane (right panel in Figure 1-6). In prokaryotic glutamate. receptors (GluR0), as well as in eukaryotic glutamate receptors, the core ion channel region is formed by M1, M2 and M3 hydrophobic segments, with M2 homologous to the K^+ channel P loop (Arinaminpathy et al., 2003). Homologous to TM2 in K^+ channel, the transmembrane M3 of GluRs is α-helical in structure. It is a major pore-lining domain and is extensively involved in channel gating (for a review see Wollmuth and Sobolevsky, 2004). Few studies have addressed the structural or functional significance of the M1 segment.

In contrast to K^+ channels and prokaryotic GluRs, all mammalian GluR subunits have an additional hydrophobic segment, the M4 segment, located C-terminal to the core of the ion channel. The function of this unique transmembrane segment is unknown. One function for the M4 segment is to attach the highly regulated C-terminus (Mori et al., 1998) to the core of the ion channel. However, the M4 is necessary for channel function.

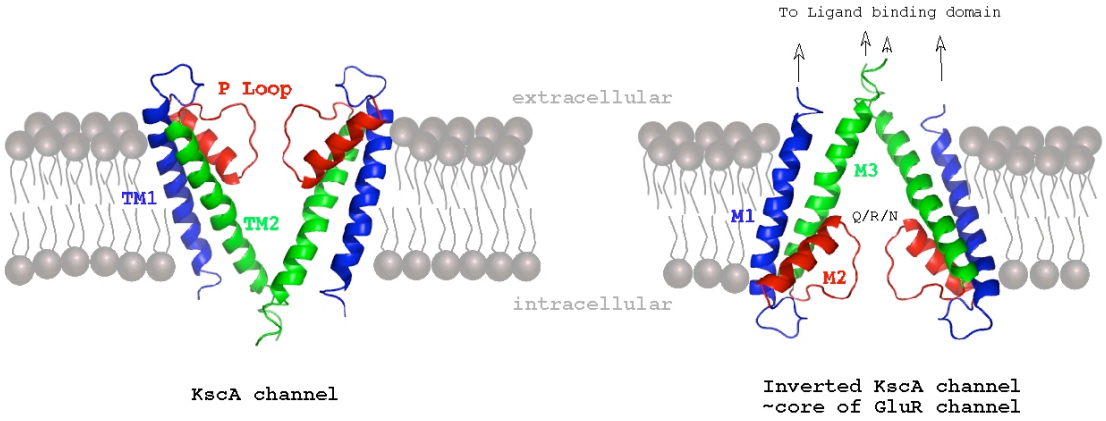

Figure 1-6 Structural relationship between the K^+ and GluR ion channel

Crystal structure of the KscA K^+ channel (1bl8) (Doyle et al., 1998) in its proper orientation (left panel) and flipped 180 ° in the membrane (right panel). For both panels, only two of the four subunits are shown with the front and back subunits removed for clarity. Homologous segments in the K^+ and GluR channels are shown in the same colors. In GluRs, the functionally critical Q/R/N site is positioned at the tip of the M2 loop (Kuner et al., 2001; Kuner et al., 1996).

Specifically, previous studies with the NMDA receptor have shown that the removal of M4 results in non-functional channels (Schorge and Colquhoun, 2003). My data with AMPA receptors show a similar dependence on the presence of M4 for function. However, these effects may reflect protein trafficking or structural changes in the protein that either directly or indirectly modify gating. The major goal of my thesis is to define the structural and functional significance of the M4 transmembrane segment to mammalian glutamate receptors.

1.4.2.1 Ion Channel Pore

The cation selectivity of GluRs requires a wider pore than the K^+ channel. Measurements of the extracellular M3 portion of the pore indicate a diameter of more than 8.5 Å (Sobolevsky et al., 2004) (Figure 1-7). Measurements of the pore of the ion channel suggest that heteromeric AMPA receptors have a pore diameter of 7 Å in the region of the M2 loop when the channel is open (Burnashev et al., 1996). Thus ions enter a funnel that may accommodate hydrated or partially hydrated ions that pass through a pore that is significantly wider than that of the K^+ channel channel (KcsA) (Doyle et al., 1998).

1.4.2.2 Channel Gating

Agonist binding closes the cleft of the LBD and conformational changes of this domain are transduced into channel opening (Figure 1-6).

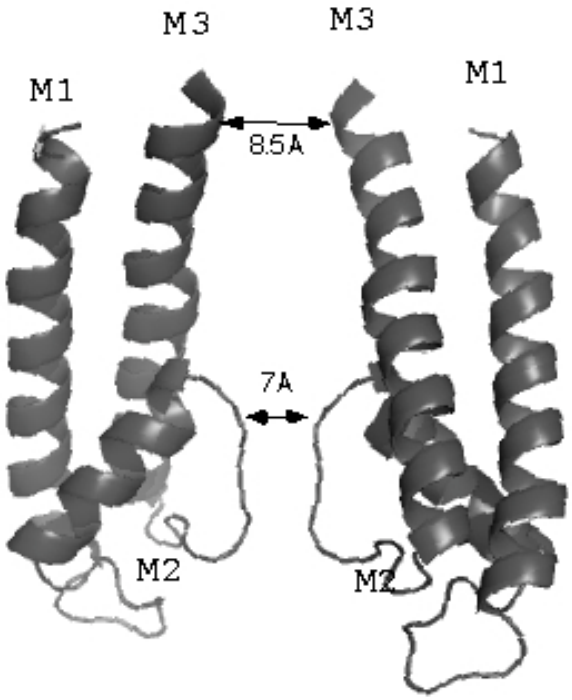

Figure 1-7 Putative pore region of Glutamate Receptors

Structure of KscA potassium channel is used as a template (18bl). Intersubunit distances have been modified to accommodate GluR model.

During gating of the ion channel the extracellular ends of M3, the major transmembrane α-helix lining the pore, are thought to follow the general movements of the LBD dimer (Sobolevsky et al., 2004). Binding of glutamate to the LBD, closes the lobes of the LBD, and opens the pore of the ion channel. During binding, distances between LBD dimers increase (Armstrong and Gouaux, 2000; Sun et al., 2002) and are thought to correlate with the expansion of the pore. The expansion of the pore may be due to increasing intersubunit distances. The M2-loop and M3 transmembrane α-helix clearly participate in this process. What is not clear is the contribution of other transmembranes α-helices to channel gating. Considering the homology to K^+ channels, we might expect that the M1 transmembrane follow the M3 in the movement during gating (Perozo et al., 1999). Less clear is the part that the M4 segment plays in this concerted event.

GluRs are expected to have a four-fold symmetry like the K^+ channels. The LBDs are dimers of dimers (Sun et al., 2002) and this two-fold symmetry is maintained in the outer part of the pore of the ion channel by the M3 transmembrane (Sobolevsky et al., 2004). It is thought that four-fold symmetry begins deep into the pore, where the M2 loop is located. Nevertheless, there is increasing evidence that suggests that the four-fold symmetry observed in K^+ channels is not maintained in GluRs (Mayer, 2006).

CHAPTER TWO

Methods

2 METHODS

The following experimental methods were used for the experiments contained in Chapters 3 and 4.

2.1 Mutagenesis and expression

All experiments were performed with previously described expression constructs for wild type rat AMPAR subunits (Burnashev et al., 1992), which were named following the nomenclature of Seeburg (Seeburg, 1993). AMPAR subunits were always in the flip splice variant form. Numbering of amino acids is for the mature protein.

Truncated AMPAR subunits, polyleucine replacements, site-directed mutations, and glycine insertions were made in and around the M4 segment of the GluR-A (GluR1) subunit. For oocyte expression, we used as a reference and as a background a construct where a leucine in the ligand binding domain was substituted with a tyrosine [GluR-A(L479Y)]. For wild type channels, this construct is essentially non-desensitizing (Stern-Bach et al., 1998) (see also Schmid et al., 2007). For simplicity, especially for constructs with additional substitutions, we refer to GluR-A(L479Y) as GluR-A'. Point mutations and insertions were generated using the QuickChange site-directed mutagenesis kit

(Stratagene, La Jolla, CA). Mutations were initially made in a pSP64T-derived vector. After the introduction of the mutation, a fragment encompassing it was subcloned back into a wild-type template either in the pSP64T-derived vector or in a pRK eukaryotic expression vector. We sequenced all constructs over the entire length of the subcloned fragment.

We generated deletions of the M4 segment (and the C-terminal domain) by replacing the valine codon, the initial position in the M4 segment (Boulter et al., 1990; Keinanen et al., 1990), with a stop codon (TGA). For GluR-A this corresponds to Val788 with the construct referred to as GluR-A(V788stop) or GluR-A-ΔM4 (or GluR-A'-ΔM4 when in the non- desensitizing background). This construct includes the entire S2-M4 linker. C-terminal domain deletion (CTD) (GluR-A-ΔCTD) was made by introducing a stop codon (ATA) at position 815 (Ser815) (GluR-A(S815stop)). This construct includes five amino acids after the end of M4.

We generated tandem constructs to study subunit arrangement and gating in transmembrane proteins. We generated a construct for AMPARs placing the GluR-A'-ΔM4 in an open reading frame with GluR-A' (GluR-A'-ΔM4/GluR-A'). Comparable to the tandem generated by Schorge and Colquhoun (Schorge and Colquhoun, 2003) with NMDARs.

cRNA was transcribed for each expression construct using SP6 RNA polymerase (Ambion Inc., Austin, TX) and examined electrophoretically on an agarose gel.

Concentration and purity were determined by UV spectroscopy using a SmartSpec™300 Spectrophotometer (Bio-Rad, Hercules, CA).

Wild type and mutant AMPAR subunits were expressed in *Xenopus laevis* oocytes and/or human embryonic kidney 293 (HEK 293) cells. Oocytes were treated as described (Sobolevsky et al., 2002; Stuhmer, 1998; Wollmuth et al., 1996) and were maintained in a nutrient OR-3 medium containing 50% L-15, 50 mg/ml penicillin-streptomycin, 5 mM glutamine, and 15 mM NaHEPES (all Gibco BRL, Grand Island, NY) (pH 7.2, NaOH) as well as in CNQX (25 μM). Unless otherwise noted, wild type constructs including GluR-A(L479Y) were injected at 0.01 μg/μl (~0.5-0.8 ng mRNA per oocyte) whereas all mutants constructs at least initially and unless otherwise noted were tested at 0.1 μg/μl (~5-8 ng of mRNA per oocyte). Recordings were typically made two to five days after injections.

HEK 293 cells were transfected with GluR subunits using FuGene 6 (Roche, Indianapolis, IN). A vector for enhanced green fluorescent protein (pEGFP-C1, Clontech, Palo Alto, CA) was co-transfected at a ratio of 1:9 (pEGFP-C1:GluR subunit). Recordings were typically made one to three days after transfection.

2.2 Current Recordings and Data Analysis

2.2.1 *Xenopus* oocytes recordings

Membrane currents in *Xenopus* oocytes were recorded at room temperature (20-23°C) using a two-electrode voltage-clamp (DAGAN TEV-200A, DAGAN Corp., Minneapolis, MN) with Cell Works software (*npi* electronic, Tamm, Germany). Microelectrodes were filled with 3 M KCl, and had resistances of 1-4 MΩ. To maximize solution exchange rates, we used a narrow flow-through recording chamber with a small volume of ~70 μl. The external solution consisted of (mM): 115 NaCl, 2.5 KCl, 0.18 $CaCl_2$, and 5 HEPES (pH 7.2, NaOH). All reagents, including glutamate (typically 1 mM), were bath applied.

2.2.2 HEK 293 recordings

Currents in the whole-cell mode or outside-out patches, isolated from HEK 293 cells, were recorded at room temperature (20-23°C) using an EPC-9 amplifier with Patchmaster software (HEKA Elektronik, Lambrecht, Germany), low-pass filtered at 2.9 kHz (-3 dB) with an 8 pole low pass Bessel filter and digitized at 10 kHz. Pipettes had resistances of 2-5 MΩ when filled with the pipette solution and measured in the standard Na^+ external solution. We did not use series resistance compensation nor did we correct for junction potentials.

For HEK 293 cell recordings, external solutions were applied using a piezo-driven double barrel application system. One barrel contained the external solution while the

other barrel contained the same solution with added glutamate (5 mM). To optimize solution exchange for fast agonist application, we briefly treated the tips of the theta glass with hydrofluoric acid to reduce the thickness of the septum. At the end of such experiments, the outside-out patch was blown off, and the open tip response was recorded. We included in the final analysis only those patches where the 10-90% rise time was <350 μs.

Our standard internal (pipette) solution consisted of (mM): 105 K-gluconate, 30 KCl, 10 HEPES, 10 phosphocreatine, 4 Mg-ATP and 0.3 GTP, pH 7.3 (KOH). The standard external solution consisted of (mM): 140 NaCl, 10 HEPES, 1.8 $CaCl_2$, and 1 $MgCl_2$, pH 7.2 (NaOH). We also tested a high K^+ containing external solution (in mM): 100 NaCl, 50 KCl, 10 HEPES, 1.8 $CaCl_2$, and 1 $MgCl_2$ pH, 7.2 (NaOH) [Chen, 1999 #1520]. Unless otherwise noted, all chemicals were obtained from Sigma (St. Louis, MO) or J.T. Baker (Phillipsburg, NJ).

2.3 Protein Chemistry

2.3.1 Biotinylation of cell surface proteins

Oocytes injected with 5-7 ng of mRNA were used 48 hours after injection. Ten oocytes were mechanically devitinilized while mantained for 20 min in a hypertonic solution (in mM): 200 K-Aspartate, 20 KCl, 5 EGTA, and 10 HEPES (pH 7.4, KOH). The oocyte plasma membrane was biotinylated with 1.5 mg/ml Sulfo-NHS-SS-Biotin

(Pierce, Rockford, IL) according to manufacturer instructions. Intact oocytes were incubated in the reagent for 30 min and washed with 100 mM glycine. Biotinylated oocytes were solubilized in 150 mM NaCl, 20 mM Tris-HCl, pH 7.6, 1% Na-Deoxycholate, 1% Triton X-100 (v/v), Protease inhibitor cocktail and 1% Nonident P40 (the last three chemicals from Roche, Palo Alto, CA). The biotin-labeled proteins were recovered overnight from the supernatant fractions using Ultralink immobilized NeutrAvidin protein Plus (Pierce). After wash, the beads were incubated in 50 mM DTT for 2 hours at room temperature to cleave the disulfide bond in the spacer arm of the biotin reagent. The proteins were separated in discontinuous SDS-PAGE gels run under reducing conditions (Laemmli, 1970).

2.3.2 Immunoblot

Proteins were transferred from the gel to 0.45 mm nitrocellulose membranes by semi-dry transfer (BioRad, Hercules, CA) using Bjerrum-Schaffer-Nielsen Buffer (Bjerrum and Schafer-Nielsen, 1986). Blots were blocked and incubated with primary antibodies overnight. The antibodies used were anti-(ATD)GluR-A (or GluR1(E6) which is directed against the N-terminal domain (ATD); sc-13152, Santa Cruz Biotechnologies, Santa Cruz, CA), anti-Na^+/K^+-ATPase β (sc-25709, Santa Cruz Biotechnologies), and anti-β-Tubuline (Axyll-H8481, Accurate Chemical & Scientific corporation, Westbury, NY). Blots were washed prior to incubation with HRP-conjugated goat anti-mouse (sc-2302) or HPR conjugated goat anti-rabbit (sc-2030) and were developed using western

blot luminol reagent (sc-2048, all reagents Santa Cruz Biotechnologies) before exposure to chemiluminescence Biomax Film (Kodak, Cedex, France).

Signal quantification of the western blot was done by scanning the films using an EPSON flat scanner (Epson Perfection V700 Photo) in an 8 bit gray scale mode, 1200 dpi, and quantified using NIH image J (1.38x) on a Mac OS X platform. GluR protein levels were expressed relative to a loading control either Na^+/K^+ ATPase β subunit (membrane expression) or β-tubulin (total expression). It was calculated as:

$$\rho_{\text{anti-(ATD)GluR-A}} / \rho_{\text{loadingcontrol}}$$

where ρ is the measured density of a defined region, expressed in arbitrary units (AU), for the N-terminal GluR-A antibody (anti-(ATD)GluR-A) or the loading control, either anti-Na^+/K^+-ATPase β or anti-β-Tubuline.

2.3.3 Immunocytochemistry

Transfected HEK 293 cells were incubated at 4ºC with anti-(ATD)GluR-A followed by conjugated Alexa Fluor® 594 goat anti-mouse or Alexa Fluor® 546 goat anti-mouse (A11005, Invitrogen, Carlsbad, CA). During the last wash a nuclear stain was done with [3 nM] 4',6-diamidino-2-phenylindole, dihydrochloride (DAPI) (Invitrogen, Carlsbad, CA). Cells were examined using an upright microscope Axio Imager Z1 with an Axiocam MR3 (Carl Zeiss, Jena, Germany) or a Zeiss LSM510 confocal laser scanning microscope.

2.4 Electrophysiology Experimental Protocols

2.4.1 Kinetics

To determine the rate and extent of desensitization, we rapidly applied glutamate for 100 ms at –60 mV to outside-out patches excised from HEK 293 cells. Time constants of desensitization (τ_{des}) were determined by fitting the current decay with a single exponential function. The extent of desensitization was based on the steady-state (I_{ss}) and peak (I_p) current amplitudes and calculated as the percent desensitization:

$$(\%_{des} = 100 \times (1 - (I_{ss}/I_p)).$$

2.4.2 Glutamate Concentration Dependance

Concentration-response curves were measured in *Xenopus* oocytes using GluR-A' as a reference. Solutions containing various concentrations of glutamate (1.3 μM to 3 mM) were applied to cells held at –60 mV. Current amplitudes normalized to the maximal response were plotted as a function of concentration and fitted with the Hill equation, $1/(1 + (EC_{50}/[Glu])^n)$, where EC_{50} is the concentration to achieve half-maximal response and *n* is the Hill coefficient.

2.4.3 Substituted cysteine accessibility method (SCAM)

AMPAR cysteine-substituted mutant channels were probed from the extracellular side of the membrane with the positively-charged methanethiosulfonate (MTS) reagent 2-(trimethylammonium)ethyl MTS (MTSET). MTSET was purchased from Toronto

Research Chemicals, Inc. (Ontario, Canada) and was prepared, stored, and applied as described (Sobolevsky et al., 2002).

2.4.3.1 Steady-State Reactions

Steady-state reactions were quantified at –60 mV. Baseline agonist-activated current amplitudes (I_{pre}) were established by three to five consecutive 15 to 20 s applications of glutamate separated by 60 to 120 s washes in glutamate free solution. Subsequent to the last wash, MTSET (2 mM) was applied for 60 s either in presence of agonists or in their absence (but in the presence of CNQX). After the MTSET exposure, current amplitudes (I_{post}) were determined again using three to five agonist applications. The change in the agonist-activated current amplitude, expressed as a percentage (% change), was calculated as:

$$\% \text{ change} = (1 - I_{post}/I_{pre}) \times 100$$

The steady-state change in the leak current amplitude, expressed as a percentage (Δ leak), was calculated as:

$$\Delta \text{ leak} = ((I_{leak\_pre} - I_{leak\_post}) / (I_{pre} + I_{leak\_pre})) \times 100$$

where I_{leak_pre} and I_{leak_post} are the leak current amplitudes before and after the MTS reagent application, respectively. Although this equation is not necessarily intuitive, we used it in this form since inhibition and potentiation of glutamate-activated currents (% change) and decreases and increases in leak current (Δ leak) are given the same positive and negative signs, respectively.

2.5 Statistical Analysis

For statistical analysis, we used Igor Pro (WaveMetrics, Inc., Lake Oswego, OR) and Microsoft Excel (Redmond, WA). Results are reported in the text as mean ± SEM and shown graphically as mean ± 2*SEM. An ANOVA or a Student's t-test was used to define statistical differences. The Tukey test was used for multiple comparisons. Significance was assumed if $P < 0.05$.

2.6 Dissertation outline

This thesis describes biochemical and electrophysiological data used to determine the structural and functional significance of the additional transmembrane segment, the M4, in mammalian glutamate receptors. Chapter 2 explains the molecular biology methods to generate the clones, the electrophysiological determination of the mutants and the biochemical techniques to confirm the data. Chapter 3 presents the effect that M4 deletion has on mammalian glutamate receptors. Chapter 4 describes the requirement of M4 interactions with other transmembrane segments for receptor function. Finally chapter 5 presents the general discussion of this study and evolutionary and therapeutics point of view for the M4 transmembrane segment.

CHAPTER THREE

AMPA Receptors Require the Additional Transmembrane Segment for Glutamate Activated Currents

3 AMPA receptors require the additional TM segment for glutamate-activated currents

3.1 Introduction

Fast excitatory neurotransmission in the brain and spinal cord is mediated primarily by ionotropic glutamate receptors (GluRs) notably N-methyl-D-aspartate (NMDA), α-amino-3-hydroxy-5-methyl-4-isoxazolepropronic acid (AMPA), and kainate (KA) receptor subtypes (Dingledine et al., 1999). GluR subtypes as well as subunits within a subtype share common structural features including membrane topology and stoichiometry (Madden, 2002; Mayer, 2006; Oswald et al., 2007; Paoletti and Neyton, 2007; Wollmuth and Sobolevsky, 2004; Yamakura and Shimoji, 1999), but they show distinct molecular and functional properties that subserve many of their unique biological contributions to synaptic physiology.

As discussed previously in the general introduction, GluR subunits are modular (Mayer, 2006; Oswald et al., 2007) being composed of four presumably evolutionarily distinct domains: an amino-terminal domain (ATD), a ligand-binding domain (LBD), a membrane domain (hydrophobic segments M1–M4), and a cytoplasmic carboxy-terminal domain (CTD) (Figure 1-3). The amino-terminal domain and the ligand-binding domain (S1 & S2 lobes) share a high sequence similarity to certain bacterial periplasmic binding proteins (Nakanishi et al., 1990; O'Hara et al., 1993). The central core of the ion

channel—hydrophobic segments M1-M3—share a limited but notable sequence similarity to pore loop channels such as K^+ and cyclic-nucleotide gated channels as well as a common membrane topology albeit being inverted 180° in the plane of the membrane (Wo and Oswald, 1995; Wood et al., 1995; see also Kuner et al., 2003). The evolutionary precursors to the M4 segment and the carboxy-terminal domain are unknown (Wo and Oswald, 1995).

In terms of function, GluRs also show some degree of modularity. The amino-terminal domain participates in subunit recognition and various gating and allosteric functions (e.g., Ayalon and Stern-Bach, 2001; Gielen et al., 2008; Oswald et al., 2007), yet its removal has only minor effects on expression and function (Pasternack et al., 2002). Similarly, the C-terminal domain which is critical for regulation of expression, distribution and function of GluRs (e.g., Derkach et al., 2007) can also largely be removed (deletion of 52 of 81 residues) while leaving basic properties intact (Suzuki et al., 2005). The ligand-binding domain also functions as a soluble protein (S1S2 construct) independent of other domains (Arvola and Keinanen, 1996). Indeed, this soluble S1S2 construct has been crystallized (Armstrong et al., 1998; Furukawa et al., 2005; Mayer, 2005; Sun et al., 2002) and has proven quite predictive of the activity of the intact receptor (e.g., Mayer, 2006).

A more complicated picture emerges when considering the ion channel itself. Clearly, the ion channel core (M1-M3) is structurally homologous to inverted pore loop channels, and two transmembrane K^+ channels, such as KcsA and inward rectifiers, can

function independent of any other structural elements (e.g., Yellen, 1999). Supporting this relationship is the "two-transmembrane" prokaryotic GluR subunit, GluR0, that is functional and has K^+ selectivity (Chen et al., 1999). GluR0 however displays very slow gating kinetics compared to mammalian GluR subtypes (Figure 3-1). In addition, there is not great functional compatibility between K^+ channels and GluR subtypes (Hoffmann et al., 2006a; Hoffmann et al., 2006b). Perhaps more surprising, the additional transmembrane segment M4 appears to be required for function, at least for NMDA receptors (Schorge and Colquhoun, 2003). Specifically, in truncated NMDA receptor subunits lacking M4, no glutamate-activated current could be detected though functional channels could be generated if these truncated subunits were co-expressed with an independently encoded M4 segment. These results suggest that in contrast to two-transmembrane K^+ channels and the prokaryotic GluR0, mammalian GluRs require an additional transmembrane segment to function but the basis for this effect—whether a trafficking, structural or gating action—is unknown.

We generated a truncated form of AMPA receptor subunits lacking the M4 segment and find that these subunits are not functional but are expressed on the membrane surface indicating that the lack of functionality is not due to trafficking or a biosynthesis defect. We also looked at several other general features of M4 including an independently encoded M4 as well as the use of truncated receptors as tandems.

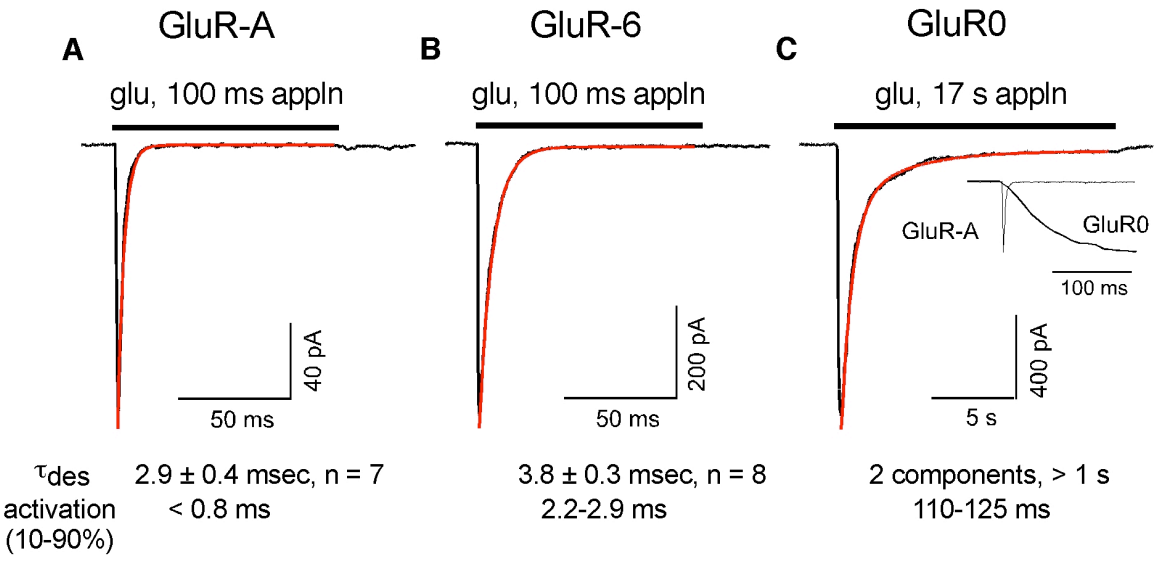

Figure 3-1 The Bacterial glutamate receptor GluR0 shows slow gating kinetics compared to mammalian glutamate receptor subunits

Currents recorded from outside-out patches in response to fast glutamate applications. Patches were isolated from HEK-293 cells transfected with GluR-A (A), GluR-6 (B) or GluR0 (C). Currents were elicited by either a 100 msec (A & B) or a 17 sec (C) application of glutamate (5 mM, solid bar). The red line through the data points is a single exponential fits. Below the current recordings are the mean values for the onset of desensitization (τ_{des}) and approximate values for activation (10-90% rise times). Inset to (C), currents for GluR-A and GluR0 on an expanded time scale showing the extremely slow activation of GluR0.

3.2 Results

To investigate the functional and structural significance of the additional transmembrane segment to mammalian GluRs, we used the AMPA receptor subunit GluR-A in the 'flip' form as a reference mainly because it functions as a homomultimer and expresses robustly, in a wild type form, in heterologous expression systems.

3.2.1 AMPA receptors require the additional TM segment for glutamate-activated currents

Figure 3-2 shows membrane currents for a *Xenopus* oocyte injected with mRNA for the non-desensitizing GluR-A(L479Y) or GluR-A'. As expected, glutamate-activated current amplitudes were robust, typically on the order of several mA (Table 3-1). HEK 293 cells transfected with wild type GluR-A similarly showed large glutamate-activated currents (Figure 3-1). In contrast, GluR-A subunits lacking M4 did not show any detectable glutamate-activated current either in *Xenopus* oocytes (Figure 3-2B), where the non-desensitizing background was used (GluR-A'-ΔM4), or in HEK 293 cells (Figure 3-1) where the wild type background was used (GluR-A-ΔM4). In oocytes injected with GluR-A'-ΔM4, glutamate-activated currents were not seen 2-7 days after injection nor did high glutamate concentrations (10 mM), kainate (30 mM) or cyclothiazide (CTZ, 30 μM) restore functionality. Similarly, in HEK 293 cells transfected with GluR-A-ΔM4, we did not detect glutamate-activated currents using fast agonist application either in the

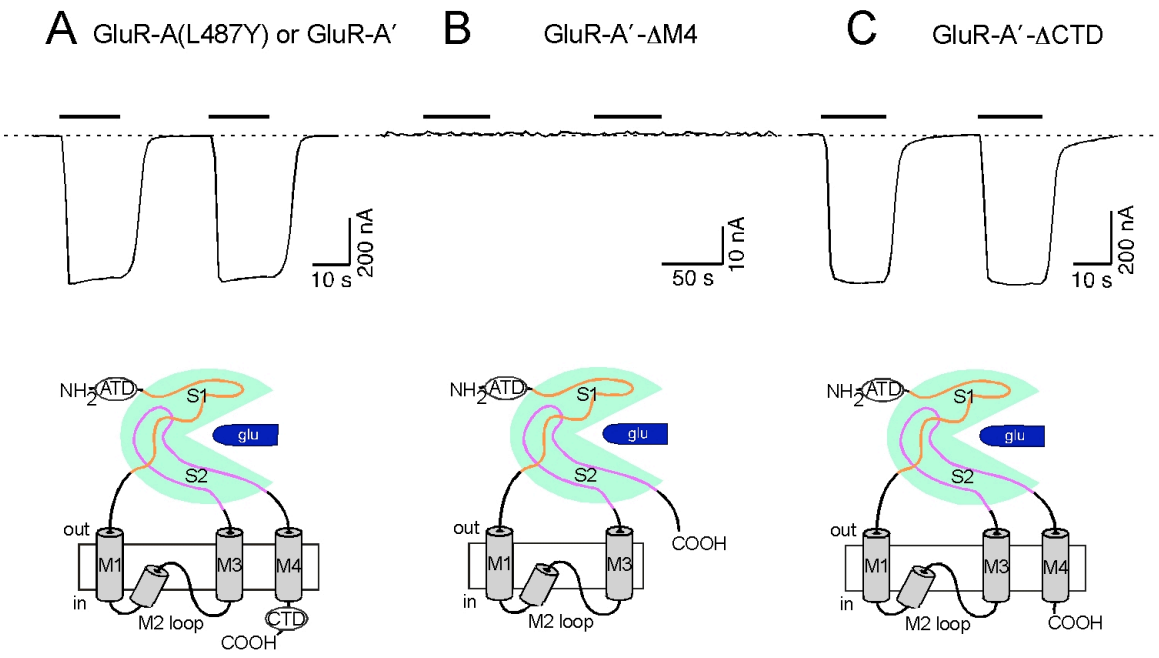

Figure 3-2 The M4 segment in AMPA receptors is required for glutamate-activated currents

Upper panels, Whole-cell currents recorded in Xenopus oocytes injected with mRNAs based on the AMPA receptor subunit GluR-A, in the flip form, containing a leucine-to-tyrosine (L479Y) substitution [GluR-A(L477Y) or GluR-A'] that blocks desensitization (Stern-Bach et al., 1998). Dashed lines indicate zero current that was based on current amplitudes before the glutamate application (thick solid lines, 1 mM, 15 to 60 secs in duration). Holding potential (Vh) was –60 mV. Lower panels, Schematics of presumed membrane topology of individual subunits of injected mRNA: (A) GluR-A'; (B) GluR-A'- with a stop codon introduced at the first position in M4 [GluR-A'(V788stop) or GluR-A'-ΔM4]; (C) GluR-A'- with a stop codon at position 815 just after M4 [GluR-A'(S815stop) or GluR-A'-ΔCTD]. GluR-A' was injected at ~0.7-0.8 ng mRNA total whereas truncated constructs at ~7-8 ng mRNA total.

Table 3-1 Functional properties of wild-type and truncated forms of the AMPA receptor GluR-A subunit expressed in *Xenopus* oocytes or HEK 293 cells.

Construct	I (nA)	n	EC50 *(μM)*	*Hill*	n
Xenopus oocytes					
GluR-A'	-1650 ± 75	15	--	--	
A'-ΔM4	nd	>20	--	--	
GluR-A'	-2190 ± 90	11	4.5 ± 0.3	1.5 ± 0.1	5
A'-ΔCTD	-2090 ± 150	10	4.6 ± 0.3	1.5 ± 0.1	4
	I (pA)	n	I_{leak} *(pA)*	τ_{des} *(ms)*	*%des*
HEK 293 Cells					
GluR-A	-3010 ± 170	11	-160 ± 10	--	
A-ΔM4	nd	11	-150 ± 10	--	
GluR-A + Stargazin	-6850 ± 1480	5	-310 ± 40	--	
A-ΔM4 + Stargazin	nd	5	-150 ± 15	--	
GluR-A (outside-out)	-71 ± 7	4	--	2.3 ± 0.1	>99%
A-ΔCTD (outside-out)	-15 ± 2	8	--	2.6 ± 0.1	>99%

Peak glutamate-activated currents (I) for wild type subunits were measured during the same injection/transfection cycles as corresponding truncated GluR-A subunits. Each construct was also expressed on at least 3 different injection or transfection rounds. EC_{50} is the concentration at half-maximal activation and *Hill* the Hill coefficient (see Experimental Methods).
Values shown are mean ± SEM. *nd*, no glutamate-activated currents detected.

presence or absence of CTZ or at extreme potentials (-150 or +150 mV) either in our standard external solution or in a solution high in external K^+ that yields currents in the two-transmembrane GluR0 (Chen et al., 1999) (Figure 3-1). Co-expression of GluR-A-ΔM4 with Stargazin (γ2) (e.g., Tomita et al., 2005) also did not restore functionality. Finally, leak currents did not show significant differences between wild type and ΔM4 transfected cells (Table 3-1) suggesting no notable constitutive current. Hence, for functionality, AMPA receptors require the M4 segment in a manner presumably similar to NMDA receptor subunits (Schorge and Colquhoun, 2003). Therefore, although kainite receptors have not been tested, it seems likely that the presence of M4 is a requirement for functionality in all mammalian GluRs.

The ΔM4 construct lacks not only M4 but also the carboxy-terminal domain (CTD) that is critical for regulating GluR expression (e.g., Derkach et al., 2007). Partial deletion of the CTD in GluR-A, leaving 29 amino acids after M4 including a PKA site, has little effect on its expression or function (Suzuki et al., 2005). To verify this point, we generated a construct where even more of the CTD was deleted, placing a stop codon at position 815 (GluR-A'-ΔCTD or GluR-A-ΔCTD), five amino acids after M4. The amplitude of glutamate-activated currents for GluR-A'-ΔCTD (Figure 3-2C & Figure 3-3A) as well as general gating properties such as concentration-response curves (Figure 3-3B & Figure 3-3C) and rates of entry into desensitization (Table 3-1) were comparable to wild type. Hence, while the CTD is critical for GluR trafficking, in our expression system its absence does not underlie the non-functional phenotype for the ΔM4 constructs.

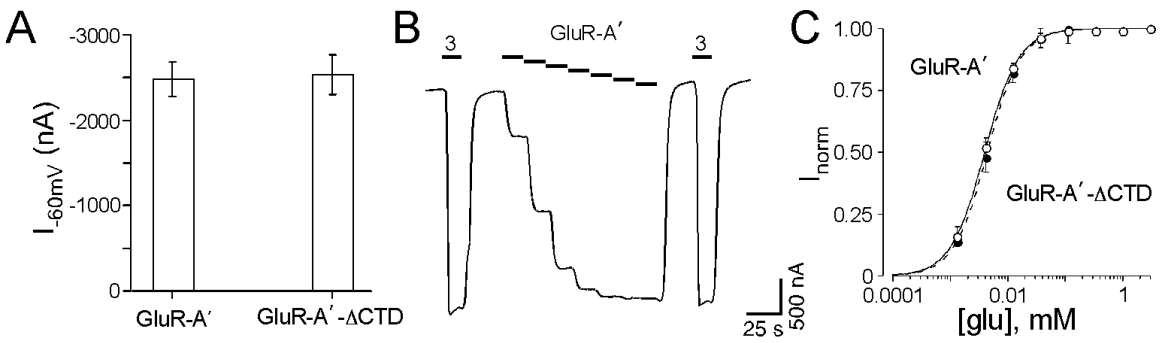

Figure 3-3 GluR-A lacking CTD does not show altered functional properties

Heterologous expression in *Xenopus* oocytes of GluR-A-L487Y (GluR-A') or GluR-A'-ΔCTD mutants.

(A) Mean current amplitudes (± 2*SEM) for GluR-A' or GluR-A'-ΔCTD (n > 10).

(B) Whole-cell currents recorded in a *Xenopus* oocyte injected with GluR-A'. Glutamate applications (solid bars) were at 3 mM (outer solid lines) or between 0.0013 and 1 mM (staggered lines).

(C) Concentration-response curves for GluR-A' (open circles) or GluR-A'-ΔCTD (solid circles). Current amplitudes, as in (E), were normalized to those in 3 mM glutamate. Points were fit with the Hill equation (see Methods) yielding EC_{50}s and Hill coefficients of 4.5 ± 0.3 μM & 1.5 ± 0.1 μM (mean ± SEM) for GluR-A' (n = 5) and 4.6 ± 0.3 μM & 1.5 ± 0.1 μM for GluR-A'-ΔCTD (n = 4).

3.2.2 ΔM4 constructs express in the membrane

The absence of functionality or glutamate-activated currents for the ΔM4 constructs could reflect that M4 is an essential component of the biosynthesis or trafficking of mammalian GluR subunits. To test this alternative, we looked for surface expression of the ΔM4 constructs in *Xenopus* oocytes (Figure 3-4) and HEK 293 cells (Figure 3-5). For oocytes, we performed Western blots of biotinylated membranes and identified that GluR-A' and GluR-A'-ΔM4 are expressed in the membrane (upper band, Figure 3-4A). To quantify membrane expression, we normalized band densities relative to that for the endogenously expressed Na^+-K^+-ATPase β subunit (lower band, Figure 3-4A). Membrane expression for both GluR-A' and GluR-A'-ΔM4 was significantly greater than background (membranes from DEPC-injected oocytes) and comparable in magnitude (Figure 3-4C). We also quantified the total (whole lysate) expression of GluR-A' and GluR-A'-ΔM4 relative to β-tubulin (Figure 3-4B & D). Again, both constructs expressed equally well suggesting that synthesis and membrane trafficking of the ΔM4 construct, at least in *Xenopus* oocytes, is not impeded.

To verify that the membrane expression was not exclusive of *Xenopus laevis* oocytes, we also tested for surface expression of wild type GluR-A and the corresponding ΔM4 construct in non-permeabilized HEK 293 cells using immunocytochemistry (Figure 3-5). Although not quantified, membrane expression of the ΔM4 construct was robust and qualitatively comparable to that of wild type. The data demonstrated that the receptor is

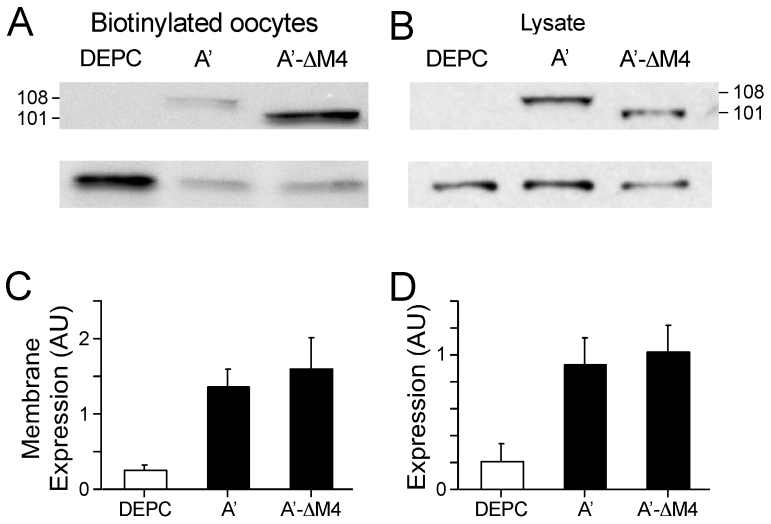

Figure 3-4 ΔM4 constructs are expressed in the membrane.

(A) Western blot of a biotinylated membrane preparation from *Xenopus* oocytes injected with either DEPC water (DEPC), GluR-A' (A') or GluR-A'-ΔM4 (ΔM4) mRNA (both at 5-6 ng). Expression was evaluated 2 days after injection using antibodies against the N-terminus of GluR1 (GluR-A) (upper band) or Na^+/K^+ ATPase β (lower band) as a loading control. Theoretical molecular weight of GluR-A' (101) and ΔM4 (91) are less than that observed (approximately 108 & 101, respectively), presumably reflecting glycosylation or other post-translational modifications.

(B) As in (A) but for whole lysate using β tubulin (lower band) as a loading control.

(C-D) Quantification of GluR-A' subunits in the membrane (C) or in whole oocyte (D) relative to the endogenous Na^+/K^+-ATPase β (C) or β tubulin (D) (see Methods). Values shown are mean ± 2*SEM (n > 7 for each). The values for A' and ΔM4 were not significantly different ($P < 0.05$).

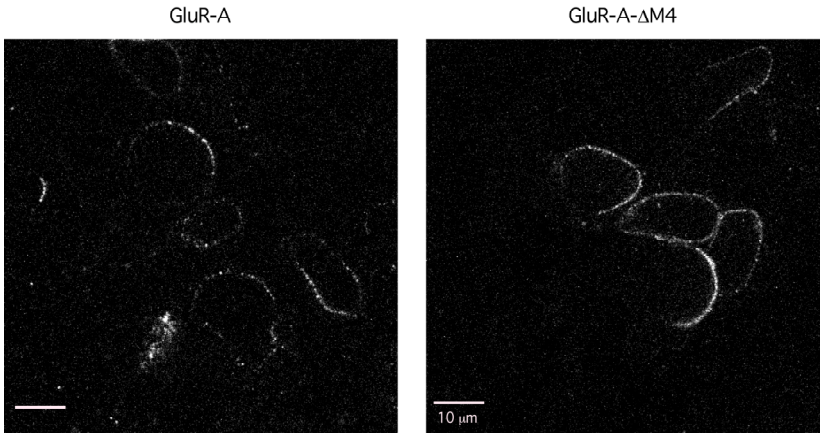

Figure 3-5 Membrane Expression of GluR-A'-ΔM4 in HEK-293 cells

Immunocytochemistry of HEK-293 cells transfected with either GluR-A (left) or GluR-A-ΔM4 (ΔM4) (right) cDNA. Non permeabilized cells, fixed with 1% paraformaldehyde were labeled with anti-ATD-GluR-A antibodies and Alexa-546 secondary antibody. Images scale bar is 10 μm. Images are representative of >6 independent experiments.

able to traffic to the plasma membrane besides deletions in the M4 transmembrane segment.

3.3 Coexpression of an independently encoded M4 with GluR-A-ΔM4

The data imply the need of M4 for receptor function. Previous experiments in NMDA receptors have shown that co-expression of an independently encoded M4 can restore limited functionality (Schorge and Colquhoun, 2003). By reproduction of comparable constructs for AMPA GluR-A receptor and cotransfection in *Xenopus* oocytes, we were able to reproduce similar results (Figure 3-6). Limited functionality was elicited with glutamate although the reproducibility of the data was limited. Several questions arise regarding the stoichiometry of the constructs and the difficulty to manage it during experimentation. Nevertheless the results are consistent with the idea that the M4 segment is important for glutamate receptor function.

3.4 Tandem constructs display properties unlike wild type receptors

To study subunit arrangement and gating in transmembrane proteins, there is an advantage to having tandem constructs where two subunits are joined together. However, in GluR subunits, the N- and C-termini of GluRs are located on opposite sides of the membrane complicating the generation of such constructs. This problem was solved by Schorge and Colquhoun (Schorge and Colquhoun, 2003) by placing a truncated form of

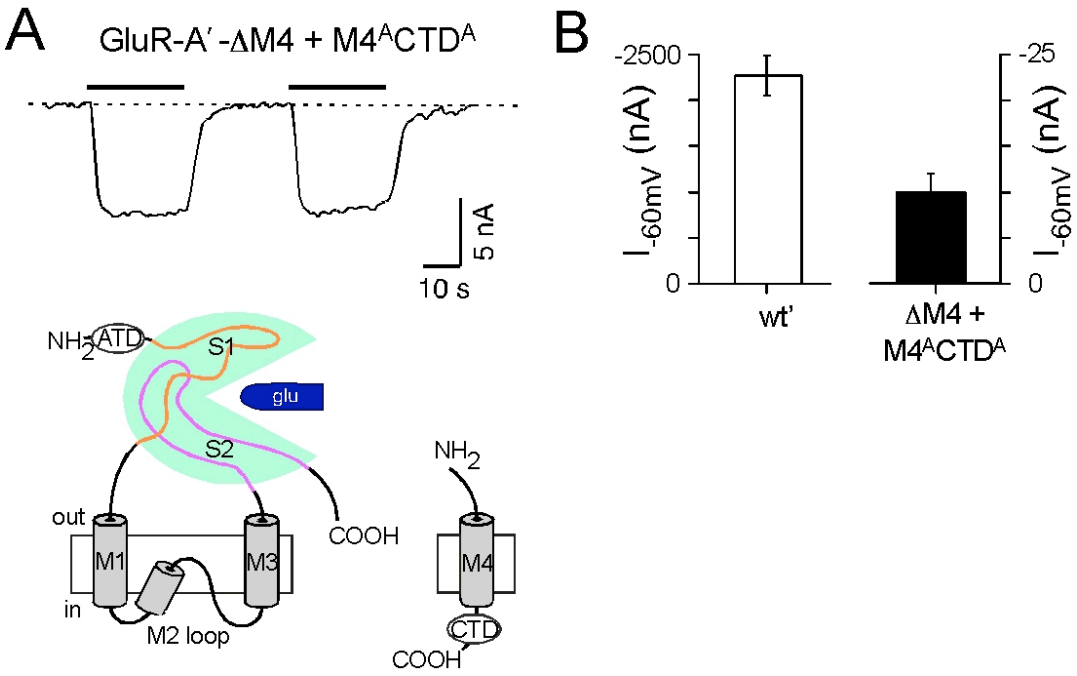

Figure 3-6 An independently encoded M4 segment can regenerate function in the ΔM4 construct

(A) Upper panel, Whole-cell currents recorded in a *Xenopus* oocytes injected with mRNA for GluR-A'-ΔM4 and an independently encoded M4 segment and C-terminal domain derived from GluR-A ($M4^{A}CTD^{A}$). Lower panels, Schematics of presumed membrane topology of injected mRNA. Data are recorded and displayed as in Figure 3-2

(B) Mean current amplitudes (± 2*SEM) for GluR-A' or GluR-A'-ΔCTD co-injected with $M4^{A}CTD^{A}$ (n = 13).

a GluR subunit lacking an M4 segment in an open reading frame with an intact subunit.

I also generated a tandem construct where two GluR-A subunits are linked in an open reading frame, in analogy to Schorge & Colquhoun (2003) for NMDA receptor subunits. The first subunit in the tandem lacks an M4/CTD permitting presumed proper folding of the second subunit. Oocytes injected with such a tandem construct show small albeit detectable glutamate-activated currents (Figure 3-7B). However, wild type GluR-A AMPA receptors are not affected by externally applied methanethiolsulfonate (MTS) reagents (e.g., Sobolevsky et al., 2003) (Figure 3-7A) indicating that possible modifications of endogenous cysteines do not affect current amplitudes. In contrast, the application of externally applied MTS reagents does reduce current amplitudes in the GluR-A'-ΔM4/GluR-A' tandem construct (Figure 3-7B & C). This result raised concerns as to how well the tandem constructs might represent wild type receptors and I therefore decided not to pursue the use of tandem constructs experimentally.

3.5 Conclusion

In summary, the M4 segment or associated CTD may affect membrane expression of GluRs, but this does not contribute notably to the lack of functionality of the ΔM4 construct. Given this finding and that co-expression of an independently encoded M4 can restore limited functionality (Schorge and Colquhoun, 2003) indicates that the M4

segment is an essential structural element for receptor function in mammalian GluRs. The mechanistic basis for this requirement is unknown and is the focus of chapter 4.

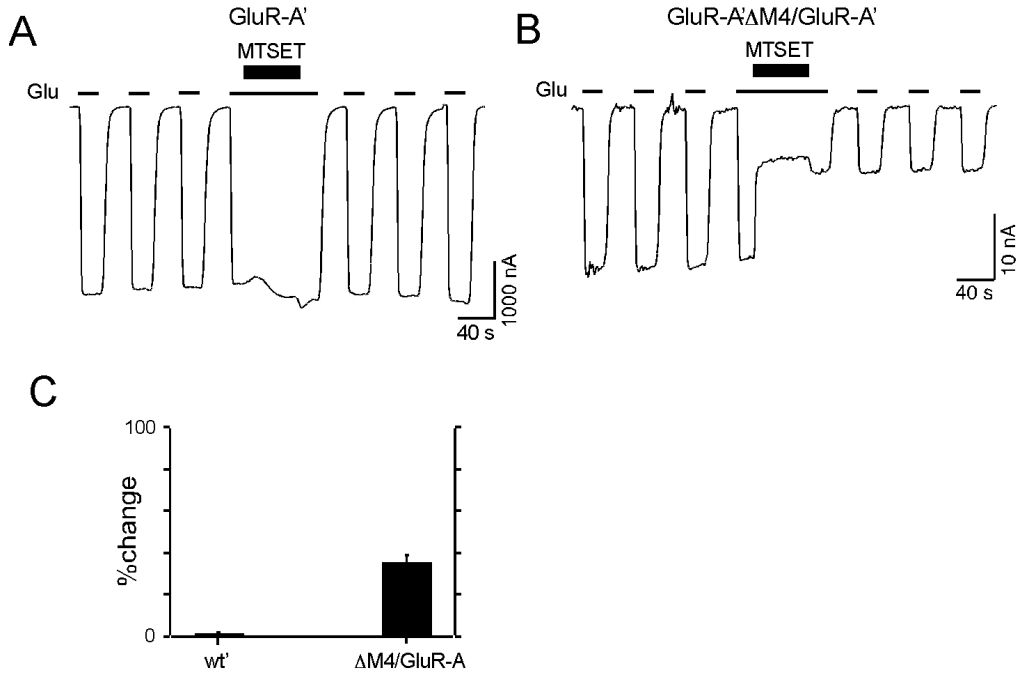

Figure 3-7 Wild type tandem constructs show an altered sensitivity to MTS reagents.

(A & B) Protocol to assay the effect of MTSET on wild type (A) and tandem (B) receptors. The protocols were made in the presence of glutamate using steady-state reactions (see Supplemental Experimental Procedures). Currents were elicited by glutamate (1 mM) (thin lines) at a holding potential (V_h) of –60 mV. MTSET (2 mM, thick lines) was applied for 60 s in the continuous presence of glutamate.

(C) Mean percent change (% change) in glutamate-activated current amplitudes measured before (I_{pre}) and after (I_{post}) exposure to MTSET in the presence of glutamate (n > 4). Filled bars indicate that the value of % change is statistically different from zero.

CHAPTER FOUR

Interaction of the M4 Segment with other Transmembrane-Segments is Required for Channel Gating in Mammalian Glutamate Receptors

4 Interaction of the M4 segment with other Transmembrane-Segments is required for Channel Gating in Mammalian Glutamate Receptors

4.1 Introduction

In contrast to K^+ channels and prokaryotic GluR (GluR0) subunits, all mammalian GluR subunits have an additional transmembrane segment, M4, located C-terminal to the core of the ion channel (M1-M3). M4 is required for the functioning of mammalian GluRs, a result found for AMPA (Figure 3-2) and NMDA (Schorge and Colquhoun, 2003) receptors. Understanding the structural and functional significance of M4 will therefore help define fundamental gating principles in mammalian GluRs. Mechanistically two general, non-mutually exclusive working models for the function of M4 can be considered. (i) M4 is needed for translation of the LBD conformational changes into the ion channel opening. In this model (Anchor Model), the anchoring of the C-terminal part of the LBD to the membrane is essential. In the extreme of this model, the specific properties of M4-outside of acting as an anchor-are unimportant. Alternatively (ii), M4 is needed for conformational changes in the ion channel itself to occur. Here, M4 provides an environment in the protein/lipid permitting other gating domains such as M3 to undergo their conformational changes (Interaction Model). In its pure form, the specific properties of M4 would be more critical. Again, both of these

working models may have some degree of validity and should not be viewed as exclusive.

Taking advantage of polyleucine transmembrane segments, recovery of function, tryptophan and cysteine mutagenesis scans, and glycine insertions, we conclude that the interaction of the M4 segment with other transmembrane segments –rather than with the ligand-binding domain- is required for channel gating in mammalian GluRs. These interactions, which apparently occurred early in the course of evolution, may represent one means to generate fast gating in mammalian glutamate receptors.

4.2 Results

4.2.1 Replacing the M4 segment with an artificial transmembrane helix does not restore functionality

One potential function of M4 is to tether the LBD and to act as an anchor so that the clam shell-like closure following glutamate binding can be converted into channel opening presumably via the M3 segment, the major gating element in GluRs (Jones et al., 2002; Sobolevsky et al., 2002). In its simplest form, the specific identity of M4 should be unimportant since only its membrane spanning or tethering capacity would be required for functionality. To test this idea, we therefore replaced the entire M4 segment in GluR-A with leucines (21 amino acids total) (Figure 4-1A). Such polyleucine (pLeu) stretches are frequently used as model transmembrane helices (e.g., Caputo and London, 2004; Zhou et al., 2001) since they form spontaneous, stable α-helices and insert naturally into membranes. We did not use a polyalanine transmembrane segment to avoid any potential helical-helical interactions.

Figure 4-1B-C shows whole-cell currents from oocytes injected with mRNA for GluR-A' (Figure 4-1A) or for a comparable construct but where the M4 segment was replaced with leucines (GluR-A'-M4^{pLeu}) (Figure 4-1C). Surprisingly, GluR-A'-M4^{pLeu} did not show any detectable glutamate-activated currents. Like the ΔM4 constructs this

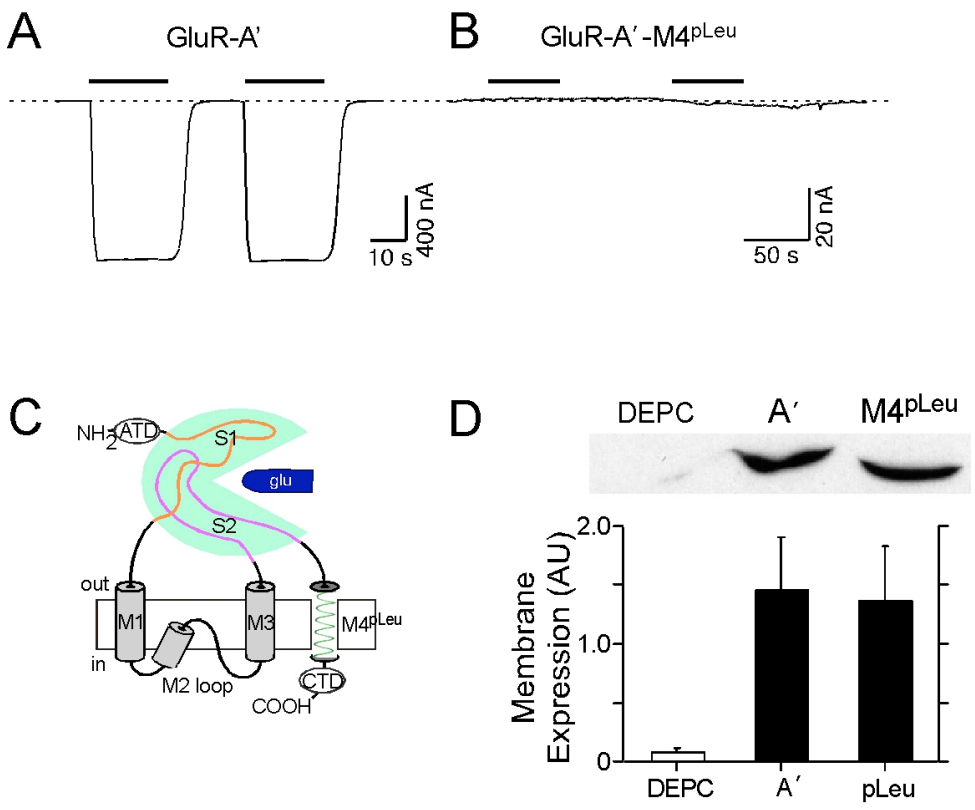

Figure 4-1 An artificial transmembrane α-helix substituted for the M4 segment.

(A & B) Whole-cell currents recorded in *Xenopus* oocytes injected with GluR-A' (B) or GluR-A'-M4^{pLeu} (C). No detectable glutamate-activated current could be detected in oocytes injected with GluR-A'-M4^{pLeu} ($n > 20$).

(C) Presumed membrane topology of a construct where the entire GluR-A' M4 segment was replaced with leucines (21 total) (GluR-A'-M4^{pLeu}). Such long runs of leucines are used as canonical transmembrane α-helices (Zhou et al., 2001).

(D) GluR-A'-M4^{pLeu} is expressed in the membrane. Western blots of biotinylated GluR-A' or GluR-A'-M4^{pLeu} (upper panel). Quantification of membrane expression, relative to endogenous Na^+/K^+-ATPase β (lower panel), as in Figure 3-4. The values for A' and A'-M4^{pLeu} were not significantly different ($P < 0.05$).

polyleucine construct still expresses on the membrane (Figure 4-1D upper panel) and at a level comparable to that for wild type GluR-A' (Figure 4-1D, lower panel). In addition, we also verified that the orientation of the polyleucine M4 was correct by looking at the positioning of the CTD. Here, we examined the reactivity of HEK 293 cells to a C-terminal antibody either in non-permeabilized or permeabilized conditions (Figure 4-2). Only in the permeabilized instance did we detect a signal consistent with the C-terminus being located intracellularly as in wild type GluR subunits.

In summary, a pLeu transmembrane helix that presumably recreates the membrane spanning property of M4 but lacks any specific identifying features does not yield functional receptors. Hence, at least to some degree, the specific features of M4 are essential to carry out its function. We therefore carried out site-directed mutagenesis scans of the GluR-A M4 segment.

4.2.2 Tryptophan and cysteine mutagenesis scans reveal a putative interacting face of the M4 segment

As an alternative to a tethering function, the M4 segment may be required for transmembrane interactions. To test this alternative, we substituted each individual position in the GluR-A M4 segment, as well as the polar clamps on either end, with either tryptophan (W) or cysteine (C) and compared glutamate-activated current amplitudes from these mutant channels to that for wild type channels. Tryptophan has a bulky,

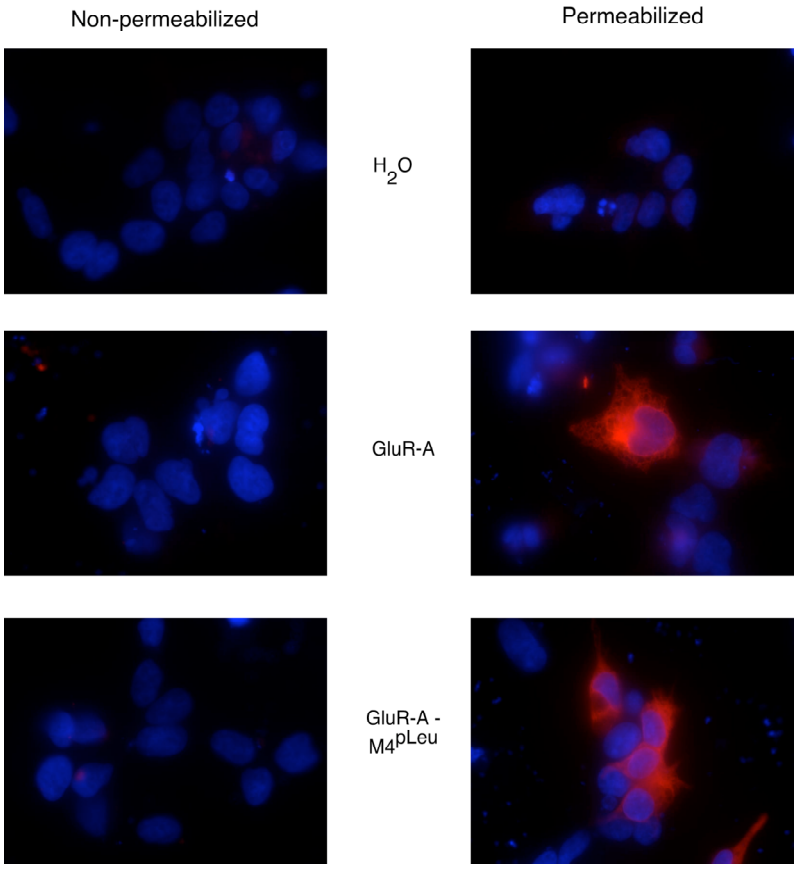

Figure 4-2 Topology of A'-M4^{pLeu} at the membrane.

Immunocytochemistry of HEK 293 cells transfected with H_2O (top row), GluR-A(middle row) or GluR-A-M4^{pLeu} (bottom row). 1% paraformaldehyde fixed cells were labeled with anti-CTD-GluR-A antibody under non-permeabilized (left column) or permeabilized (0.05% Tween-20) conditions (right column). Cells signal was only detected under permeabilized conditions suggesting the pLeu transmembrane segment is at the membrane and the GluR-A-M4^{pLeu} mutant is topologically oriented like a wild type. Nuclear DAPI staining. Bar 10 μm.

hydrophobic side chain that is tolerated in a lipid environment but less so at points of helix-helix interactions (Liu et al., 2004; Moore et al., 2008). Hence, we anticipated that if transmembrane helix interactions are important for receptor function—at least in some state of the receptor—, then positions located at such interfaces when substituted with tryptophan should yield receptors with altered function. Cysteine has a smaller side chain than tryptophan and might be more tolerated at least at less sensitive positions. We also used it to test for reactivity with a methanethiolsulfonate (MTS) reagent (see below).

Figure 4-3 shows glutamate-activated currents for GluR-A' as well as in these instances tryptophan-substituted receptors. Figure 4-4A and Figure 4-4B summarize current amplitudes, normalized to those for GluR-A', for either the tryptophan- (Figure 4-4A, left panel) or cysteine- (Figure 4-4A, right panel) substituted receptors. Many of the mutant receptors showed robust glutamate-activated current amplitudes on the order of wild type (Table 4-1, Table 4-2). On the other hand, many showed no glutamate-activated current (demarcated by an 'X') (Figure 4-4), like the ΔM4 construct, or showed greatly reduced current amplitudes. As a cut-off and mainly to focus on a more limited set of positions, presumably the most critical, we considered the most significant only those positions that showed normalized responses <0.3 of that of wild type. For tryptophan-substituted receptors, this cut-off was unnecessary because normalized

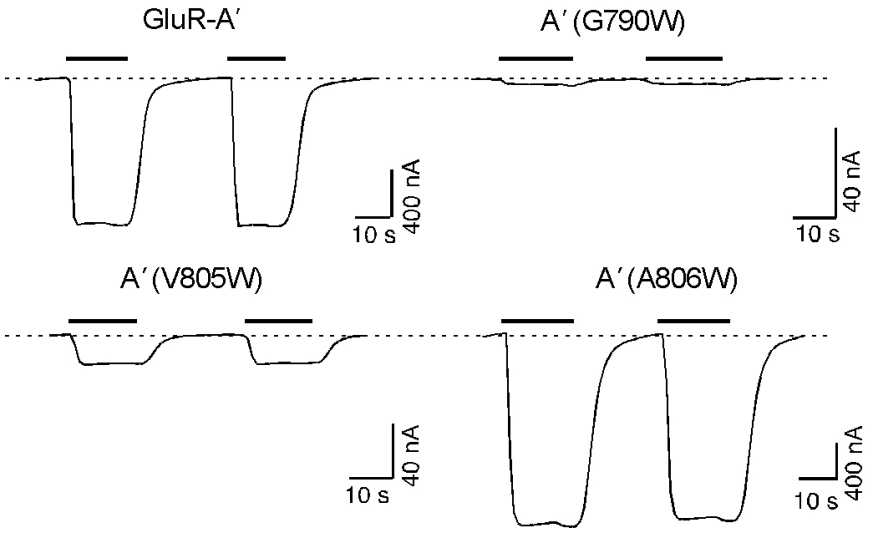

Figure 4-3 Tryptophan mutagenesis scan of residues in the M4 segment

Representative whole-cell currents recorded from *Xenopus* oocytes injected with GluR-A', GluR-A'(G790W), GluR-A'(V805W) or GluR-A'(A806W). Currents recorded and displayed as in Figure 3-2.

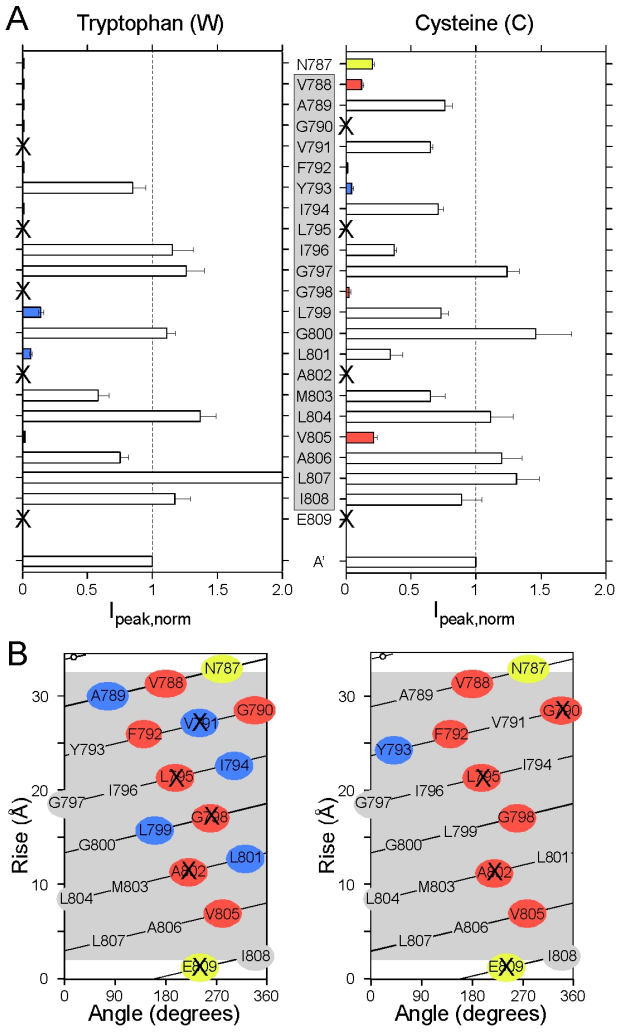

Figure 4-4 Tryptophan and cysteine mutagenesis scans of residues in the M4 segment.

(A) Mean whole-cell glutamate-activated current amplitudes (± 2*SEM) at –60 mV and in 1 mM glutamate normalized to those obtained in wild type (GluR-A') injected and recorded during the same cycle for either tryptophan (*left panel*) or cysteine (*right panel*) substitutions (n > 7). Each position was injected and recorded on at least 3 different injection cycles. Wild type current amplitudes were -2120 ± 39 (n = 32) for those done in association with tryptophan substitutions and -1100 ± 41 (n = 32) with cysteine substitutions (Table 4-1, Table 4-2). Positions that did not show detectable glutamate-activated currents are demarcated by an 'X'. Positions that showed current amplitudes <0.3 of wild type are colored: yellow for polar clamps; blue if occuring only in a single scan; and red if occuring for both scans.

(B) Helical net representation of the results shown in (B). All positions tested including the polar clamps and those within the M4 segment (highlighted in grey) are shown. The same color scheme as used in (B) is used here (yellow for polar clamp, blue for single scan, and red for both scans). Positions that did not show detectable glutamate-activated currents are demarcated by an 'X'.

Table 4-1 Functional properties of Wild Type and Tryptophan-substituted GluR-A' receptors expressed in *Xenopus* oocytes.

Construct	I (nA)	n	EC50 *(μM)*	*Hill*	n
GluR-A'	-2120 ± 40	32	4.2 ± 0.1	1.6 ± 0.1	14
N787W	-14 ± 2	7 (13)	nt		
V788W	-66 ± 2	3 (16)	nt		
A789W	-15 ± 1	14 (18)	14.8 ± 1.0	1.8 ± 0.1	6
G790W	-14 ± 2	11 (21)	nt		
V791W	nd	7	nt		
F792W	-4 ± 1	2 (9)	nt		
Y793W	-2430 ± 100	11	5.6 ± 0.2	1.5 ± 0.1	6
I794W	-7 ± 1	7 (16)	nt		
L795W	nd	10	nt		
I796W	-3440 ± 160	11	3.0 ± 0.3	1.2 ± 0.1	5
G797W	-2940 ± 160	10	3.7 ± 0.2	1.4 ± 0.1	5
G798W	nd	7	nt		
L799W	-310 ± 20	13	7.8 ± 0.2	1.5 ± 0.1	8
G800W	-2970 ± 80	13	3.9 ± 0.1	1.3 ± 0.1	6
L801W	-140 ± 10	11	7.2 ± 0.3	1.6 ± 0.1	7
A802W	nd	7	nt		
M803W	-1100 ± 60	10	8.0 ± 0.5	1.4 ± 0.1	6
L804W	-3350 ± 110	12	3.0 ± 0.1	1.3 ± 0.1	6
V805W	-36 ± 2	12	11.0 ± 0.3	1.4 ± 0.1	6
A806W	-2070 ± 70	10	3.0 ± 0.1	1.5 ± 0.1	5
L807W	-5670 ± 120	13	3.0 ± 0.1	1.5 ± 0.1	6
I808W	-2990 ± 80	12	4.1 ± 0.1	1.3 ± 0.1	6
E809W	nd	9	nt		

Values shown and displayed as in Table 1. *nd*, no glutamate-activated currents detected. *nt*, not tested. For some mutations, injected oocytes showed either no detectable glutamate-activated currents or very small current amplitudes. In these instances, the *n* values in parenthesis indicates the total number of oocytes recorded whereas the other number indicates those that showed a detectable glutamate-activated current. The average current amplitude is only of those recordings that showed detectable currents.

Table 4-2 Functional properties of wild type and Cysteine-substituted GluR-A' receptors expressed in *Xenopus* oocytes.

Construct	I (nA)	n
GluR-A'	-1099 ± 41	32
N787C	-221 ± 14	18
V788C	-155 ± 9	21
A789C	-945 ± 46	21
G790C	-nd	
V791C	-751 ± 38	22
F792C	- 5.1 ± 38	5
Y793C	-60 ± 5	18
I794C	-900 ± 42	19
L795C	nd	
I796C	-458 ± 24	17
G797C	-1154 ± 62	17
G798C	-17 ± 2	15
L799C	-803 ± 62	18
G800C	-4143 ± 553	4
L801C	-666 ± 65	4
A802C	nd	
M803C	-2192 ± 583	4
L804C	-2455 ± 201	6
V805C	-676 ± 67	8
A806C	-4386 ± 484	8
L807C	-3475 ± 285	8
I808C	-2175 ± 253	6
E809C	nd	

Values shown and displayed as in Table 4-1.

responses were either <0.1 or non-functional or comparable to wild type (>0.5). Not unsurprisingly, given the nature of its side chain, the cysteine-substituted receptors showed less distinct responses though there was considerable overlap between the two scans (see below).

To give a structural meaning to these results and assuming that the membrane spanning M4 is α-helical, we plotted them out on helical nets (Figure 4-4B) for either the tryptophan (*left panel*) or cysteine (*right panel*) substitutions. All positions tested are shown in these plots but only those that showed greatly reduced amplitudes (<0.3) are colored: yellow for polar clamps; blue if occurring in a single scan; and red if occurring in both scans. Clearly, the number of red (and yellow) positions of the total number of colored positions between the two scans are quite high (9 of 14 for the tryptophan scan and 9 of 10 for the cysteine scan). Also notable is that, with the exception of either G790 or F792 all of the red positions fall on one face of a canonical α-helix, extending from the N-terminus end (V788) to the C-terminus end (V805). Even the blue highlighted positions, with the exception of Y793, typically surround the red positions. Hence, given the disruption of function including for the small cysteine, these results suggest that the interaction of M4 with other transmembrane segments—possibly the core of the ion channel (M1-M3) or even the M4 segment itself—is an important component of receptor function in GluRs.

4.2.3 Tryptophan-substituted receptors are expressed in the membrane

The tryptophan-substituted receptors showed a distinct pattern of current amplitudes either being greatly reduced (<0.1) or comparable to (>0.5) that of wild type. We therefore focused subsequent analysis on these receptors. Initially, we verified that the reduced current amplitudes did not reflect a trafficking or biosynthesis problem and quantified membrane expression using biotinylated membranes from oocytes (Figure 4-6). Like the ΔM4 construct, all non-functional (V791W, L795W, G798W, A802W, E809W) (Figure 4-6A) and reduced current amplitude (N787W, V788W, A789W, G790W, F792W, I794W, V805W) (Figure 4-6B) tryptophan constructs expressed in the membrane and at a level significantly greater than DEPC injected oocytes. Several non-functional tryptophan constructs (L795W) did show a level significantly less than GluR-A' possibly suggesting some contribution to trafficking/biosynthesis. Nevertheless, these results suggest that the tryptophan substitutions and alterations of the M4 segment in general are not altering trafficking but rather are altering an intrinsic property of the receptor in the membrane.

4.2.4 The M4 segment in GluR-A is not water accessible

The channel of GluR-A is a water filled pore, like in other ion channels. Residues that form these pore domain have been identified in the M3 transmembrane segment and the M2-reentry loop. Then, the participation of residues of the M4 transmembrane helix in pore formation was tested. To identify whether positions in the GluR-A M4 segment

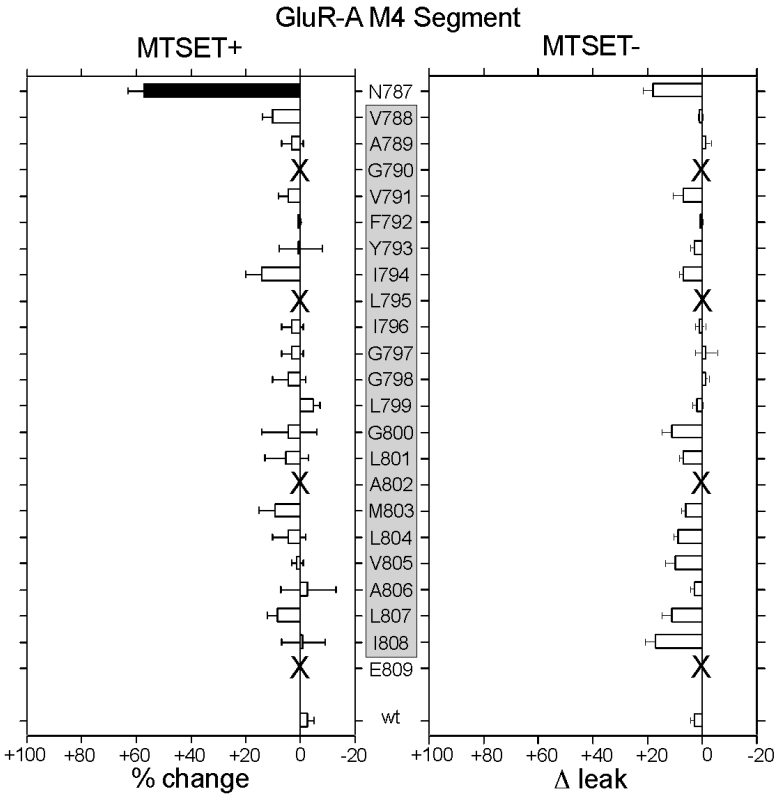

Figure 4-5 The M4 segment in GluR-A is not water accessible

Mean percent change (% change) in glutamate-activated current amplitudes measured before (I_{pre}) and after (I_{post}) exposure to MTSET (MTSET + Glu) in the presence of glutamate. Left and right pointing bars indicate inhibition and potentiation, respectively (n > 4). Filled bars indicate that the value of % change is statistically different from zero.

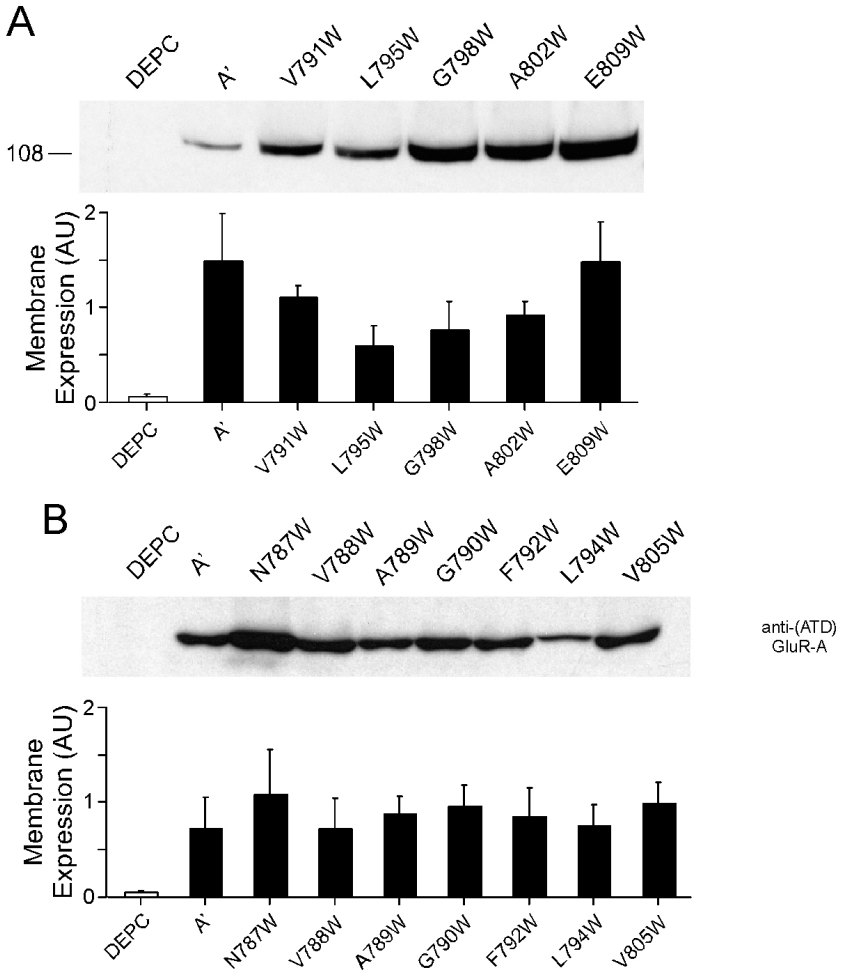

Figure 4-6 Tryptophan-substituted receptors express in the membrane

(A & B) Western blots of biotinylated membrane preparations from Xenopus oocytes injected either with DEPC water (DEPC), GluR-A', or various tryptophan-substituted GluR-A' receptors either those that showed no glutamate-activated current (A) or very low levels of current (B). Protocol as in Figure 3-4 ($n > 4$ for each position).

are water accessible y used the Cysteine scanning mutagenesis. I tested all positions with cysteine substitutions for their accessibility to the positively charged MTSET (see (Sobolevsky et al., 2003). Although the polar N787 was accessible in the presence of glutamate (MTSET +), none of the other positions showed a significant change in current amplitude following MTSET application. Hence, in AMPA receptors the M4 segment does not appear water accessible in contrast to the NR1:NR2C M4 segment (Beck et al., 1999; Sobolevsky et al., 2007).

4.2.5 Recovery of function in the polyleucine background

Given the observation that certain residues are necessary for receptor function (Figure 4-5) we considered the opposite scenario—the minimum number of these key residues to restore function in a non-functioning background. Hence, starting with the non-functional polyleucine background (Figure 4-1), we systematically re-introduced key (red colored) residues to identify the minimum residues needed for function (Figure 4-7).

Figure 4-7A shows mainly conserved sequence alignments for the M4 segments from non-NMDA (*upper panel*) and NMDA (*lower panel*) receptor subunits. In general, residues within a class (non-NMDA versus NMDA) are conserved either in terms of identity or functional properties (see Discussion) especially for those positions that are demarcated 'red' by the tryptophan and cysteine scans. The most conserved positions in the M4 segments, G790 and F792 in GluR-A, both are demarcated by red in Figure 4-7

but when reintroduced into the M4 polyleucine background (GluR-A'-pLeu^{GF}) were not enough to yield glutamate-activated currents (raw data not shown, Figure 4-7C). Reintroducing a number of other conserved residues (e.g., G798, A802) in a stepwise fashion also did not yield functional receptors. However, when a cluster of residues were converted back to their native conformation (L790G/L791V/L792F/L798G/L802A/ L805V; note a conserved, red leucine, L795, is already present in the polyleucine background), currents, albeit small were now detected (Figure 4-7B & C). A slightly different strategy starting with the addition of V788 yielded a comparable outcome.

Figure 4-8 highlights the distribution of those positions presumably necessary to recover function on a canonical α-helix for the M4 segment. They suggest that these positions clearly lie on one face of the segment supporting the notion that its interaction with other transmembrane segments is necessary for receptor function.

4.2.6 Chimeras between GluR-A and the M4 segment of other GluRs

The M4 sequence identity is presumably relevant for receptor function. To further identify the specificity of its character, we assemble GluR-A' receptors with the M4 transmembrane segment of GluR-6, KA2, NR2A or NR2B subunits. *Xenopus* oocytes injected with the chimeric proteins elicited glutamate activated currents only when the M4 exchange was made within the same GluR subfamily (Figure 4-9). Nevertheless, the currents were not fully reestablished even the receptor was functional.

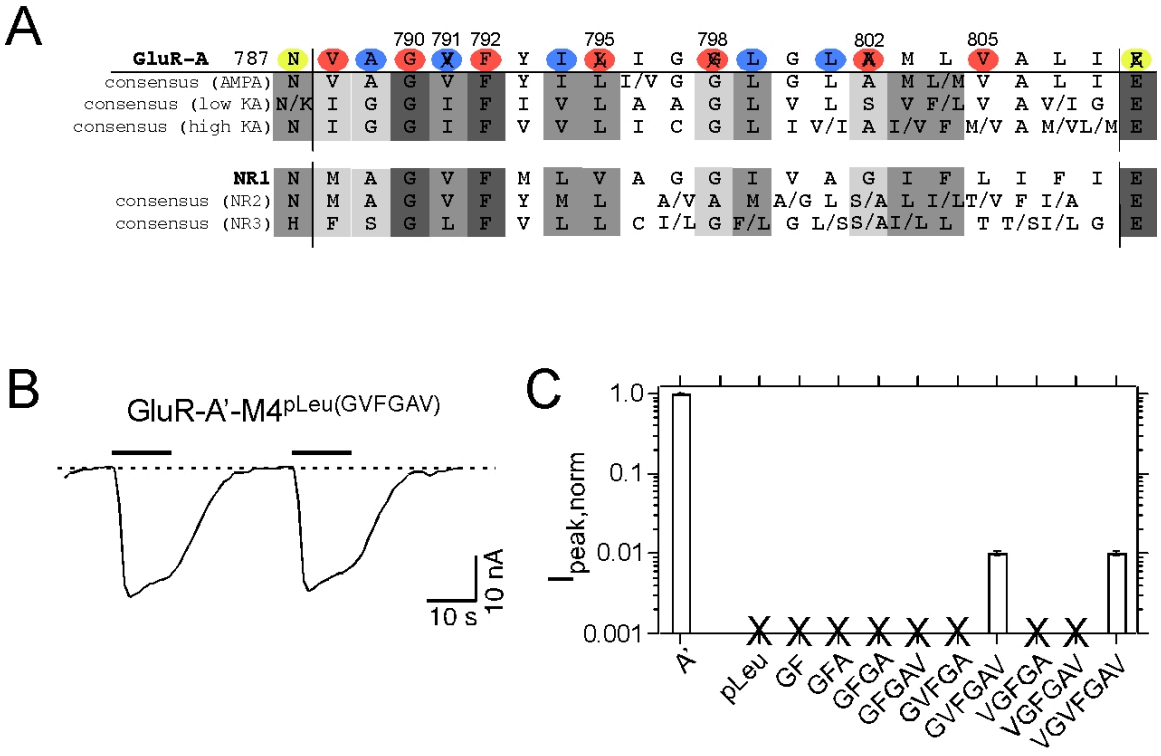

Figure 4-7 **Recovery of function in the non-functional polyleucine background.**

(A) Sequence alignment of residues in and around the M4 segments in non-NMDA (upper panel) and NMDA (lower panel) receptor subunits. Outside of GluR-A and NR1, consensus sequences are shown for AMPA (A-D), low affinity kainate (low KA) (GluR5-7), high affinity kainate (high KA) (KA1 & KA2), NR2 (A-D) or NR3 (A & B) subunits. If a position is blank, it is not conserved. The degree of shading corresponds to conservation: completely conserved positions are shaded dark gray whereas those that have no conservation are not shaded. Numbering is given only for the GluR-A subunit. Positions where function was affected in the tryptophan scan are and are highlighted in yellow (polar clamps), blue (occurring in only one scan) or red (occurring in both scans) as for previous figures.

(B) Representative whole-cell currents recorded from a *Xenopus* oocyte injected with GluR-A'-M4^{pLeu}(GVFGAV). In this construct, the GluR-A' M4 segment was in the polyleucine background (see Fig. 3) but certain positions had been mutated back to their wild type form: L790G/L791V/L792F/L798G/L802A/L805V (GVFGAV). Currents recorded and displayed as in Figure 3-2.

(C) Mean whole-cell glutamate-activated current amplitudes (± 2*SEM) at –60 mV and in 1 mM glutamate normalized to those obtained in wild type (GluR-A') injected and recorded during the same cycle (n > 6). Each mutant was injected and recorded on at least 3 different cycles. Wild type current amplitudes were -1760 ± 50 (n = 20). Positions that did not show detectable glutamate-activated currents are demarcated by an 'X'. All mutant constructs were in the M4 polyleucine (pLeu) background where certain positions were reverted back to their native residue: GF (L790G/L792F); GFA (GF + L802A); GFGA (GFA + L798G); GFGAV (GFGA + L805V); GVFGA (GFGA + L791V); GVFGAV (GVFGA + L805V); VGFGA (GFGA + L788V); VGFGAV (VGFGA + L805V); and VGVFGAV (VGFGAV + L791V).

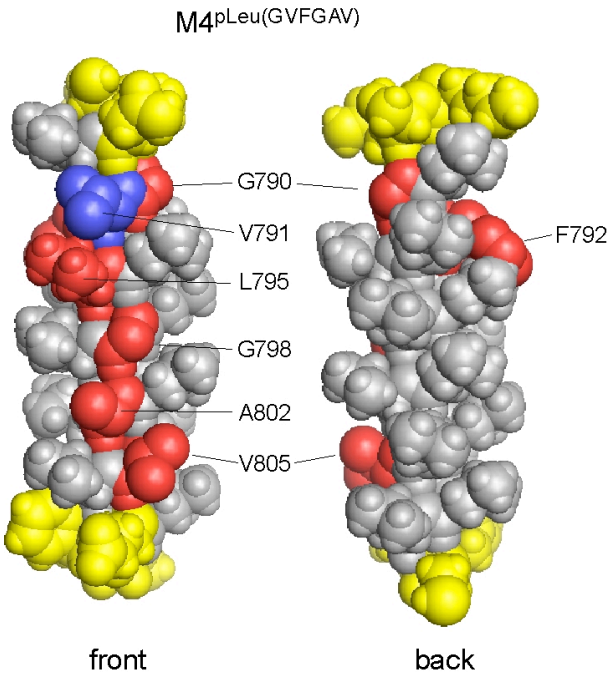

Figure 4-8 Putative M4 transmembrane interaction face

Canonical α-helical representation of the M4 segment illustrating the putative location of the GVFGAV positions, the minimal motif to regain function. Note that one of the leucines (L795) was also demarcated red (see Figure 4-7A).

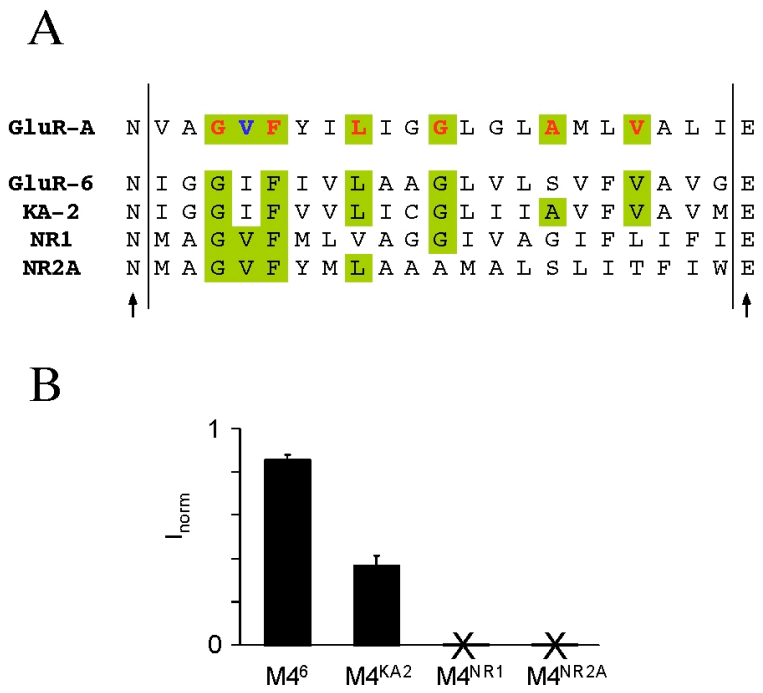

Figure 4-9 M4 chimeras of GluR-A

(A) Sequence comparison of the M4 transmembrane used for chimera Arrows: polar clamp residues; red and blue positions identified with the Tryptophan and Cysteine scanning as putative interacting face under green background. Conserved residues of M4 GluR-A subunit highlighted in the other M4 sequences.

(B) GluR-A M4 segment was replaced by M4 from other subunits. The M4 of GluR-6 and KA2 (non-NMDA receptors) and NR1 and NR2A (NMDA receptors) were used for the substitutions. Normalized Current amplitudes of wild type (A') or chimeric GluR-A'-$M4^{6}$ ($M4^{6}$), GluR-A'-$M4^{KA2}$ ($M4^{KA2}$), GluR-A'-$M4^{NR1}$ ($M4^{NR1}$) or GluR-A'-$M4^{NR2A}$ ($M4^{NR2A}$). Mutants were stimulated with 1 mM glutamate. The values shown are mean ±2*SEM (n>3).

4.2.7 The M4 segment contributes to channel gating

The interaction of M4 with other transmembrane segments appears critical for receptor function, but less clear is the specific function of M4. In part, it could be to simply provide structural integrity to the protein. Alternatively, it may be an active participant in channel gating by lending its surface for dynamic interactions with other gating elements (e.g., M3 and/or M1). Although many of the positions at the putative interface are mutation-intolerant (at least when mutated to tryptophan or the much smaller cysteine), certain positions (e.g., L801, & V805) showed marked reduction in current amplitudes and also fall on the putative interacting face of the α-helix.

We considered a simple gating model for AMPA receptors (Figure 4-10) where we assume, for simplicity, that binding occurs in a step-wise fashion and that the final gating step is concerted. Although this model certainly is inappropriate in detail (e.g., Robert and Howe, 2003), it encompasses the essence of binding/gating in a ligand-gated ion channel including GluRs. We also reasoned that, since mutations of M4 were in a transmembrane segment, that they were unlikely to have any significant effect on a binding step, occurring in the extracellular ligand-binding domain. Later results are consistent with this idea. As illustrated in Figure 4-10A (right panel) increases in α or decrease in β (stabilizing the closed state) produce strong reduction in P_{open} as well as rightward shifts in the apparent concentration dependence (EC_{50}, right panel). Figure 4-10B illustrates concentration-response curves for GluR-A' (*open circles*) and several tryptophan-substituted receptors. Many of the tryptophan-substituted receptors,

especially those that showed normal current amplitudes, showed concentration-response curves indistinguishable from wild type (Table 4-1). However many of the poorer expressing ones showed a rightward shift in their concentration-response curves as would be anticipated from a decreased β (or increased α). We observed that for wild type GluR-A' receptors the EC_{50} is not correlated with current amplitude (Figure 4-11). Figure 4-10C plots normalized EC_{50} against normalized I_{peak} for the tryptophan-substituted receptors for which concentration response curves could be measured. It also plots normalized EC_{50} versus normalized P_{open} for the simplified kinetic model (red line). Hence, for those mutations that expressed well enough to measure a concentration-response curve, there was a strong correlation between EC_{50} and I_{peak}, suggesting that at least some component of the disruption of function is due to a gating effect.

Hence, an interaction of the M4 segment with other transmembrane segments appears to be an essential step in the energetics of gating in mammalian GluRs. This function in channel gating, based on previous results and the rather weak effects on alterations in EC_{50}, is probably more passive providing an environment for other major gating domains such as M3 to carry out their function. Nevertheless, we cannot completely rule out that some of the actions of M4 are to affect the desensitized conformation of the receptor. Still, later results argue against this possibility.

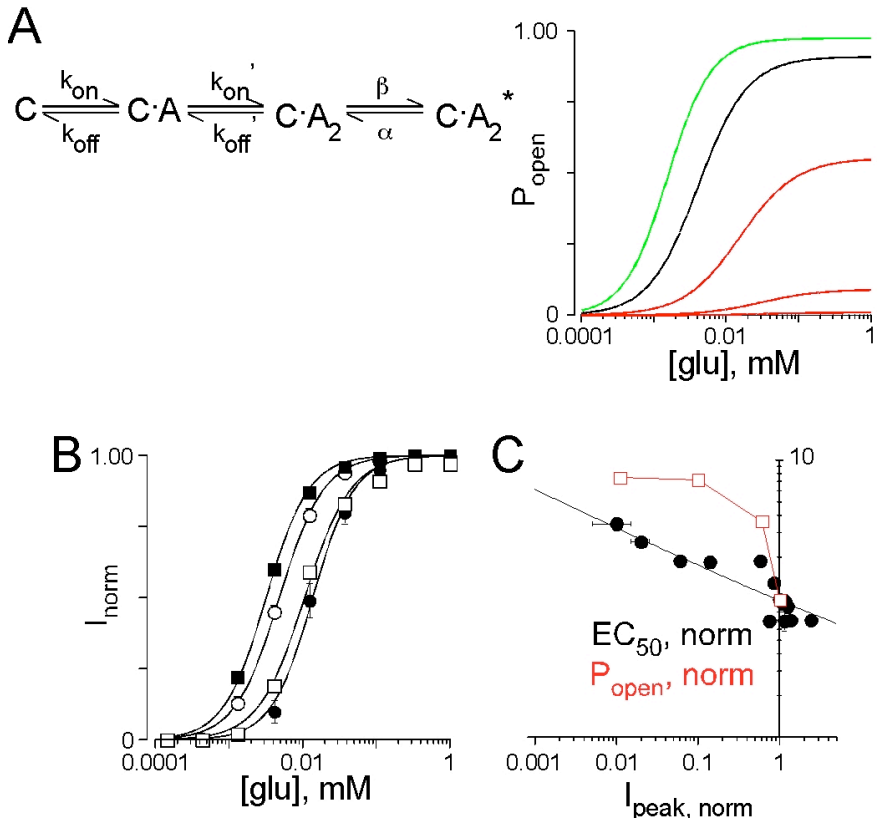

Figure 4-10 **The M4 segment contributes to channel gating.**

(A) Simplified kinetic model of AMPA receptors gating. C corresponds to unliganded, closed channel, C-A to singly liganded, C-A2 doubly liganded and C-A2* to doubly liganded, open channel. Model is adapted from (Partin et al., 1996) using ChannelLab (Synaptosoft, Atlanta, GA) but with desensitization states removed and with β (3.0 x 10^4 sec-1) and α (3.0 x 10^3 sec-1) adjusted to yield concentration response curves comparable to GluR-A' (EC_{50} ≈ 4.1 μM, black curve in right panel). Right panel, concentration-P_{open} curves for simplified kinetic model with variations in b: increasing 2-fold (green curve) or decreasing it 8-, 100- or 1000-fold (consecutive red curves).

(B) Concentration-response curves for GluR-A' (open circles), GluR-A'(A789W) (solid circles), GluR-A'(V805W) (open squares), or GluR-A'(L807W) (solid squares). Points were fit with the Hill equation (see Methods) yielding EC_{50}s and Hill coefficients of 4.8 ± 0.1 mM & 1.4 ± 0.1 for GluR-A' (n = 14); 13.7 ± 0.6 mM & 1.5 ± 0.1 for A789W (n = 6); 10.6 ± 0.7 mM & 1.4 ± 0.1 for V805W (n = 6); and 3.2 ± 0.1 mM & 1.5 ± 0.1 for L807W (n = 7).

(C) Plot of EC_{50} for tryptophan-substituted GluR-A' receptors normalized to that for GluR-A' (see Table 4-1) plotted against normalized peak current amplitude. The solid line is a linear regression. The red diamonds are a plot of the normalized EC_{50} potted against normalized P_{open} for the kinetic model shown in (A).

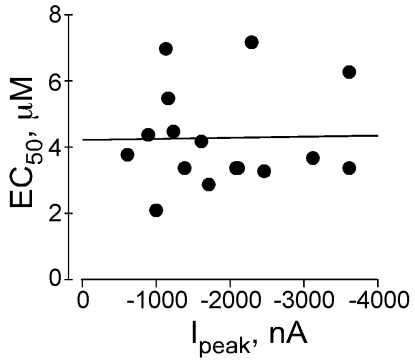

Figure 4-11 The EC_{50} is not correlated with current amplitude

Plot of EC_{50} versus peak current for wild type (GluR-A') receptors. The solid line is a linear regression.

4.2.8 Decoupling of the M4 segment from the ligand-binding domain has no effect on function

The results presented so far clearly indicate that the interaction of M4 with other transmembrane segments is a critical determinant of its function. Nevertheless, they do not rule out that at least part of the functional significance of M4 is to act as a tether for the ligand-binding domain. The interaction of M4 with other transmembrane segments will be essential for its proper location in the ion channel. To test this alternative, we introduced up to 8 glycine residues in the linker coupling M4 to the ligand-binding domain, the S2-M4 linker (Figure 4-12). Glycine is a strong helix breaker for soluble proteins and due to the absence of a side chain, such polyglycine stretches will introduce flexibility and length to the linker which should decouple the ligand-binding domain from M4. Hence, if tethering is an important function of M4, we anticipate that the addition of these glycines to S2-M4 should produce a phenotype comparable to ΔM4 constructs or tryptophan substitutions lining the interacting face, that is either poorly or non-functional in terms of glutamate-activated currents with altered functional properties.

As shown in Figure 4-12B-C, the expression level of glycine-introduced receptors, in terms of glutamate-activated currents, was indistinguishable from wild type. In terms of functional properties the additional glycines had no notable effect, producing a small leftward shift in the concentration-response curve (Figure 4-12D) and having no effect on desensitization and activation gating (Figure 4-12 E & F). These results indicate that the interaction of the M4 segment with the ligand-binding domain is not a significant

component of the function of M4. They also support the idea, albeit indirectly, that decoupling M4 from the LBD has little or no effect on its ability to bind agonist.

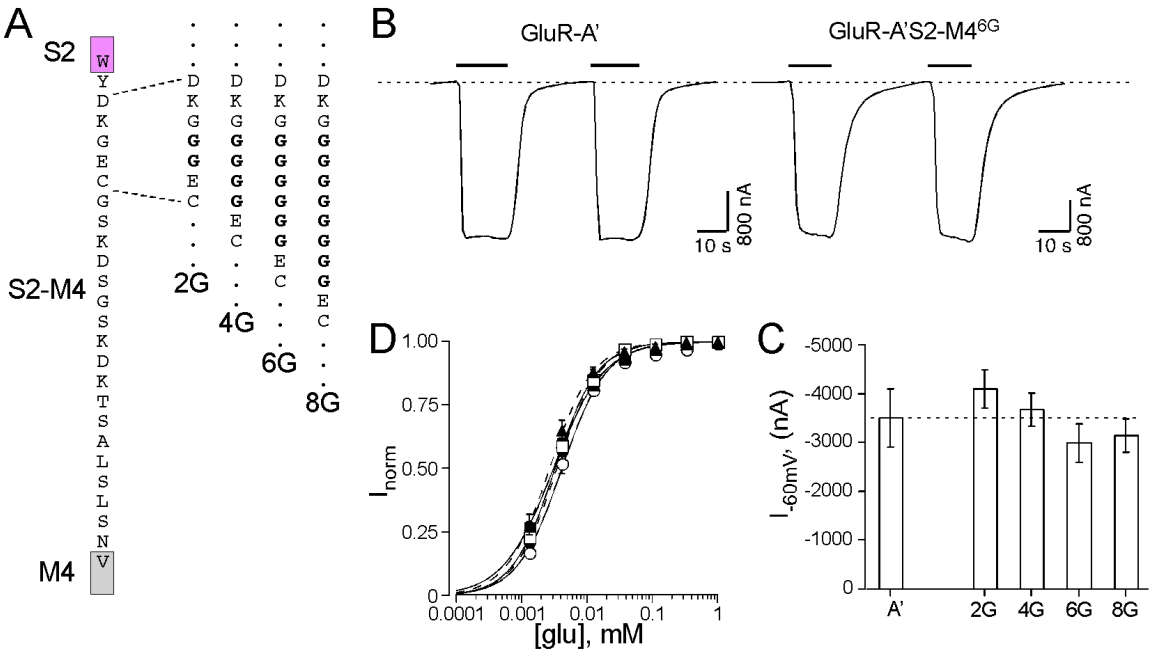

Figure 4-12 Addition of glycines to the S2-M4 linker has no notable effect on channel function.

(A) Schematic indicating the sites of glycine (G) insertions in the S2-M4 linker in the GluR-A' or GluR-A background.

(B) Representative whole-cell currents recorded from Xenopus oocytes injected with GluR-A' or GluR-A' S2-M4^{6G}. Currents recorded and displayed as in Figure 3-2.

(C) Mean current amplitudes (± 2*SEM) of whole cell glutamate-activated currents recorded in wild type GluR-A' or GluR-A' with inserted glycines in S2-M4. All constructs were injected at ~0.7-0.8 ng mRNA. None of the values were significantly different from GluR-A' ($P < 0.05$)

(D) Concentration-response curves for GluR-A' (open circles), GluR-A' S2-M4^{2G} (solid circles), GluR-A' S2-M4^{4G} (solid squares), GluR-A' S2-M4^{6G} (open squares), or GluR-A' S2-M4^{8G} (solid triangles). Points were fit with the Hill equation (see Methods) yielding EC_{50}s and Hill coefficients of 4.1 ± 0.2 mM & 1.4 ± 0.1 for GluR-A' (n = 7); 3.5 ± 0.2 mM & 1.5 ± 0.1 for S2-M4^{2G} (n = 5); 3.1 ± 0.2 mM & 1.2 ± 0.1 for S2-M4^{4G} (n = 7); 3.2 ± 0.3 mM & 1.5 ± 0.1 for S2-M4^{6G} (n = 4); and 2.7 ± 0.2 mM & 1.4 ± 0.1 for S2-M4^{8G} (n = 5).

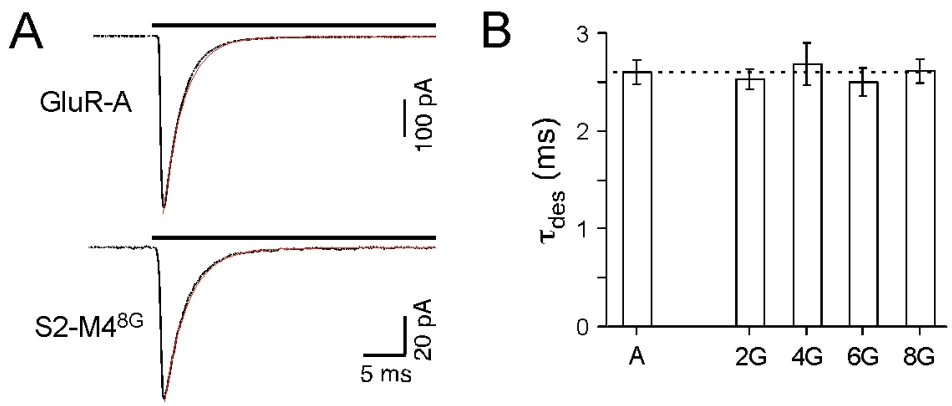

Figure 4-13 Effect of additional glycines in desensitization of GluR-A (LBD-M4-uncoupling)

(A) Currents recorded from outside-out patches, isolated from HEK 293 cells, expressing GluR-A or GluR-A S2-M4^{8G}. Solid bar indicates the time of the fast glutamate application (3 mM) (see Experimental Methods). Holding potential was –60 mV.

(B) Mean values for the entry into desensitization (± 2*SEM) for GluR-A or S2-M4 glycine-inserted GluR-A subunits.

4.3 Discussion

In contrast to K^+ channels and prokaryotic GluRs, all mammalian GluR subunits have an additional transmembrane segment, M4, located C-terminal to the ion channel core. The lack of functionality for GluRs not having an M4 is surprising since two transmembrane K^+ channels are functional as is a two transmembrane segment prokaryotic GluR (GluR0) (Chen et al., 1999) (Figure 3-1). This requirement for an additional transmembrane segment suggests that the core of the mammalian GluR, while it shares common structural features with K^+ channels, may have certain distinct needs for channel gating.

4.3.1 Interaction of M4 with other transmembrane segments is required for receptor function

Our results demonstrate the significance of the M4 segment to the function of mammalian GluRs and delineate, at least to an initial level, the basis for this. Specifically, we find that to function, mammalian GluRs require the interaction of M4 with other transmembrane segments either M1, M3 and/or M4 itself. Various lines of evidence support this idea. First, the tryptophan and cysteine mutagenesis scans revealed a distinct pattern of positions (highlighted by red or blue in Figure 4-4) that disrupt function. Here Red positions—disrupted in both mutagenesis scans—largely line one face of a canonical α-helix (Figure 4-4B & Figure 4-8). In addition, strategic reintroduction of these same residues in the non-functioning polyleucine background is required to regain function

(Figure 4-7). Like the rescue polyleucine mutant, M4-chimeric constructs that present the potential interacting face, but have a different background are functional (Figure 4-9). In contrast, an alternative mechanism for the action of M4—that it is required for the functioning of the LBD—appears unlikely because decoupling the ligand-binding domain from M4 has no notable effect on receptor function (Figure 4-12). Similarly, an artifical α-helix cannot replace M4 (Figure 4-1) suggesting that its specific properties are important. Finally, the M4 segment does not appear to have a major role in assembly or trafficking of GluRs (Figure 3-4, Figure 3-5 & Figure 4-6).

Helix-helix interactions are an important structural element for the folding, stability, and functioning of transmembrane proteins including ion channels (Moore et al., 2008). These interacting faces often display specific amino acid side chains or even unique sequence motifs that facilitate such interactions. In this regard, the M4 segment shows two notable features. First, analysis of the composition of helix-helix interacting faces, based largely on available high-resolution structures, has developed the concept of helix packing, a quantitative description of the propensity of amino acids to be located at an interacting face (Eilers et al., 2002; Liu et al., 2004). As shown in Figure 4-14, positions defined by Red in the present study match quite well with the putative helix packing vectors predicted by such models. In addition, at the core of this interacting face is a GxxxG-like sequence (G798xxxA802), a motif well-known to be located at points of transmembrane helix-helix interactions (Moore et al., 2008; Russ and Engelman, 2000; Senes et al., 2004). Indeed, the positioning of small amino acid side chains, typically glycine but also alanine and serine, separated by 3 amino acids is quite common and

substitutions of either G798 or A802 had strong effects on function in both mutagenesis scans. Hence, available structural evidence supports the idea that the M4 segment represents an important element for transmembrane helix-helix interactions.

4.3.2 Functionality in the ΔM4 construct

Modularity of multi-domain proteins including ion channels (e.g., Alabi et al., 2007) is a prevalent theme. GluR subunits are also largely modular (see Introduction) yet truncation of the M4 segment (ΔM4 constructs), yielding a subunit with a topology like the functional GluR0, express on the membrane but are non-functional. The ΔM4 constructs might function under some condition, but their lack of function under normal ionic conditions in either *Xenopus* oocytes or a mammalian cell line (Figure 3-2; Table 3-1) supports the idea that M4 is a critical structural element for receptor function. Although not essential to our argument, the lack of function or the poorly functioning single substituted tryptophan- or cysteine-substituted receptors (Figure 4-4) presumably disrupt function in a manner similar to ΔM4.

On the other hand, the ΔM4 construct could distort receptor structure possibly disrupting (a) membrane folding, (b) tetramerization, or (c) the specific arrangement of M1-M3 in a tetramerized receptor. We think alternatives (a) and (b) are highly unlikely for a variety of reasons. First, the ΔM4 construct is expressed in the membrane, both in *Xenopus* oocytes as well as in HEK 293 cells (Figure 3-4 and Figure 3-5) and function can be regenerated when co-expressed with an independently encoded M4 segment (Schorge and Colquhoun, 2003). In terms of membrane expression, a misfolded protein

or a monomer/dimer would be unlikely to get past the ER quality control system (Mah et al., 2005). This is especially true since we did not see any significant difference in terms of quantitative membrane expression or total expression (Figure 3-4). In addition, the core of the ion channel, which is structurally homologous to 2TM K^+ channels remains intact in truncated and single substituted mutant channels (Deutsch, 2002) and other elements in GluRs important for tetramer formation (Greger et al., 2007) are unaltered. Therefore, it seems unlikely that there are great structural changes in these constructs.

Alternative (c) is not inconsistent with our general hypothesis. Hence, our proposal is that the ΔM4 construct, in a tetrameric form, gets to the membrane and that the ion channel largely in an intact form can no longer gate either because M1-M3 are in a distorted conformation or because they have largely their native (closed) conformation. In either scenario, the free energy provided by ligand-binding is now insufficient to overcome the energetics of the ion channels to open. Presumably small but subtle evolutionary changes in the nature of the side chains in the ion channel core (M1-M3) have been altered the dynamics of gating in two transmembrane to three transmembrane GluRs.

4.3.3 Mechanistic role of the M4 segment

Although our results resolve important features of the functional significance of M4 to mammalian glutamate receptors, key issues remain unresolved. Perhaps most notable is what transmembrane segment(s) specifically interact with M4 and why this interaction is

needed for channel gating. For the tryptophan scan, the disruption of function was more extensive at the extreme N-terminal end of M4, encompassing all sides of a canonical α-helix (Figure 4-14). In contrast, starting at about two turns down the helix in the vicinity of F792, disruption of function was restricted to one face. Although we are uncertain as to the basis for this distinction between the N- and C-terminal ends of M4, it might reflect that M4 interacts with multiple helices—either M1, M3 or even M4—at the extreme N-terminus and is more restricted elsewhere or that there are more dynamic helical interactions at the N-terminal end. On the other hand, and an alternative we cannot rule out, the putative helix-cap of M4 is composed of only small residues (VAGV), and substitution of them with the bulky tryptophan might dramatically change the helix landscape. In any case, depending on the vertical depth M4 may interact with different transmembrane helices. The identity of these interacting helices remain unknown. Still, given the homology to K^+ channels (Wo and Oswald, 1995; Wood et al., 1995), which would place M1 more peripheral, it probably represents at least one of these helices. High resolution structures of the intact GluR as well as more extensive mutagenesis will be needed to clarify these helix-helix interactions.

A second major unresolved functional issue is why the M4 interactions are necessary for channel gating. It seems unlikely that M4 itself undergoes extensive conformational changes during gating, an idea supported by the results shown in Figure 4-12 and Figure 4-13.

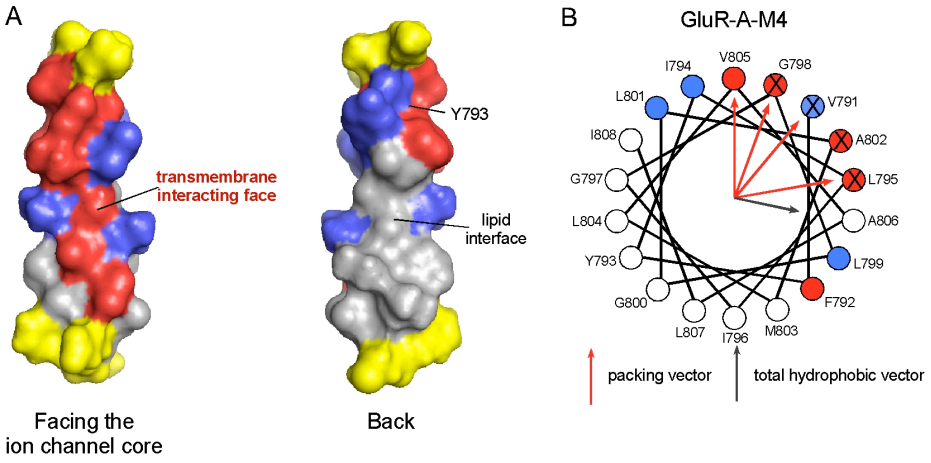

Figure 4-14 The interaction of the M4 segment with other transmembrane segments.

(A) Canonical α-helix of the M4 segment. The N- and C-termini including the polar clamps are highlighted in yellow. Those positions that presumably form the major interacting face are highlighted in red, whereas those presumably more peripheral to this interacting face are highlighted in blue. Those positions that are presumably in contact with lipid are highlighted in gray.
(B) Helix packing moment of the GluR-A M4 segment (Liu et al., 2004). Helical wheel representation of the GluR-A M4 segment (positions V791-I808). Results are shown for tryptophan substitution. The red arrows are the packing vectors whereas the light gray arrow is the total hydrophobic vector (citation). The residues identified in the putative interacting face colocalize with the helix packing moments predictions.

Rather, it is the M3 segment and probably to a lesser degree the M1 segment that undergo the conformational changes necessary for channel gating (Beck et al., 1999; Sobolevsky et al., 2007). Given this, several potential functions for the M4 segment helix-helix interactions can be considered. First, the M4 segments might help reduce the energetic landscape for gating by providing an environment, presumably by protecting against the lipid interface, for other gating domains to undergo their conformational change. Alternatively, the helix-helix interacting face may be necessary to permit select key residues—either in the helix-helix interface or in adjacent areas (e.g., proximal S2-M4 linker) to interact.

4.3.4 Evolution of M4 segment and associated C-terminal domain

In the present context, we have emphasized the significance of M4 to mammalian GluRs mainly because the gating properties of numerous mammalian GluR subtypes in heterologous expression systems are well defined. Nevertheless, the M4 segment and associated C-terminal domain are found in all eukaryotic GluRs. In figure Figure 4-4, red positions are defined by their functional effects on receptor function. These aminoacids tend to be conserved in invertebrate GluRs, including Caenorhabditis elegans, Drosophila and Trichoplax (Figure 4-15).

In terms of the evolution of M4 and the associated C-terminal domain several key issues remain unresolved. The first is the origin of M4 itself. Although we have yet to identify any single pass transmembrane proteins via BLAST searches that display

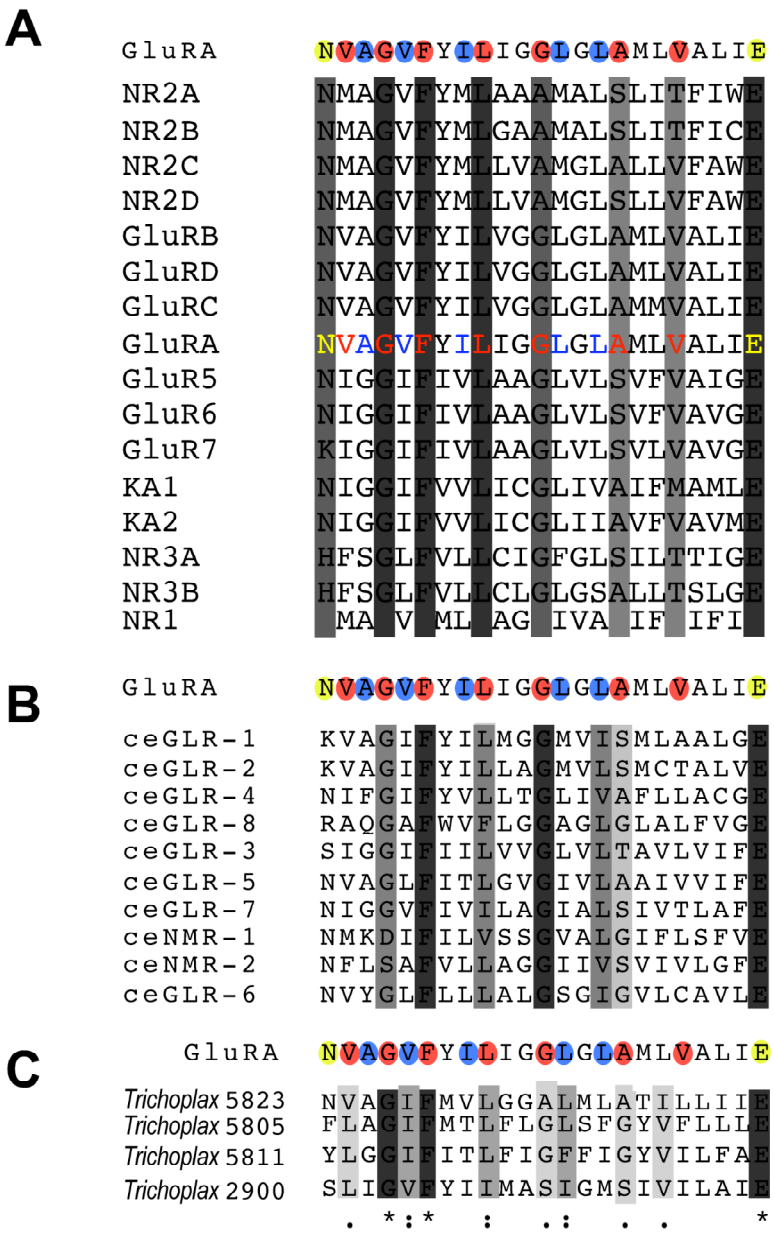

Figure 4-15 M4 Sequence Alignment of Glutamate receptors

Sequence alignment with clustalw. M4 transmembrane sequences in A) mammalian glutamate receptors, B) *C. elegans and C)* Tricoplax. GluR-A has color coded, yellow polar clamp residues, red and blue residues identified in the mutagenesis as potential interacting face. Highly conserve residues denoted with * or dark gray. 50% conserved residues ":" or medium gray, and low conservation with light gray or ".".
Cap of residues at the N-terminus of the alpha helix and the (small)xxx(small) motif (GxxxG-like) is present in all the alignments.

homology to M4, numerous examples of single pass transmembrane proteins exist that modulate ion channel function (Moore et al., 2008). The second major issue is what drove the evolution of M4. M4 in its own right has functional significance, yet it is also critical for attaching the highly regulated C-terminal domain to the core of the ion channel. Hence, in the course of evolution, either the M4 or the C-terminal domain may have been the initial evolutionary advantage of M4/C-terminal domain complex with the other element becoming a synaptic experiment. A better understanding of the distribution and function of invertebrate GluRs subtypes will further delineate these issues.

4.3.5 Perturbations of M4 as a pathway for modulation of receptor function

Modulation of GluR function is critical in regulating synaptic activity including plasticity (e.g., Derkach et al., 2007)] and can occur by a variety of means such as phosphorylation, membrane phospholipid composition, and auxiliary proteins (Derkach et al., 2007; Nicoll et al., 2006; Wilding et al., 1998). At present, the molecular mechanism by which these agents act remain largely undefined. Although speculative, perturbations of the topology of M4 relative to other transmembrane segments in the plane of the membrane could represent one such mechanism. Notable here are those agents whose action is affected by Q/R site editing such as membrane fatty acids (Wilding et al., 2008; Wilding et al., 2005) and Type II TARPs (Kato et al., 2008). Nevertheless, specific experiments will be needed to address any potential role for the topology of M4 as a regulatory mechanism of GluR function.

CHAPTER FIVE

General Discussion

5 GENERAL DISCUSSION

The core of the ion channel (M1-M3) in GluRs is not functional (Chapters 3 & 4). GluRs have three transmembrane segments (M1, M3, M4) and a reentry pore loop (M2). The GluR ion channel has an evolutionary link with two transmembrane K^+ channels (Wo and Oswald, 1995), although the core of the ion channel (M1 to M3) has an inverted topology in the membrane. Bacterial GluRs with only two transmembrane segments and a reentry pore loop are functional (Chen et al., 1999) (Figure 3-1). This information strengthens the idea that the ion channel core of GluRs has a relationship to K^+ channel. Several components of the ion channel in GluRs resemble the counterpart of K^+ channels even though signature sequences are not identical (Cordero-Morales et al., 2006; Liu et al., 2001; Perozo et al., 1999; Sprengel et al., 2001). In this frame, the M4 transmembrane segment was thought to be more a redundant element in the structure of the channel than a relevant player for its function. My data suggest a more significant role for M4 in channel function.

The M4 segment interaction with other transmembrane domains is relevant for channel function. When transmembrane interactions of M4 are totally disrupted but LBD domain connection is maintained the receptor is not functional (polyleucine mutant in Figure 4-1). The functional receptor is reestablished when a set of residues, implied in packing (Eilers et al., 2000; Javadpour et al., 1999; Richardson et al., 2006) are reintroduced into several M4 backgrounds (Figure 4.7 GluR-A-M4^{pLeu}, Figure 4-9 GluR-

A-M4^{KA2} and GluR-A-M4^{KA6} chimeras). An intrahelical interaction motif, (small)xxx(small), is observed. Where small represents glycine, alanine, serine or cysteine residues and X denote any residue. It is considered that this is a potential place for helix-helix interaction or even tertiary structure determination (Kleiger et al., 2002). Although not surprisingly, M4 requires additional amino acids in the interacting face, as the context of this motif is important for stable helix interactions (Schneider and Engelman, 2004). The set of residues that line one face of the alpha-helix constitute a putative site for helix-helix interaction. The N-*terminal* cluster (G790, V791, F792, L795) is of specific interest and will be discussed below.

Tryptophan mutations in M4 transmembrane segment stabilize the close state of the receptor. These substitutions in M4 show a strong correlation between their EC_{50} and peak currents (Figure 4.10) suggesting that at least some components of the disruption of function is due to a gating effect. M4 is not forming the pore of the ion channel (Figure 4-5), and therefore probably support other gating elements (M3 or M1) for its function.

5.1 Evolution

The construction of GluRs from bacterial precursors (O'Hara et al., 1993) is supported by the presence of plant GluRs (Lam et al., 1998), insects and bacterial predecessors (Chen et al., 1999; McFeeters and Oswald, 2004). Mosaic or modular proteins like GluRs occurred in many eukaryotic proteins, at the time of the metazoan

radiation (Patthy, 1999). Each module is a large region of sequence that can be associated with specific function. GluR ligand gated ion channels is a mosaic produced by genes assembled via processes such as exon shuffling (Wo and Oswald, 1995). Each module or domain is encoded by a different exon, but the exon-intron boundaries are not coincident with the junctional sites of the domains described (ATD, LBD, ion channel). One possibility is that the original intron pattern is hidden by deletion and insertion of introns during the evolutionary history of GluRs. It is interesting to note that the core of the ion channel in GluR Drosophila genes (DGluR1, DGluRII) is encoded by a single exon. It is proposed that one module of GluRs (the ion channel) was formed from a structure related to K^+ channel based on hydropathy profiles, sequence similarities, mutational studies and effects of RNA editing. GluRs evolution might have come by splicing of a primordial channel structure into a prokaryotic periplasmic amino acid binding protein.

The fourth module of GluRs that includes M4 and the CTD has no identified evolutionary link. The unique origin of this module can be seen by the presence of an intron between the extracellular bacterial-periplasmic-binding protein like domain and M4 transmembrane. M4 sequence analysis for the GluR family shows conservation of the packing interface identified in this study (Figure 4-9 & Figure 4-14A). The residue identity is maintained within the subfamilies. Additionally conservative substitutions in and around the packing residues can be observed between subfamilies (Figure 5-1). When mutations that altered our identified packing pattern exist (like for NMDA

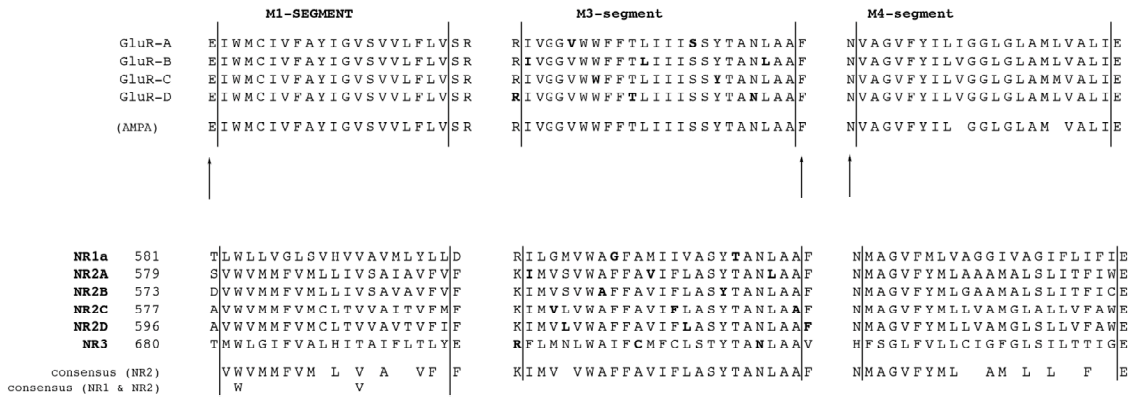

Figure 5-1 Sequence alignment of Glutamate Receptor transmembrane segments

Glutamate receptor sequences were aligned using clustalw. Vertical lanes denote the boundary of the lipid bilayer. Arrow indicates the extracellular polar clamp amino acid of each transmembrane alpha helix. AMPA receptors (upper panel) are highly conserved while NMDA receptors (lower panel) show some variability towards the C-terminal half of M1 and M4 transmembrane segment.

receptors), enrichment in beta-branch residues or the increase hydrophobicity in the region occurs. M4 coevolution with the core of the ion channel must have shaped this divergence between subfamilies. For AMPA receptors, the M1 and M3 segments are identical (Figure 5-1). M4 has two conservative substitutions outside of the packing face. AMPAR M4 exchange would not alter the specific properties of the subunit original background. It also will imply that the subunit composition of AMPA receptors is determined mainly by other domains in the subunits because the ion channel can be promiscuous. In NMDA receptors, the more intracellular segment of M1 has high variability. This might be an indication of the specific coevolution with M4. On the other hand, the intracellular half of M3 segment is also quite variable. Future studies will be needed to define the evolutionary force that shape the current M4 sequence.

In chapter four (4), I suggested that the evolution of M4 might be linked to the CTD. Another alternative to consider is the evolution of M4 as the last structural element of the LBD. During the mosaic formation of proteins some structural elements are maintained. Alpha helices and beta-sheets are usually structures preserved from mRNA splice junctions and help to define invisible modules in the architecture of proteins (Barik, 2004). Venus Fly-Trap structural superfamilies includes, among others, members of the DNA binding repressors like the Lac repressor. These proteins, form tetramers and their last structural elements are alpha-helix that binds DNA or help for tetramerization. When sequences of the M4 of GluR-A and the last helix sequence of Lac repressor are compared, some residue similarities exist (Figure 5-2). Of interest is that the pattern of polar residues is in the opposite face of the packing of M4. The preliminary phylogenetic

Figure 5-2 Glutamate receptor and Lac repressor sequence alignment

The M4 transmembrane of GluR-A and the Lac repressor sequences were aligned using ClustalW. Yellow polar clamp residues of M4-GluR-A, red residues are the putative transmembrane interaction face of M4; * polar residues important for DNA binding.

analysis done in Figure 4-15 demonstrates that the origins of M4 go beyond Trichoplax and cyanobacterias. An indication that the use of the superfamily of periplasmic binding proteins (venus fly-trap superfamily) for the mosaic formation is plausible and that by selective pressures the structural last alpha-helix might have been inserted at the membrane. It is notable that the GxxxG-like motif (represented in M4 sequence as small xxx small motif) is also prevalent in soluble proteins (Kleiger et al., 2002). Some investigation of sequences that includes other venus flytrap domain proteins need to be used to evaluate this phylogenetic hypothesis.

5.2 Glutamate Receptor structure

The core of the ion channel has structural homology with two transmembrane K^+ channels (Wo and Oswald, 1995). Our data demostrate that M4 plays a pivotal role in ion channel gating of glutamate receptors. Modifications of the putative packing interface of M4 lock the receptor in a dysfunctional conformation. These critically constrained positions at the packing interface might be forming hydrogen bonds and the disruptions of these by mutations can destabilize the helical structure/interaction and altered the functional dynamics of the receptor. Three questions are raised regarding M4: what does it interact with, how is it located in the tetramer and how is its mechanistic function during gating. The identification of transmembrane interactions may provide helpful structural insights into understanding GluRs gating mechanism.

5.2.1 **M4 transmembrane interactions**

The putative helix-helix interation motif of M4 transmembrane segment can be defined as:

N(small)(small)(small)(small)FxxLxx(small)xxx(small)xxVxxx**E**

Where small is any residue between glycine, serine, alanine, or cysteine. The cluster of small residues near the N-terminal asparagine (N) is maintained in all GluR(s) indicating that, size exclusion might be influencing this pattern. Visual analysis of the sequences in Figure 5-1 shows a conserved Tryptophan in the M1 transmembrane and the conserved tyrosine of the M3-SYTANLAAF motif. Both residues large in size will fit the knob made by the cluster of small residues of M4. Which transmembrane interact with M4 (M1 or M3) is not clear yet, or if both of them form interactions. The M3 segment with the 45° bend will add some constrains to the M3-M4 contact but the spring movement of it might release and facilitate interaction (Sobolevsky et al., 2004). It can occur that M3 toggle with M1 the space of M4 during gating.

The second region of interaction (small)xxx(small) motif start at the middle of the bilayer and toward the C-terminal half of the transmembrane. The motif is at the center of the transmembrane in agreement with the fact that the interactions are stronger in the low-polarity center of the bilayer than closer to the head group regions of the lipid (Zhou et al., 2001). Chimeric constructs were only possible when this motif was present, and the best results for rescue came with the presence of serine, (GxxxS), a residue known to facilitate hydrogen bond formation. The major forces that drive interactions between

transmembrane segments are initiated by hydrogen bonds and cemented by Van der Waals forces. We can speculate that this motif stabilizes the structure by a hydrogen bond with the Serine present at M1 transmembrane. M3 has a Tryptophan in the equivalent position, and a knob in the hole interaction can also fit the experimental results. M1 and M3 present structural elements that can interact with M4. Ruling out exclusive interactions will only be possible after experimentation. Still, the M4 alpha-helix might be tilted at the membrane, a conformation that permits interaction with M1 and M3 simultaneously. The type of interactions that M4 provides will help in the association with other transmembranes during the packing of the ion channel.

5.2.2 M4 transmembrane location

No data exist about the location of M4 relative to the core of the ion channel. The putative interaction face identified, gives us the possibility to orient the alpha helix in the membrane space. Using the crystal structure of K^+ channel (1bl8, Doyle et al., 1998)) as a template, I consider, two potential places for M4 location.

One is in the crevice left by TM1 and TM2. It is a peripheric position that allow for the interaction with M1 and M3 of the same subunit. Another possibility is the location of M4 between subunits. This will raise the chance of interaction with adjacent subunits and intervene strongly in the packing of the tetramer. A crystal structure or computer modeling might be more informative. I considered that in the second model the interactions between residues in the transmembrane helices may serve to provide

structural stability and oligomerization specificity. It will be in agreement with the dimerization power that has been identified for this type of motif (Senes et al., 2004).

5.2.3 M4 mechanism in gating

The interactions M4 facilitates allow for the structural flexibility required for channel function. The helices in the ion channel are considered to be loosely packed but closely associated. Breaking and reforming of hydrogen bonds at the helical interfaces can be the result of the conformational changes that the ion channel experience during gating. The putative interaction face, has a motif (small xxx small) that directs helix-helix interaction. Transmembrane contacts are important when conformational changes are required for functional states of a protein. When the sequence constrains of this interaction is reduced or eliminated (as in the tryptophan scan) global conformational changes occurred and the transmembrane α-helices rearrange in a state that is not mobile. Hydrogen bond might be lost and indeed the mechanism for channel gating is broken. The packing motif is a hinge for the core of the ion channel to function.

Something that is not clear is if the non-tolerant mutants (no glutamate activated currents) prevent the formation of assembly competent dimers or attenuates the packing of two dimers into tetramers. Is M4 providing the environment for the transition from the two fold to the four fold symmetry?

5.3 Folding

The M4 transmembrane segment might affect the tetramerization of Glutamate receptors. GluRs are modular polypeptides. The distinct domains of the receptors (ATD, LBD, ion channel and CTD) participate in intersubunit contacts during the oligomer assembly (Greger and Esteban, 2007; Greger et al., 2003; Mah et al., 2005). The ATD and LBD fold and assemble in the ER lumen. The subsequent synthesis of the core of the ion channel is embedded in the lipid bilayer by assistance of the translocon channel. The organization of the domains in the transcript and the modular nature of GluRs suggest that the domains fold sequencially (Figure 1-3). The ATD will fold and establish intersubunit contacts while other domains are being translated and translocated into the ER membrane (Greger and Esteban, 2007). Similar to K^+ channels and acetylcholine receptors the folding and assembly of GluRs might be a concurrent event.

AMPA receptors assemble as a dimer of dimers. The dimerization is initiated at the ATD by interactions that define compatibility of subfamily subunits (Ayalon et al., 2005; Ayalon and Stern-Bach, 2001). The second point of assembly is provided by the LBD and the core of the ion channel. LBD folding might follow the ion channel due to their presence in the transcript. The transmembrane helices provide a tetramerization step that involves of the core of the ion channel. This is followed by the LBD formation of dimer of dimers interaction, who will tighten the tetramer. Tertiary folding supported by LBD will facilitate packing and aligning of the transmembrane segments. M4 transmembrane might play a role in the final folding of the structure.

Our ΔM4 construct is apparently able to pass control machinery and exit the ER (Figures 3-4, 3-5, 4-1, 4-2). The already tetrameric receptor traffics towards the membrane. The influence of M4 in packing can pass the control machinery but do not support channel funcion. Gating motions evaluated during the ER transit are not impaired (Penn et al., 2008). Experiments that measure oligomerization state of the receptor like blue native polyacrylamide gels (BN-PAGE) might give a false indication of a process that is occurring deeply and clearly in the membrane. An assay for in vitro refolding of the ion channel will be a better indicator of the M4 influence in oligomerization and the packing effect that M4 transmembrane deploy.

5.4 Therapeutic potential for M4

Targeting the specific interactions between transmembrane helices of GluRs can be a method to disrupt receptor function for application in drug design and structure function studies of the receptor (Tarasova et al., 1999). My thesis describes a specific sequence of amino acids in the M4 transmembrane segment that represent the putative interaction face with other transmembrane elements of the ion channel. Structural analogs of this individual transmembrane sequence can possibly serve as a potent and specific receptor antagonist. Individual domains of GluRs that were precipitated, refold and are functional (Chen et al., 1998). The function of inactive truncated receptors can be rescued by expression of the missing transmembrane (Schorge and Colquhoun, 2003)or the here identified transmembrane sequence (as shown here in figures 4-4; 4-8;

3-6). The ion channel is a flexible structure that allows conformational changes during the gating process. The proper packing of the ion channels facilitates flexibility and functionality of the receptor but alterations of it can destroy the balance and render an inactive receptor. Peptides derived from the M4 transmembrane of GluRs that mimics their packing face can potentially abolish channel gating.

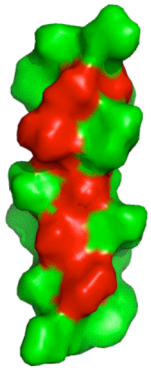

REFERENCES

Acher, F.C., and Bertrand, H.O. (2005). Amino acid recognition by Venus flytrap domains is encoded in an 8-residue motif. Biopolymers *80*, 357-366.

Ahmed, A.H., Wang, Q., Sondermann, H., and Oswald, R.E. (2008). Structure of the S1S2 glutamate binding domain of GLUR3. Proteins.

Alabi, A.A., Bahamonde, M.I., Jung, H.J., Kim, J.I., and Swartz, K.J. (2007). Portability of paddle motif function and pharmacology in voltage sensors. Nature *450*, 370-375.

Andrews, P.I., and McNamara, J.O. (1996). Rasmussen's encephalitis: an autoimmune disorder? Curr Opin Neurobiol *6*, 673-678.

Arinaminpathy, Y., Biggin, P.C., Shrivastava, I.H., and Sansom, M.S.P. (2003). A prokaryotic glutamate receptor: homology modelling and molecular dynamics simulations of GluR0. Febs Letters *553*, 321-327.

Armstrong, N., and Gouaux, E. (2000). Mechanisms for activation and antagonism of an AMPA-sensitive glutamate receptor: crystal structures of the GluR2 ligand binding core. Neuron *28*, 165-181.

Armstrong, N., Sun, Y., Chen, G.Q., and Gouaux, E. (1998). Structure of a glutamate-receptor ligand-binding core in complex with kainate. Nature *395*, 913-917.

Arvola, M., and Keinanen, K. (1996). Characterization of the ligand-binding domains of glutamate receptor (GluR)-B and GluR-D subunits expressed in Escherichia coli as periplasmic proteins. J Biol Chem *271*, 15527-15532.

Ayalon, G., Segev, E., Elgavish, S., and Stern-Bach, Y. (2005). Two regions in the N-terminal domain of ionotropic glutamate receptor 3 form the subunit oligomerization interfaces that control subtype-specific receptor assembly. J Biol Chem *280*, 15053-15060.

Ayalon, G., and Stern-Bach, Y. (2001). Functional assembly of AMPA and kainate receptors is mediated by several discrete protein-protein interactions. Neuron *31*, 103-113.

Barik, S. (2004). When proteome meets genome: the alpha helix and the beta strand of proteins are eschewed by mRNA splice junctions and may define the minimal indivisible modules of protein architecture. J Biosci *29*, 261-273.

Barria, A., Muller, D., Derkach, V., Griffith, L.C., and Soderling, T.R. (1997). Regulatory phosphorylation of AMPA-type glutamate receptors by CaM-KII during long-term potentiation. Science *276*, 2042-2045.

Beck, C., Wollmuth, L.P., Seeburg, P.H., Sakmann, B., and Kuner, T. (1999). NMDAR channel segments forming the extracellular vestibule inferred from the accessibility of substituted cysteines. Neuron *22*, 559-570.

Benn, C.L., Slow, E.J., Farrell, L.A., Graham, R., Deng, Y., Hayden, M.R., and Cha, J.H. (2007). Glutamate receptor abnormalities in the YAC128 transgenic mouse model of Huntington's disease. Neuroscience *147*, 354-372.

Berciano, J., Boesch, S., Perez-Ramos, J.M., and Wenning, G.K. (2006). Olivopontocerebellar atrophy: toward a better nosological definition. Mov Disord *21*, 1607-1613.

Bjerrum , O.J., and Schafer-Nielsen, C. (1986). Buffer Systems and Transfer Parameters for Semidry Electroblotting with a Horizontal Apparatus. In Electrophoresis '86, M.J. Dunn, ed. (Weinheim: VCH Verlagsgesellschaft), pp. 315-327.

Boulter, J., Hollmann, M., O'Shea-Greenfield, A., Hartley, M., Deneris, E., Maron, C., and Heinemann, S. (1990). Molecular cloning and functional expression of glutamate receptor subunit genes. Science *249*, 1033-1037.

Bowie, D., Garcia, E.P., Marshall, J., Traynelis, S.F., and Lange, G.D. (2003). Allosteric regulation and spatial distribution of kainate receptors bound to ancillary proteins. J Physiol *547*, 373-385.

Bowie, D., and Mayer, M.L. (1995). Inward rectification of both AMPA and kainate subtype glutamate receptors generated by polyamine-mediated ion channel block. Neuron *15*, 453-462.

Burbea, M., Dreier, L., Dittman, J.S., Grunwald, M.E., and Kaplan, J.M. (2002). Ubiquitin and AP180 regulate the abundance of GLR-1 glutamate receptors at postsynaptic elements in C-elegans. Neuron *35*, 107-120.

Burnashev, N., Monyer, H., Seeburg, P.H., and Sakmann, B. (1992). Divalent ion permeability of AMPA receptor channels is dominated by the edited form of a single subunit. Neuron *8*, 189-198.

Burnashev, N., Villarroel, A., and Sakmann, B. (1996). Dimensions and ion selectivity of recombinant AMPA and kainate receptor channels and their dependence on Q/R site residues. J Physiol *496 (Pt 1)*, 165-173.

Caputo, G.A., and London, E. (2004). Position and ionization state of Asp in the core of membrane-inserted alpha helices control both the equilibrium between transmembrane and nontransmembrane helix topography and transmembrane helix positioning. Biochemistry *43*, 8794-8806.

Cavara, N.A., and Hollmann, M. (2008). Shuffling the deck anew: how NR3 tweaks NMDA receptor function. Mol Neurobiol *38*, 16-26.

Chen, B.S., Braud, S., Badger, J.D., 2nd, Isaac, J.T., and Roche, K.W. (2006). Regulation of NR1/NR2C N-methyl-D-aspartate (NMDA) receptors by phosphorylation. J Biol Chem *281*, 16583-16590.

Chen, G.Q., Cui, C.H., Mayer, M.L., and Gouaux, E. (1999). Functional characterization of a potassium-selective prokaryotic glutamate receptor. Nature *402*, 817-821.

Chen, G.Q., Sun, Y., Jin, R., and Gouaux, E. (1998). Probing the ligand binding domain of the GluR2 receptor by proteolysis and deletion mutagenesis defines domain boundaries and yields a crystallizable construct. Protein Sci *7*, 2623-2630.

Chen, L., Chetkovich, D.M., Petralia, R.S., Sweeney, N.T., Kawasaki, Y., Wenthold, R.J., Bredt, D.S., and Nicoll, R.A. (2000). Stargazin regulates synaptic targeting of AMPA receptors by two distinct mechanisms. Nature *408*, 936-943.

Chen, P.E., and Wyllie, D.J. (2006). Pharmacological insights obtained from structure-function studies of ionotropic glutamate receptors. Br J Pharmacol *147*, 839-853.

Cho, K., Francis, J.C., Hirbec, H., Dev, K., Brown, M.W., Henley, J.M., and Bashir, Z.I. (2003). Regulation of kainate receptors by protein kinase C and metabotropic glutamate receptors. Journal of Physiology-London *548*, 723-730.

Citri, A., and Malenka, R.C. (2008). Synaptic plasticity: multiple forms, functions, and mechanisms. Neuropsychopharmacology *33*, 18-41.

Collingridge, G.L., and Isaac, J.T.R. (2003). Functional roles of protein interactions with AMPA and kainate receptors. Neuroscience Research *47*, 3-15.

Cordero-Morales, J.F., Cuello, L.G., Zhao, Y., Jogini, V., Cortes, D.M., Roux, B., and Perozo, E. (2006). Molecular determinants of gating at the potassium-channel selectivity filter. Nat Struct Mol Biol *13*, 311-318.

Coyle, J.T., Tsai, G., and Goff, D.C. (2002). Ionotropic glutamate receptors as therapeutic targets in schizophrenia. Curr Drug Targets CNS Neurol Disord *1*, 183-189.

Cull-Candy, S., Brickley, S., and Farrant, M. (2001). NMDA receptor subunits: diversity, development and disease. Curr Opin Neurobiol *11*, 327-335.

Cull-Candy, S.G., and Leszkiewicz, D.N. (2004). Role of distinct NMDA receptor subtypes at central synapses. Sci STKE *2004*, re16.

Derkach, V.A., Oh, M.C., Guire, E.S., and Soderling, T.R. (2007). Regulatory mechanisms of AMPA receptors in synaptic plasticity. Nat Rev Neurosci *8*, 101-113.

Deutsch, C. (2002). Potassium channel ontogeny. Annu Rev Physiol *64*, 19-46.

DiAntonio, A., and Hicke, L. (2004). Ubiquitin-dependent regulation of the synapse. Annual Review of Neuroscience *27*, 223-246.

Dingledine, R., Borges, K., Bowie, D., and Traynelis, S.F. (1999). The glutamate receptor ion channels. Pharmacological Reviews *51*, 7-61.

Dingledine, R., Kleckner, N.W., and McBain, C.J. (1990). The glycine coagonist site of the NMDA receptor. Adv Exp Med Biol *268*, 17-26.

Dirnagl, U., Iadecola, C., and Moskowitz, M.A. (1999). Pathobiology of ischaemic stroke: an integrated view. Trends in Neurosciences *22*, 391-397.

Dirson, G., Desjardins, P., Tannenberg, T., Dodd, P., and Butterworth, R.F. (2002). Selective loss of expression of glutamate GluR2/R3 receptor subunits in cerebellar tissue from a patient with olivopontocerebellar atrophy. Metab Brain Dis *17*, 77-82.

Doyle, D.A., Morais Cabral, J., Pfuetzner, R.A., Kuo, A., Gulbis, J.M., Cohen, S.L., Chait, B.T., and MacKinnon, R. (1998). The structure of the potassium channel: molecular basis of K+ conduction and selectivity. Science *280*, 69-77.

Eastwood, S.L., McDonald, B., Burnet, P.W., Beckwith, J.P., Kerwin, R.W., and Harrison, P.J. (1995). Decreased expression of mRNAs encoding non-NMDA glutamate receptors GluR1 and GluR2 in medial temporal lobe neurons in schizophrenia. Brain Res Mol Brain Res *29*, 211-223.

Ehlers, M.D. (2000). Reinsertion or degradation of AMPA receptors determined by activity-dependent endocytic sorting. Neuron *28*, 511-525.

Ehlers, M.D. (2003). Activity level controls postsynaptic composition and signaling via the ubiquitin-proteasome system. Nature Neuroscience *6*, 231-242.

Eilers, M., Patel, A.B., Liu, W., and Smith, S.O. (2002). Comparison of helix interactions in membrane and soluble alpha-bundle proteins. Biophys J *82*, 2720-2736.

Eilers, M., Shekar, S.C., Shieh, T., Smith, S.O., and Fleming, P.J. (2000). Internal packing of helical membrane proteins. Proc Natl Acad Sci U S A *97*, 5796-5801.

Furukawa, H., Singh, S.K., Mancusso, R., and Gouaux, E. (2005). Subunit arrangement and function in NMDA receptors. Nature *438*, 185-192.

Gahring, L.C., Rogers, S.W., and Twyman, R.E. (1997). Autoantibodies to glutamate receptor subunit GluR2 in nonfamilial olivopontocerebellar degeneration. Neurology *48*, 494-500.

Gielen, M., Le Goff, A., Stroebel, D., Johnson, J.W., Neyton, J., and Paoletti, P. (2008). Structural rearrangements of NR1/NR2A NMDA receptors during allosteric inhibition. Neuron *57*, 80-93.

Gilman, S., Little, R., Johanns, J., Heumann, M., Kluin, K.J., Junck, L., Koeppe, R.A., and An, H. (2000). Evolution of sporadic olivopontocerebellar atrophy into multiple system atrophy. Neurology *55*, 527-532.

Granata, T., Fusco, L., Gobbi, G., Freri, E., Ragona, F., Broggi, G., Mantegazza, R., Giordano, L., Villani, F., Capovilla, G.*, et al.* (2003). Experience with immunomodulatory treatments in Rasmussen's encephalitis. Neurology *61*, 1807-1810.

Greger, I.H., and Esteban, J.A. (2007). AMPA receptor biogenesis and trafficking. Curr Opin Neurobiol *17*, 289-297.

Greger, I.H., Khatri, L., Kong, X., and Ziff, E.B. (2003). AMPA receptor tetramerization is mediated by Q/R editing. Neuron *40*, 763-774.

Greger, I.H., Ziff, E.B., and Penn, A.C. (2007). Molecular determinants of AMPA receptor subunit assembly. Trends Neurosci *30*, 407-416.

Guo, S., Shi, Y., Zhao, X., Duan, S., Zhou, J., Meng, J., Yang, Y., Gu, N., Feng, G., Liu, H.*, et al.* (2004). No genetic association between polymorphisms in the AMPA receptor subunit GluR4 gene (GRIA4) and schizophrenia in the Chinese population. Neurosci Lett *369*, 168-172.

Hall, B.J., and Ghosh, A. (2008). Regulation of AMPA receptor recruitment at developing synapses. Trends Neurosci *31*, 82-89.

Heintz, N., and Zoghbi, H.Y. (2000). Insights from mouse models into the molecular basis of neurodegeneration. Annu Rev Physiol *62*, 779-802.

Hirbec, H., Francis, J.C., Lauri, S.E., Braithwaite, S.P., Coussen, F., Mulle, C., Dev, K.K., Couthino, V., Meyer, G., Isaac, J.T.R.*, et al.* (2003). Rapid and differential regulation of AMPA and kainate receptors at hippocampal mossy fibre Synapses by PICK1 and GRIP. Neuron *37*, 625-638.

Hoffmann, J., Gorodetskaia, A., and Hollmann, M. (2006a). Ion pore properties of ionotropic glutamate receptors are modulated by a transplanted potassium channel selectivity filter. Mol Cell Neurosci *33*, 335-343.

Hoffmann, J., Villmann, C., Werner, M., and Hollmann, M. (2006b). Investigation via ion pore transplantation of the putative relationship between glutamate receptors and K+ channels. Mol Cell Neurosci *33*, 358-370.

Hsieh, H., Boehm, J., Sato, C., Iwatsubo, T., Tomita, T., Sisodia, S., and Malinow, R. (2006). AMPAR removal underlies Abeta-induced synaptic depression and dendritic spine loss. Neuron *52*, 831-843.

Huettner, J.E. (2003). Kainate receptors and synaptic transmission. Prog Neurobiol *70*, 387-407.

Huggins, D.J., and Grant, G.H. (2005). The function of the amino terminal domain in NMDA receptor modulation. J Mol Graph Model *23*, 381-388.

Jaskolski, F., Coussen, F., and Mulle, C. (2005). Subcellular localization and trafficking of kainate receptors. Trends Pharmacol Sci *26*, 20-26.

Javadpour, M.M., Eilers, M., Groesbeek, M., and Smith, S.O. (1999). Helix packing in polytopic membrane proteins: role of glycine in transmembrane helix association. Biophys J *77*, 1609-1618.

Jellinger, K.A. (2003). Neuropathological spectrum of synucleinopathies. Mov Disord *18 Suppl 6*, S2-12.

Jin, R., Banke, T.G., Mayer, M.L., Traynelis, S.F., and Gouaux, E. (2003). Structural basis for partial agonist action at ionotropic glutamate receptors. Nat Neurosci *6*, 803-810.

Jones, K.S., VanDongen, H.M., and VanDongen, A.M. (2002). The NMDA receptor M3 segment is a conserved transduction element coupling ligand binding to channel opening. J Neurosci *22*, 2044-2053.

Kalia, L.V., Kalia, S.K., and Salter, M.W. (2008). NMDA receptors in clinical neurology: excitatory times ahead. Lancet Neurol *7*, 742-755.

Kamboj, S.K., Swanson, G.T., and Cull-Candy, S.G. (1995). Intracellular spermine confers rectification on rat calcium-permeable AMPA and kainate receptors. J Physiol *486 (Pt 2)*, 297-303.

Kang, C.H., Gokcen, S., and Ames, G.F. (1992). Crystallization and preliminary X-ray studies of the liganded lysine, arginine, ornithine-binding protein from Salmonella typhimurium. J Mol Biol *225*, 1123-1125.

Kato, A.S., Siuda, E.R., Nisenbaum, E.S., and Bredt, D.S. (2008). AMPA receptor subunit-specific regulation by a distinct family of type II TARPs. Neuron *59*, 986-996.

Kawahara, Y., Ito, K., Sun, H., Aizawa, H., Kanazawa, I., and Kwak, S. (2004). Glutamate receptors: RNA editing and death of motor neurons. Nature *427*, 801.

Keinanen, K., Wisden, W., Sommer, B., Werner, P., Herb, A., Verdoorn, T.A., Sakmann, B., and Seeburg, P.H. (1990). A family of AMPA-selective glutamate receptors. Science *249*, 556-560.

Kew, J.N., and Kemp, J.A. (2005). Ionotropic and metabotropic glutamate receptor structure and pharmacology. Psychopharmacology (Berl) *179*, 4-29.

Kim, E.J., and Sheng, M. (2004). PDZ domain proteins of synapses. Nature Reviews Neuroscience *5*, 771-781.

Kleiger, G., Grothe, R., Mallick, P., and Eisenberg, D. (2002). GXXXG and AXXXA: common alpha-helical interaction motifs in proteins, particularly in extremophiles. Biochemistry *41*, 5990-5997.

Koh, D.S., Burnashev, N., and Jonas, P. (1995). Block of native Ca(2+)-permeable AMPA receptors in rat brain by intracellular polyamines generates double rectification. J Physiol *486 (Pt 2)*, 305-312.

Kornau, H.C., Schenker, L.T., Kennedy, M.B., and Seeburg, P.H. (1995). Domain interaction between NMDA receptor subunits and the postsynaptic density protein PSD-95. Science *269*, 1737-1740.

Krupp, J.J., Vissel, B., Heinemann, S.F., and Westbrook, G.L. (1998). N-terminal domains in the NR2 subunit control desensitization of NMDA receptors. Neuron *20*, 317-327.

Kuner, T., Beck, C., Sakmann, B., and Seeburg, P.H. (2001). Channel-lining residues of the AMPA receptor M2 segment: structural environment of the Q/R site and identification of the selectivity filter. J Neurosci *21*, 4162-4172.

Kuner, T., and Schoepfer, R. (1996). Multiple structural elements determine subunit specificity of Mg2+ block in NMDA receptor channels. J Neurosci *16*, 3549-3558.

Kuner, T., Seeburg, P.H., and Guy, H.R. (2003). A common architecture for K+ channels and ionotropic glutamate receptors? Trends Neurosci *26*, 27-32.

Kuner, T., Wollmuth, L.P., Karlin, A., Seeburg, P.H., and Sakmann, B. (1996). Structure of the NMDA receptor channel M2 segment inferred from the accessibility of substituted cysteines. Neuron *17*, 343-352.

Kuusinen, A., Abele, R., Madden, D.R., and Keinanen, K. (1999). Oligomerization and ligand-binding properties of the ectodomain of the alpha-amino-3-hydroxy-5-methyl-4-isoxazole propionic acid receptor subunit GluRD. J Biol Chem *274*, 28937-28943.

Kuusinen, A., Arvola, M., and Keinanen, K. (1995). Molecular dissection of the agonist binding site of an AMPA receptor. EMBO J *14*, 6327-6332.

Kwak, S., and Kawahara, Y. (2005). Deficient RNA editing of GluR2 and neuronal death in amyotropic lateral sclerosis. J Mol Med *83*, 110-120.

Kwon, H.B., and Castillo, P.E. (2008). Role of glutamate autoreceptors at hippocampal mossy fiber synapses. Neuron *60*, 1082-1094.

Laemmli, U.K. (1970). Cleavage of structural proteins during the assembly of the head of bacteriophage T4. Nature *227*, 680-685.

Lam, H.M., Chiu, J., Hsieh, M.H., Meisel, L., Oliveira, I.C., Shin, M., and Coruzzi, G. (1998). Glutamate-receptor genes in plants. Nature *396*, 125-126.

Lavezzari, G., McCallum, J., Lee, R., and Roche, K.W. (2003). Differential binding of the AP-2 adaptor complex and PSD-95 to the C-terminus of the NMDA receptor subunit NR2B regulates surface expression. Neuropharmacology *45*, 729-737.

Lee, S.H., Liu, L.D., Wang, Y.T., and Sheng, M. (2002). Clathrin adaptor AP2 and NSF interact with overlapping sites of GluR2 and play distinct roles in AMPA receptor trafficking and hippocampal LTD. Neuron *36*, 661-674.

Leonard, A.S., Davare, M.A., Horne, M.C., Garner, C.C., and Hell, J.W. (1998). SAP97 is associated with the alpha-amino-3-hydroxy-5-methylisoxazole-4-propionic acid receptor GluR1 subunit. J Biol Chem *273*, 19518-19524.

Lerma, J. (2006). Kainate receptor physiology. Curr Opin Pharmacol *6*, 89-97.

Leuschner, W.D., and Hoch, W. (1999). Subtype-specific assembly of alpha-amino-3-hydroxy-5-methyl-4-isoxazole propionic acid receptor subunits is mediated by their n-terminal domains. J Biol Chem *274*, 16907-16916.

Liu, W., Eilers, M., Patel, A.B., and Smith, S.O. (2004). Helix packing moments reveal diversity and conservation in membrane protein structure. Journal of Molecular Biology *337*, 713-729.

Liu, Y.S., Sompornpisut, P., and Perozo, E. (2001). Structure of the KcsA channel intracellular gate in the open state. Nat Struct Biol *8*, 883-887.

MacKinnon, R. (2003). Potassium channels. Febs Letters *555*, 62-65.

Madden, D.R. (2002). The inner workings of the AMPA receptors. Curr Opin Drug Discov Devel *5*, 741-748.

Magri, C., Gardella, R., Valsecchi, P., Barlati, S.D., Guizzetti, L., Imperadori, L., Bonvicini, C., Tura, G.B., Gennarelli, M., Sacchetti, E., and Barlati, S. (2008). Study on GRIA2, GRIA3 and GRIA4 genes highlights a positive association between schizophrenia and GRIA3 in female patients. Am J Med Genet B Neuropsychiatr Genet *147B*, 745-753.

Mah, S.J., Cornell, E., Mitchell, N.A., and Fleck, M.W. (2005). Glutamate receptor trafficking: Endoplasmic reticulum quality control involves ligand binding and receptor function. Journal of Neuroscience *25*, 2215-2225.

Maier, W., Schemm, R., Grewer, C., and Laube, B. (2007). Disruption of interdomain interactions in the glutamate binding pocket affects differentially agonist affinity and efficacy of N-methyl-D-aspartate receptor activation. J Biol Chem *282*, 1863-1872.

Martin, S., and Henley, J.M. (2004). Activity-dependent endocytic sorting of kainate receptors to recycling or degradation pathways. Embo Journal *23*, 4749-4759.

Mayer, M. (2004). Structure and function of glutamate receptors. Ann N Y Acad Sci *1038*, 125-130.

Mayer, M.L. (2005). Crystal structures of the GluR5 and GluR6 ligand binding cores: molecular mechanisms underlying kainate receptor selectivity. Neuron *45*, 539-552.

Mayer, M.L. (2006). Glutamate receptors at atomic resolution. Nature *440*, 456-462.

McFeeters, R.L., and Oswald, R.E. (2002). Structural mobility of the extracellular ligand-binding core of an ionotropic glutamate receptor. Analysis of NMR relaxation dynamics. Biochemistry *41*, 10472-10481.

McFeeters, R.L., and Oswald, R.E. (2004). Emerging structural explanations of ionotropic glutamate receptor function. FASEB J *18*, 428-438.

McNamara, J.O., Whitney, K.D., Andrews, P.I., He, X.P., Janumpalli, S., and Patel, M.N. (1999). Evidence for glutamate receptor autoimmunity in the pathogenesis of Rasmussen encephalitis. Adv Neurol *79*, 543-550.

Metzler, M., Gan, L., Wong, T.P., Liu, L., Helm, J., Georgiou, J., Wang, Y., Bissada, N., Cheng, K., Roder, J.C.*, et al.* (2007). NMDA receptor function and NMDA receptor-dependent phosphorylation of huntingtin is altered by the endocytic protein HIP1. J Neurosci *27*, 2298-2308.

Mi, R., Sia, G.M., Rosen, K., Tang, X., Moghekar, A., Black, J.L., McEnery, M., Huganir, R.L., and O'Brien, R.J. (2004). AMPA receptor-dependent clustering of synaptic NMDA receptors is mediated by Stargazin and NR2A/B in spinal neurons and hippocampal interneurons. Neuron *44*, 335-349.

Midgett, C.R., and Madden, D.R. (2008). The quaternary structure of a calcium-permeable AMPA receptor: conservation of shape and symmetry across functionally distinct subunit assemblies. J Mol Biol *382*, 578-584.

Moore, D.T., Berger, B.W., and DeGrado, W.F. (2008). Protein-protein interactions in the membrane: sequence, structural, and biological motifs. Structure *16*, 991-1001.

Mori, H., Manabe, T., Watanabe, M., Satoh, Y., Suzuki, N., Toki, S., Nakamura, K., Yagi, T., Kushiya, E., Takahashi, T.*, et al.* (1998). Role of the carboxy-terminal region of the GluR epsilon2 subunit in synaptic localization of the NMDA receptor channel. Neuron *21*, 571-580.

Morimoto-Tomita, M., Zhang, W., Straub, C., Cho, C.H., Kim, K.S., Howe, J.R., and Tomita, S. (2009). Autoinactivation of neuronal AMPA receptors via glutamate-regulated TARP interaction. Neuron *61*, 101-112.

Moriyoshi, K., Iijima, K., Fujii, H., Ito, H., Cho, Y., and Nakanishi, S. (2004). Seven in absentia homolog 1A mediates ubiquitination and degradation of group 1 metabotropic glutamate receptors. Proc Natl Acad Sci U S A *101*, 8614-8619.

Nakagawa, T., Cheng, Y., Sheng, M., and Walz, T. (2006). Three-dimensional structure of an AMPA receptor without associated stargazin/TARP proteins. Biol Chem *387*, 179-187.

Nakanishi, N., Shneider, N.A., and Axel, R. (1990). A family of glutamate receptor genes: evidence for the formation of heteromultimeric receptors with distinct channel properties. Neuron *5*, 569-581.

Nicoll, R.A., Tomita, S., and Bredt, D.S. (2006). Auxiliary subunits assist AMPA-type glutamate receptors. Science *311*, 1253-1256.

O'Hara, P.J., Sheppard, P.O., Thogersen, H., Venezia, D., Haldeman, B.A., McGrane, V., Houamed, K.M., Thomsen, C., Gilbert, T.L., and Mulvihill, E.R. (1993). The ligand-binding domain in metabotropic glutamate receptors is related to bacterial periplasmic binding proteins. Neuron *11*, 41-52.

Oh, M.C., Derkach, V.A., Guire, E.S., and Soderling, T.R. (2006). Extrasynaptic membrane trafficking regulated by GluR1 serine 845 phosphorylation primes AMPA receptors for long-term potentiation. J Biol Chem *281*, 752-758.

Olney, J.W., Sharpe, L.G., and Feigin, R.D. (1972). Glutamate-Induced Brain-Damage in Infant Primates. Journal of Neuropathology and Experimental Neurology *31*, 464-488.

Oswald, R.E., Ahmed, A., Fenwick, M.K., and Loh, A.P. (2007). Structure of glutamate receptors. Curr Drug Targets *8*, 573-582.

Paoletti, P., and Neyton, J. (2007). NMDA receptor subunits: function and pharmacology. Curr Opin Pharmacol *7*, 39-47.

Partin, K.M., Fleck, M.W., and Mayer, M.L. (1996). AMPA receptor flip/flop mutants affecting deactivation, desensitization, and modulation by cyclothiazide, aniracetam, and thiocyanate. J Neurosci *16*, 6634-6647.

Pasternack, A., Coleman, S.K., Jouppila, A., Mottershead, D.G., Lindfors, M., Pasternack, M., and Keinanen, K. (2002). Alpha-amino-3-hydroxy-5-methyl-4-isoxazolepropionic acid (AMPA) receptor channels lacking the N-terminal domain. J Biol Chem *277*, 49662-49667.

Patthy, L. (1999). Genome evolution and the evolution of exon-shuffling--a review. Gene *238*, 103-114.

Peng, P.L., Zhong, X., Tu, W., Soundarapandian, M.M., Molner, P., Zhu, D., Lau, L., Liu, S., Liu, F., and Lu, Y. (2006). ADAR2-dependent RNA editing of AMPA receptor subunit GluR2 determines vulnerability of neurons in forebrain ischemia. Neuron *49*, 719-733.

Penn, A.C., Williams, S.R., and Greger, I.H. (2008). Gating motions underlie AMPA receptor secretion from the endoplasmic reticulum. EMBO J *27*, 3056-3068.

Perozo, E., Cortes, D.M., and Cuello, L.G. (1999). Structural rearrangements underlying K+-channel activation gating. Science *285*, 73-78.

Pinheiro, P., and Mulle, C. (2006). Kainate receptors. Cell Tissue Res *326*, 457-482.

Richardson, J., Blunck, R., Ge, P., Selvin, P.R., Bezanilla, F., Papazian, D.M., and Correa, A.M. (2006). Distance measurements reveal a common topology of prokaryotic voltage-gated ion channels in the lipid bilayer. Proc Natl Acad Sci U S A *103*, 15865-15870.

Robert, A., and Howe, J.R. (2003). How AMPA receptor desensitization depends on receptor occupancy. J Neurosci *23*, 847-858.

Rodriguez-Moreno, A., and Sihra, T.S. (2007). Kainate receptors with a metabotropic modus operandi. Trends Neurosci *30*, 630-637.

Rogers, S.W., Andrews, P.I., Gahring, L.C., Whisenand, T., Cauley, K., Crain, B., Hughes, T.E., Heinemann, S.F., and McNamara, J.O. (1994). Autoantibodies to glutamate receptor GluR3 in Rasmussen's encephalitis. Science *265*, 648-651.

Rosenmund, C., Stern-Bach, Y., and Stevens, C.F. (1998). The tetrameric structure of a glutamate receptor channel. Science *280*, 1596-1599.

Russ, W.P., and Engelman, D.M. (2000). The GxxxG motif: a framework for transmembrane helix-helix association. J Mol Biol *296*, 911-919.

Samarasinghe, S., Virgo, L., and de Belleroche, J. (1996). Distribution of the N-methyl-D-aspartate glutamate receptor subunit NR2A in control and amyotrophic lateral sclerosis spinal cord. Brain Res *727*, 233-237.

Schmid, S.M., Korber, C., Herrmann, S., Werner, M., and Hollmann, M. (2007). A domain linking the AMPA receptor agonist binding site to the ion pore controls gating and causes lurcher properties when mutated. J Neurosci *27*, 12230-12241.

Schneider, D., and Engelman, D.M. (2004). Motifs of two small residues can assist but are not sufficient to mediate transmembrane helix interactions. J Mol Biol *343*, 799-804.

Schorge, S., and Colquhoun, D. (2003). Studies of NMDA receptor function and stoichiometry with truncated and tandem subunits. Journal of Neuroscience *23*, 1151-1158.

Seeburg, P.H. (1993). The TiPS/TINS lecture: the molecular biology of mammalian glutamate receptor channels. Trends Pharmacol Sci *14*, 297-303.

Seeburg, P.H., and Hartner, J. (2003). Regulation of ion channel/neurotransmitter receptor function by RNA editing. Curr Opin Neurobiol *13*, 279-283.

Senes, A., Engel, D.E., and DeGrado, W.F. (2004). Folding of helical membrane proteins: the role of polar, GxxxG-like and proline motifs. Curr Opin Struct Biol *14*, 465-479.

Sheng, M., and Hoogenraad, C.C. (2007). The postsynaptic architecture of excitatory synapses: a more quantitative view. Annu Rev Biochem *76*, 823-847.

Shepherd, J.D., and Huganir, R.L. (2007). The cell biology of synaptic plasticity: AMPA receptor trafficking. Annu Rev Cell Dev Biol *23*, 613-643.

Sobolevsky, A.I., Beck, C., and Wollmuth, L.P. (2002). Molecular Rearrangements of the extracellular vestibule in NMDAR channels during gating. Neuron *33*, 75-85.

Sobolevsky, A.I., Prodromou, M.L., Yelshansky, M.V., and Wollmuth, L.P. (2007). Subunit-specific contribution of pore-forming domains to NMDA receptor channel structure and gating. J Gen Physiol *129*, 509-525.

Sobolevsky, A.I., Yelshansky, M.V., and Wollmuth, L.P. (2003). Different gating mechanisms in glutamate receptor and K+ channels. Journal of Neuroscience *23*, 7559-7568.

Sobolevsky, A.I., Yelshansky, M.V., and Wollmuth, L.P. (2004). The outer pore of the glutamate receptor channel has 2-fold rotational symmetry. Neuron *41*, 367-378.

Soderling, T.R., and Derkach, V.A. (2000). Postsynaptic protein phosphorylation and LTP. Trends Neurosci *23*, 75-80.

Sprengel, R., Aronoff, R., Volkner, M., Schmitt, B., Mosbach, R., and Kuner, T. (2001). Glutamate receptor channel signatures. Trends Pharmacol Sci *22*, 7-10.

Stern-Bach, Y., Bettler, B., Hartley, M., Sheppard, P.O., O'Hara, P.J., and Heinemann, S.F. (1994). Agonist selectivity of glutamate receptors is specified by two domains structurally related to bacterial amino acid-binding proteins. Neuron *13*, 1345-1357.

Stern-Bach, Y., Russo, S., Neuman, M., and Rosenmund, C. (1998). A point mutation in the glutamate binding site blocks desensitization of AMPA receptors. Neuron *21*, 907-918.

Stuhmer, W. (1998). Electrophysiologic recordings from Xenopus oocytes. Ion Channels, Pt B *293*, 280-300.

Sun, Y., Olson, R., Horning, M., Armstrong, N., Mayer, M., and Gouaux, E. (2002). Mechanism of glutamate receptor desensitization. Nature *417*, 245-253.

Suzuki, E., Kessler, M., and Arai, A.C. (2005). C-terminal truncation affects kinetic properties of GluR1 receptors. Mol Cell Neurosci *29*, 1-10.

Tarasova, N.I., Rice, W.G., and Michejda, C.J. (1999). Inhibition of G-protein-coupled receptor function by disruption of transmembrane domain interactions. J Biol Chem *274*, 34911-34915.

Tomita, S., Adesnik, H., Sekiguchi, M., Zhang, W., Wada, K., Howe, J.R., Nicoll, R.A., and Bredt, D.S. (2005). Stargazin modulates AMPA receptor gating and trafficking by distinct domains. Nature *435*, 1052-1058.

Virgo, L., Samarasinghe, S., and de Belleroche, J. (1996). Analysis of AMPA receptor subunit mRNA expression in control and ALS spinal cord. Neuroreport *7*, 2507-2511.

Wall, M.J., Robert, A., Howe, J.R., and Usowicz, M.M. (2002). The speeding of EPSC kinetics during maturation of a central synapse. Eur J Neurosci *15*, 785-797.

Weston, M.C., Gertler, C., Mayer, M.L., and Rosenmund, C. (2006). Interdomain interactions in AMPA and kainate receptors regulate affinity for glutamate. J Neurosci *26*, 7650-7658.

Wheeler, T.C., Chin, L.S., Li, Y.K., Roudabush, F.L., and Li, L.A. (2002). Regulation of synaptophysin degradation by mammalian homologues of Seven in Absentia. Journal of Biological Chemistry *277*, 10273-10282.

Wilding, T.J., Chai, Y.H., and Huettner, J.E. (1998). Inhibition of rat neuronal kainate receptors by cis-unsaturated fatty acids. J Physiol *513 (Pt 2)*, 331-339.

Wilding, T.J., Fulling, E., Zhou, Y., and Huettner, J.E. (2008). Amino acid substitutions in the pore helix of GluR6 control inhibition by membrane fatty acids. J Gen Physiol *132*, 85-99.

Wilding, T.J., Zhou, Y., and Huettner, J.E. (2005). Q/R site editing controls kainate receptor inhibition by membrane fatty acids. J Neurosci *25*, 9470-9478.

Wo, Z.G., and Oswald, R.E. (1995). Unraveling the Modular Design of Glutamate-Gated Ion Channels. Trends in Neurosciences *18*, 161-168.

Wollmuth, L.P., Kuner, T., Seeburg, P.H., and Sakmann, B. (1996). Differential contribution of the NR1- and NR2A-subunits to the selectivity filter of recombinant NMDA receptor channels. Journal of Physiology-London *491*, 779-797.

Wollmuth, L.P., and Sobolevsky, A.I. (2004). Structure and gating of the glutamate receptor ion channel. Trends in Neurosciences *27*, 321-328.

Wood, M.W., VanDongen, H.M., and VanDongen, A.M. (1995). Structural conservation of ion conduction pathways in K channels and glutamate receptors. Proc Natl Acad Sci U S A *92*, 4882-4886.

Wyllie, D.J., Behe, P., and Colquhoun, D. (1998). Single-channel activations and concentration jumps: comparison of recombinant NR1a/NR2A and NR1a/NR2D NMDA receptors. J Physiol *510 (Pt 1)*, 1-18.

Xia, H., Hornby, Z.D., and Malenka, R.C. (2001). An ER retention signal explains differences in surface expression of NMDA and AMPA receptor subunits. Neuropharmacology *41*, 714-723.

Yamakura, T., and Shimoji, K. (1999). Subunit- and site-specific pharmacology of the NMDA receptor channel. Prog Neurobiol *59*, 279-298.

Yamazaki, M., Ohno-Shosaku, T., Fukaya, M., Kano, M., Watanabe, M., and Sakimura, K. (2004). A novel action of stargazin as an enhancer of AMPA receptor activity. Neurosci Res *50*, 369-374.

Yellen, G. (1999). The bacterial K+ channel structure and its implications for neuronal channels. Curr Opin Neurobiol *9*, 267-273.

Zhang, W., Robert, A., Vogensen, S.B., and Howe, J.R. (2006). The relationship between agonist potency and AMPA receptor kinetics. Biophys J *91*, 1336-1346.

Zhang, W., St-Gelais, F., Grabner, C.P., Trinidad, J.C., Sumioka, A., Morimoto-Tomita, M., Kim, K.S., Straub, C., Burlingame, A.L., Howe, J.R., and Tomita, S. (2009). A transmembrane accessory subunit that modulates kainate-type glutamate receptors. Neuron *61*, 385-396.

Zhou, F.X., Merianos, H.J., Brunger, A.T., and Engelman, D.M. (2001). Polar residues drive association of polyleucine transmembrane helices. Proceedings of the National Academy of Sciences of the United States of America *98*, 2250-2255.

Zucker, R.S., and Regehr, W.G. (2002). Short-term synaptic plasticity. Annu Rev Physiol *64*, 355-405.